Fall 12-2020

# Assessing the Nursery-Role Function of Pelagic Sargassum for Juvenile Fishes in the Northern Gulf of Mexico

Courtney Stachowiak

# ASSESSING THE NURSERY-ROLE FUNCTION OF PELAGIC *SARGASSUM* FOR JUVENILE FISHES IN THE NORTHERN GULF OF MEXICO

by

Courtney Stachowiak

A Thesis
Submitted to the Graduate School,
the College of Arts and Sciences
and the School of Ocean Science and Engineering
at The University of Southern Mississippi
in Partial Fulfillment of the Requirements
for the Degree of Master of Science

Approved by:

Frank Hernandez, Committee Chair
Kevin Dillon
Mark S. Peterson

December 2020

***Published by the Graduate School***

ABSTRACT

*Sargassum*, a genus of holopelagic brown algae, floats at the ocean's surface using air-filled bladders and forms a complex comprised of two species, *S. natans* and *S. fluitans*. Oceanic processes (e.g., Langmuir circulation, etc.) aggregate *Sargassum* into mats and weedlines, and primarily distribute the algal complex throughout the North Atlantic Ocean and the Gulf of Mexico (GOM). These floating habitats provide shelter and feeding opportunities for a diverse community of invertebrates and fishes. *Sargassum* is a presumed nursery habitat for juvenile stages of commercially- and recreationally-targeted fishery species. In this study, I estimated the standardized abundances of juvenile fishes, fish assemblages, and diets of *Sargassum*-associated fishes in the northern GOM, and investigated temporal, spatial, and environmental variability in these estimates. I observed some interannual variability in fish density and diversity, but species' distributions were often related to surface chlorophyll, spatial variables, or surface features (Loop Current or associated eddies). Diets were analyzed for juvenile Gray Triggerfish, Greater Amberjack, Lesser Amberjack, Almaco Jack, and Tripletail, and were found to be spatially variable (especially with distance from shelf break). I observed a continuum of dependency on *Sargassum* for feeding by these different species, from more obligate (e.g., Gray Triggerfish and Tripletail) to transient feeders on the habitat (e.g., Amberjack spp.). The results of this thesis fill a knowledge gap of diet information for *Sargassum*-associated juvenile fishes in the northern GOM, and provide an understanding of the factors contributing to variability in juvenile fish abundances and assemblages.

ACKNOWLEDGMENTS

First, I would like to thank my advisor, Frank Hernandez, for giving me the opportunity to join his lab, where I've had the privilege to gain valuable experience in field and lab processes. His support and guidance has helped me grow as a scientist, and the work in this thesis is reflective of a highly collaborative effort made possible by him. I would also like to thank Kevin Dillon and Mark S. Peterson for serving on my thesis committee. I would like to acknowledge Kevin Dillon for his assistance in developing methodology for condition analyses as well as collaborating on presentations. I'd like to thank Mark S. Peterson for providing his expertise in statistical analyses and editing.

I'd like to acknowledge the University of South Florida Optical Oceanography lab members, especially Chuanmin Hu, Mengqiu Wang, and Yingjun Zhang, who provided HYCOM images and remote sensing surface chlorophyll estimates for this thesis. I would like to acknowledge many past and present members of the Fisheries Oceanography and Ecology lab, all who were crucial in completing this project. I'd like to thank Olivia Lestrade, Eric Haffey, Angie Hoover, and Valeria Nunez for their hard work in completing fish identifications, fish processing, and diet analysis. Carley Zapfe and Carla Culpepper were also vital to this project, as they assisted me with zooplankton prey identifications. I'd like to acknowledge Verena Wang, who was always willing to assist with statistical analyses. I am grateful to have had the opportunity to work with such dedicated lab members, and I thank them for providing me with support throughout this whole process. I'd like to thank Brian Jones for assistance in fish identifications at sea, and the captains and crew of the *R/V Point Sur*. I'd like to acknowledge the financial support provided by the NOAA Restore Science Program (Award # NA17NOS4510099)

and the Division of Coastal Sciences. Additional travel funding was provided by the Graduate School and the Vice President for Research.

# DEDICATION

I would like to dedicate this thesis to my biggest supporters; my parents, sister, and boyfriend. Mom and dad, I would not have accomplished all I have without your undying support and I thank you both for fostering my love of learning and science. Madison, thank you for always lending a listening ear and being so supportive of me. Joshua, I'd like to thank you for always reminding me of all that I am capable of.

TABLE OF CONTENTS

LIST OF TABLES

LIST OF ILLUSTRATIONS

# CHAPTER I – SPATIAL AND TEMPORAL VARIABILITY IN *SARGASSUM*-ASSOCIATED JUVENILE FISH ASSEMBLAGES

## 1.1 Introduction

### 1.1.1 Background and Significance

Holopelagic *Sargassum* (composed of *S. natans* and *S. flutians*) is a brown algae that forms floating mats and weedlines on the ocean's surface and was first reported in 1492 in Christopher Columbus's ship log (Rand 1982). *Sargassum* is primarily found in the North Atlantic Ocean and the Gulf of Mexico (GOM), but is also distributed throughout the Pacific and Indian Oceans, Caribbean Sea, and the Red Sea (Dooley 1972). *Sargassum* distribution is dependent on winds, currents, and gyres that transport *Sargassum* within and between bodies of water. Early research in the North Atlantic Ocean estimated *Sargassum* covered approximately 5.2 million square kilometers (Krummel 1891), however these estimates were based on shipboard observations. Recent studies have focused on quantifying *Sargassum* biomass and tracking its distribution using satellite imagery (Gower and King 2011), resulting in annual estimates of up to six million tons in the GOM alone. In general, high concentrations of *Sargassum* are observed in satellite imagery in the northwest GOM in March to June, indicating growth within the GOM. Gower and King (2011) indicated *Sargassum* disperses east through the GOM and is transported via the Loop Current and Gulf Stream to the Atlantic Ocean by July. The Gulf Stream and the North Atlantic gyre circulate *Sargassum* in the Atlantic Ocean, resulting in large accumulations in the Sargasso Sea, which serves as an end-member repository for *Sargassum* (Gower and King 2011).

Since 2011, large *Sargassum* blooms have been observed along the equatorial Atlantic and in the Caribbean Sea, with major environmental and economic impacts in these regions (Wang et al. 2019). Termed the "Great Atlantic *Sargassum* Belt," these bloom events in recent years are likely a result of upwelling and increased nutrient discharge in West African waters and the Amazon River. Some portion of the bloom-derived *Sargassum* enters the GOM each year, but it is currently unknown whether this transported *Sargassum* provides the same ecosystem services as GOM-derived *Sargassum*.

The *Sargassum* canopy provides various organisms with structured habitat for foraging, shelter, and refuge (Dooley 1972). *Sargassum* facilitates nitrogen fixation by cyanobacteria found on the surface of the pneumatocysts and blades (Phlips et al. 1986). These bacteria and other colonizing organisms support the complex food web and rich diversity of invertebrates and fishes associated with *Sargassum.* Diverse fish assemblages have been observed in surveys sampling *Sargassum* in the GOM in which carangids and monocanthids were found to be among the dominant fish taxa (Bortone et al. 1977; Wells and Rooker 2004; Hoffmayer et al. 2005; Kramer 2014). Bortone et al. (1977) collected 40 different fish species from 16 families using dip nets and neuston net tows in the eastern GOM. Using a plankton purse seine, Wells and Rooker (2004) collected 36 species from 17 families collected in the western GOM off the coast of Texas. These GOM studies demonstrate the high richness and diversity of fishes associated with *Sargassum* and the variability observed when using various sampling methods.

Because *Sargassum* supports high species diversity and abundance of juvenile fishes, it is recognized as Essential Fish Habitat and a management plan is in place for the

South Atlantic (SAFMC 2002). This plan prompted research evaluating the function of *Sargassum* as nursery habitat for juvenile fishes in the Atlantic Ocean, which found significantly more individuals of the same fish species within *Sargassum* when compared to samples from open water sites using the same gear (Casazza and Ross 2008). This study also observed individuals of the same species to be larger in size when found within *Sargassum*. Though *Sargassum* has a presumed nursery-role function for many fish species, evidence of the spatial and temporal variability in fish assemblages associated with *Sargassum* in the northern GOM is relatively limited.

### 1.1.2 *Sargassum* Biomass - Juvenile Fish Relationships

Previous studies have reported generally positive relationships between *Sargassum* biomass and number of fish collected. For example, a positive linear relationship was observed between *Sargassum* wet weight (kg) and the number of fishes collected with neuston net tows, dip netting, and purse seine sets in the northern GOM (Kramer 2014). Similarly, a significant positive linear relationship between total fish collected and *Sargassum* biomass was observed in samples collected in neuston net tows off the coast of North Carolina in the Atlantic Ocean (Casazza and Ross 2008). There were also significant, positive relationships observed between the *Sargassum* wet weight (kg) and number of individuals of dominant taxa, including Planehead Filefish, Atlantic Flyingfish, Almaco Jack, Gray Triggerfish and Sailfin Flyingfish (Casazza and Ross 2008). In addition, Wells and Rooker (2004) reported positive relationships between the volume of *Sargassum* mats (length x width x depth) and the number of fishes collected in purse seine sets in the northwestern GOM. As sampling methods in *Sargassum* features

are highly variable between studies, the wet weight of *Sargassum* collected may be a common metric to standardize fishing effort for cross-study comparisons.

### 1.1.3 Juvenile Fish Assemblages

Diverse juvenile fish assemblages have been observed in samples collected in *Sargassum* in the GOM and the Atlantic, with variable spatial and temporal trends. In the northwestern GOM, mean catch-per-unit-effort (CPUE) of juvenile fishes associated with *Sargassum* were found to be lowest in August and highest in May while sampling using a plankton purse seine (Wells and Rooker 2004). Seven species comprised about 97% of the catch, and CPUE estimates of these dominant taxa were found to be significantly higher offshore relative to inshore. Similarly, in the eastern GOM, Bortone et al. (1977) reported higher fish abundances in *Sargassum* habitats sampled offshore relative to inshore using dip nets and neuston nets. Shannon species diversity (H') in the northwestern GOM was reported to be generally higher in the late summer relative to earlier in the year, and higher relative to latitude (Wells and Rooker 2004). In the eastern GOM, H' was found to have a large range of values (Bortone et al. 1977). Kramer (2014) also reported variation in H' in relation to *Sargassum* morphology, with generally higher values associated with weedlines relative to mats and scattered clumps. Because differently gear types were used, these studies are not directly comparable; however, combined these studies suggest patterns of spatial and temporal variability in *Sargassum*-associated juvenile fish abundance, diversity, and distribution.

*Sargassum* is recognized as a juvenile fish nursery habitat, but incorporating information related to *Sargassum*-fish associations as a tool to inform fisheries management has not previously been investigated. My thesis research is one component

of a larger project funded by the National Oceanic and Atmospheric Administration (NOAA) RESTORE Science Program. The overall goal of the RESTORE project is to test the efficacy of using remote-sensing estimates of *Sargassum* biomass, field collections of *Sargassum*-associated juvenile fishes, and relevant oceanographic and fisheries data to estimate the contribution that *Sargassum* has to subsequent recruitment of fishes to a fishery. By estimating variability in juvenile fish assemblages and the contribution of environmental drivers, the relationship between *Sargassum* and recreational and commercial fisheries in the GOM can be better understood.

### 1.1.4 Chapter Objectives

The overall objective of this chapter is to estimate variability in juvenile fish assemblages associated with *Sargassum* in the GOM and to determine the factors that contribute to this variability. First, the relationship between *Sargassum* biomass and number of fishes collected was quantified. Then, spatial and temporal patterns in fish density, relative abundance, diversity, and community structure were compared among four cruises (July 2017, June 2018, July 2018, and June 2019). The contribution of measured environmental factors potentially driving spatial or temporal variability were also investigated. Here, I also investigate the direct role of mesoscale eddies and the Loop Current (hereafter LC/Eddy) on the juvenile fishes assemblages associated with *Sargassum*, a relationship that has not previously been examined.

## 1.2 Materials and Methods

### 1.2.1 Study Region

Sampling was conducted in the northern GOM during four research cruises aboard the *R/V Point Sur* in 2017, 2018, and 2019 (Figure 1.1; Table 1.1). *Sargassum*

habitats were located using daily Alternative Floating Algal Index (AFAI) and Floating Algal Density (FA_Density) remote sensing products (Hu 2009; Wang and Hu 2016; available at https://optics.marine.usf.edu/). During all cruises, most *in situ* observations and samples associated with *Sargassum* mats were collected beyond the 200 m contour, however, sampling stations and associated oceanographic conditions varied within and among cruises (Figure 1.2). During the July 2017 cruise, sampling stations were located southeast of the Louisiana Birdfoot Delta, and in offshore waters of the northeastern GOM generally between 27.8-29.0° N (Figure 1.1). One station was located outside the northernmost edge of the Loop Current (Figure 1.2a). During the June 2018 cruise, sampling stations were largely located southeast of the Louisiana Birdfoot Delta and along the northwestern edge of the Loop Current (Figure 1.1, 1.2b). One station was located in "common water" between the northwestern edge of the Loop Current and an anticyclonic eddy. During the July 2018 cruise, sampling stations were generally located further south relative to previous cruises (south of 28.2° N) (Figure 1.1). Several stations were located along the northern edge of a large anticyclonic eddy that recently pinched off the Loop Current (Figure 1.2c). Additional sampling stations were located north and west of this eddy feature. During the June 2019 cruise, sampling stations were spread over a larger spatial area than previous cruises (Figure 1.1). Several stations were located along the edge of the Florida continental shelf (200 m contour), while others were located on the eastern, northern and western edges of the Loop Current (Figure 1.2d). One

additional station in June 2019 was located south of the Birdfoot Delta away from the Loop Current influence.

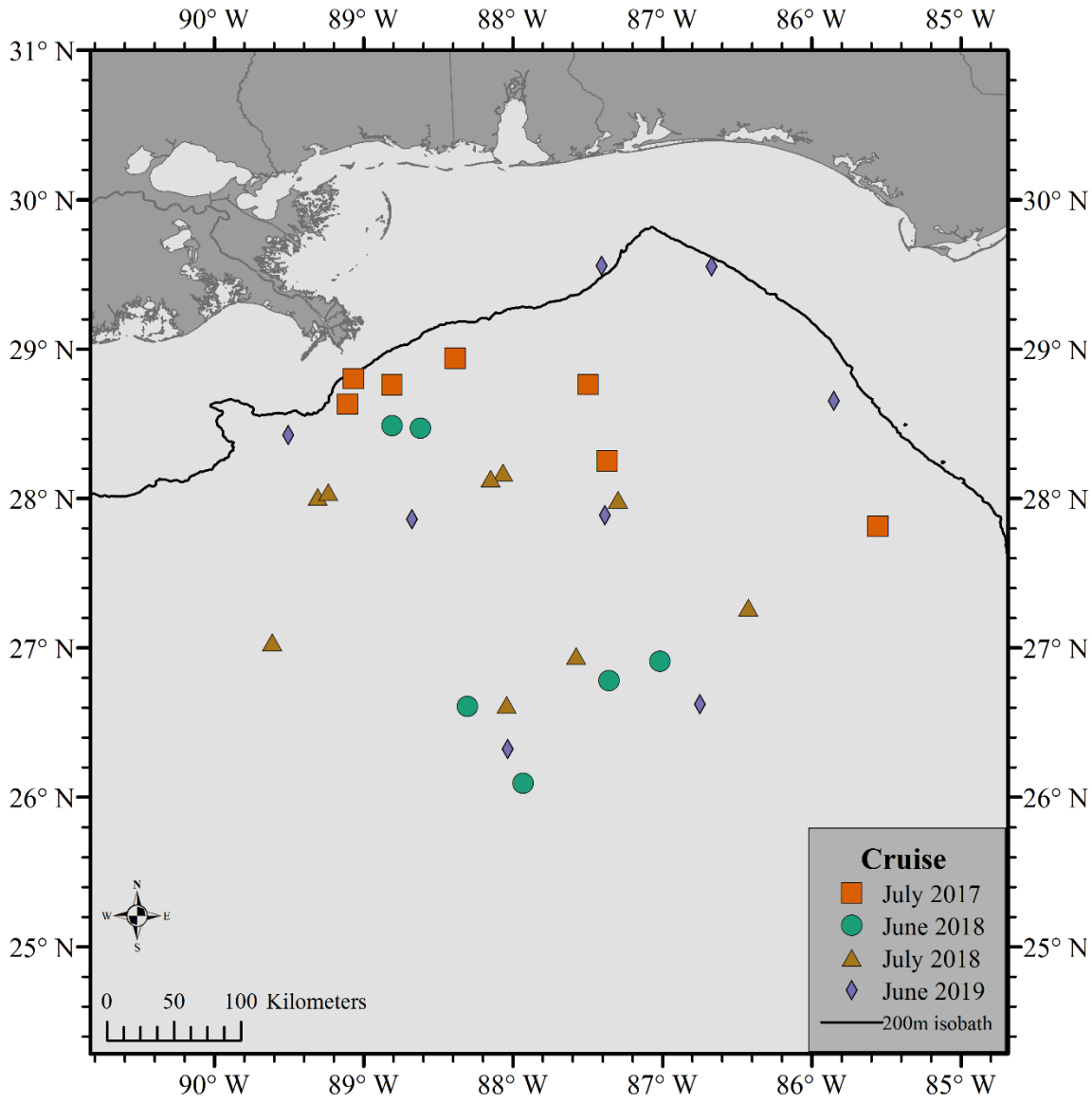


Figure 1.1 *Sargassum* neuston net sampling stations during four research cruises in 2017 – 2019. The black line represents the 200m isobath. Cruise dates and station data are provided in Table 1.1.

Table 1.1 Sample collection data for *Sargassum* and open water stations sampled during four research cruises (2017-2019). For simplicity, the second and fourth cruises are referred to as "June 2018" and "June 2019", respectively throughout the chapter, although each cruise departed in late May.

| Cruise | Dates | No. of *Sargassum* Stations | No. of Neuston Net Samples | No. of Hook-and-Line Samples |
|---|---|---|---|---|
| July 2017 | 7/20/2017 – 7/27/2017 | 7 | 7 | 6 |
| June 2018 | 5/30/2018 – 6/6/2018 | 6 | 10 | 4 |
| July 2018 | 7/9/2018 – 7/16/2018 | 9 | 13 | 7 |
| June 2019 | 5/28/2019 – 6/4/2019 | 8 | 10 | 6 |

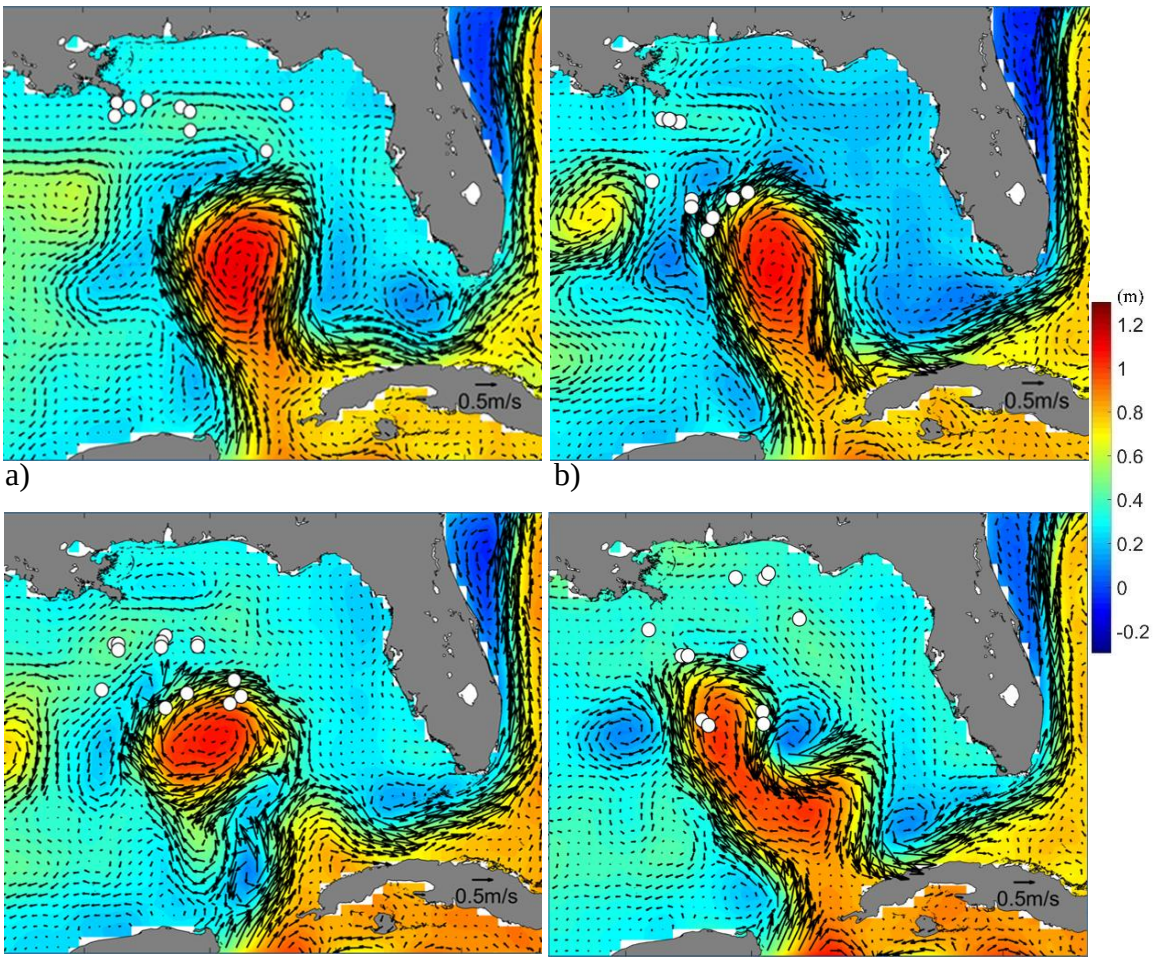


Figure 1.2 Locations of *Sargassum* neuston net stations (white circles) sampled during cruises in a) July 2017, b) June 2018, c) July 2018, and d) June 2019 in relation to sea surface currents (HYCOM) and sea surface height (SSH) anomalies (m).

### 1.2.2 Data Collection

*Sargassum* and associated juvenile fishes were collected using a 1x2 m neuston net (505 µm mesh) towed at the surface through *Sargassum* mats (sampling depth 0.5-0.75 m). Tow times varied (range of 14-262 s) depending on *Sargassum* biomass; in general, the neuston net was retrieved when it was about 1/4-1/3 full of *Sargassum*. The surface area of *Sargassum* sampled ($m^2$) during each tow was estimated by multiplying the distance towed by the width of the neuston net. Once on board, *Sargassum* was removed from the net, rinsed using seawater to remove organisms, weighed (wet) to the nearest 0.1 kg, and returned to sea. Fishes and invertebrates removed from *Sargassum* during the rinse were collected in a 0.333 mm sieve, and then either preserved in 95% ethanol or frozen. In addition to neuston net samples, standardized hook-and-line (hereafter H-L) fishing sets (four anglers, 30 minute duration) were conducted at *Sargassum* sampling stations using Sabiki bait rigs (hook sizes four and eight). Fish were measured (standard length, SL, to nearest 1.0 mm), weighed (to nearest 0.1 g), and then either preserved in 95% ethanol or frozen.

All juvenile fish (specimens >4.75 mm SL) collected were identified to the lowest taxonomic level possible in the lab using meristic counts and morphometric characteristics. A subset of juvenile fish identifications (n = 273 individuals) was confirmed using DNA barcoding of caudal fin clip samples. Barcoding was completed by the Marine Genomics Laboratory at Texas A&M University-Corpus Christi.

A suite of environmental data was collected at each sampling station prior to fish sampling. Water depth (m) and location (latitude and longitude, decimal degrees) was recorded at each station using the vessel's navigation instrumentation package. Near-

surface (4.5 m depth) observations of temperature (°C) and salinity, as well as the depth of maximum chlorophyll concentration (m) were collected using a SBE 09 Plus CTD (SBE 11 deck box). Distance from shore (km) and distance from the continental shelf break (km) was estimated using the proximity tool in ArcGIS, which calculates a point-to-line distance between the sampling coordinates and either the 200 m isobath line (continental shelf) or the closest continental border (shore). This tool accounts for curvature of the earth using the "geodesic" method, and estimates the distance by determining the closest point-to-line distance in any direction from the point. Sea surface chlorophyll concentration ($mg/m^3$) was estimated using remote sensing products provided by collaborators at the University of South Florida's Optical Oceanography lab. Lastly, stations were classified as being associated with a LC/Eddy surface feature or not associated (Other) based on remote sensing observations of sea surface height anomalies and HYCOM-derived current velocities (Figure 1.2; Table 1.2).

### 1.2.3 Data Analysis

RStudio software was used for all statistical analyses. Total fish counts (all taxa) and taxon-specific fish counts from neuston net samples were standardized by *Sargassum* biomass (fish per 10 kg of *Sargassum*) and by surface area sampled (fish per $m^2$ of *Sargassum*). Total fish abundance and species-level fish abundances from H-L samples were standardized as catch per unit effort (CPUE), i.e., number of fish caught per 30 min fishing period. Estimates of fish abundances derived from neuston net samples and H-L samples were analyzed separately, as each gear has biases and are not directly comparable. All analyses for fishes collected in neuston nets were processed separately

for biomass (fish per 10 kg *Sargassum*) and surface area (fish per $m^2$ *Sargassum*) standardized abundances.

Table 1.2 Summary of sampling effort for all neuston net and hook-and-line samples collected at *Sargassum* stations in the northern Gulf of Mexico (2017-2019). Surface feature influence denoted with "LC/Eddy" if the station was within a mesoscale eddy feature or the Loop Current, and "Other" if not associated with a surface current feature. Number of samples (by gear) collected at each station denoted by "n".

| | | | Neuston Net | | | Hook & Line | | |
|---|---|---|---|---|---|---|---|---|
| Cruise | Date | Station | n | Total No. Fish | Total *Sargassum* (kg) | n | Total No. Fish | Surface Feature |
| July 2017 | Jul 20 | 02 | 1 | 103 | 49.2 | 1 | 1 | Other |
| July 2017 | Jul 21 | 03 | 1 | 66 | 59.8 | 1 | 4 | Other |
| July 2017 | Jul 22 | 06 | 1 | 99 | 36.0 | 1 | 1 | Other |
| July 2017 | Jul 23 | 09 | 1 | 137 | 85.1 | - | - | Other |
| July 2017 | Jul 24 | 11 | 1 | 225 | 53.4 | 1 | 38 | Other |
| July 2017 | Jul 26 | 14 | 1 | 164 | 53.1 | 1 | 93* | Other |
| July 2017 | Jul 27 | 16 | 1 | 38 | 55.3 | 1 | 22 | Other |
| June 2018 | Jun 1 | 22 | 1 | 6 | 143.5 | 1 | 9 | LC/Eddy |
| June 2018 | Jun 2 | 24 | 2 | 6 | 53.9 | 1 | 5 | LC/Eddy |
| June 2018 | Jun 3 | 26 | 1 | 10 | 36.5 | 1 | 38 | Other |
| June 2018 | Jun 4 | 28 | 3 | 67 | 132.5 | - | - | Other |
| June 2018 | Jun 5 | 30 | 2 | 3 | 59.4 | 1 | 12 | LC/Eddy |
| June 2018 | Jun 6 | 31 | 1 | 11 | 68.1 | - | - | LC/Eddy |
| July 2018 | Jul 9 | 32 | 1 | 5 | 151.9 | 1 | 1 | Other |
| July 2018 | Jul 10 | 33 | 2 | 12 | 192.1 | 1 | 5 | Other |
| July 2018 | Jul 11 | 36 | 1 | 1 | 80.4 | 1 | 88 | LC/Eddy |
| July 2018 | Jul 12 | 39 | 1 | 9 | 92.4 | 1 | 53 | LC/Eddy |
| July 2018 | Jul 12 | 40 | 1 | 7 | 72.7 | - | - | LC/Eddy |
| July 2018 | Jul 13 | 42 | 1 | 12 | 132.3 | 1 | 47 | Other |
| July 2018 | Jul 14 | 43 | 2 | 106 | 71.5 | - | - | Other |
| July 2018 | Jul 15 | 44 | 3 | 59 | 214.4 | 1 | 7 | Other |
| July 2018 | Jul 16 | 46 | 1 | 4 | 58.3 | 1 | 45* | Other |
| June 2019 | May 28 | 48 | 1 | 11 | 147.2 | - | - | Other |
| June 2019 | May 29 | 50 | 2 | 14 | 179.7 | 1 | 35* | Other |
| June 2019 | May 30 | 52 | 1 | 21 | 143.0 | 1 | 3 | Other |
| June 2019 | May 31 | 54 | 1 | 16 | 75.1 | 1 | 35 | LC/Eddy |
| June 2019 | Jun 1 | 56 | 1 | 94 | 94.2 | 1 | 50* | LC/Eddy |
| June 2019 | Jun 2 | 59 | 1 | 25 | 121.4 | - | - | LC/Eddy |
| June 2019 | Jun 3 | 60 | 2 | 67 | 179.4 | 1 | 6 | LC/Eddy |
| June 2019 | Jun 4 | 62 | 1 | 30 | 120.0 | 1 | 60 | Other |

*denotes abbreviated fishing period of 15 minutes

#### 1.2.3.2 Neuston Net Standardization

To compare fish abundances with previous studies, total fish counts from neuston net samples were examined in relation to the amount of *Sargassum* biomass (kg) sampled using a linear model. Second-order polynomial and cubic regression spline models were also used to assess which model had the best fit. In addition, fish abundances were standardized by the surface area ($m^2$) of *Sargassum* sampled, and relationships with respect to canopy cover were examined using linear, second-order polynomial, and cubic regression spline models as above. Prior to each analysis, fish count data were $\log_{10}(x+1)$-transformed, and both *Sargassum* biomass (kg) and surface area ($m^2$) were $\log_{10}(x)$-transformed. There was insufficient data to estimate surface area for the July 2017 cruise, so the models for this method are limited to the June 2018, July 2018, and June 2019 cruises. A linear regression was then fitted to $\log_{10}$-transformed estimates of *Sargassum* biomass and surface area sampled to make an inference about how the two methods may provide different information about the structure of the habitat. Then, $\log_{10}(x+1)$-transformed fish count data for dominant taxa and $\log_{10}(x)$-transformed *Sargassum* biomass and surface area data were fitted using linear regressions to capture variability between method and taxa.

#### 1.2.3.3 Juvenile Fish Abundance

The size distributions of four species (*Caranx crysos, C. ruber, Seriola dumerili, S. rivoliana*) collected in both neuston net and H-L sampling were compared using length frequency distribution plots expressed as the proportional number of individuals observed within 5 mm size bins. To determine whether the length frequency distributions of the

same species were different between gear types, a two-sample Kolmogorov-Smirnov (K-S) goodness-of-fit test (Massey 1951) was used for each of four species.

Standardized fish density and CPUE for total fish and target taxa collected using neuston net and H-L sampling, respectively, were compared separately among cruises (July 2017, June 2018, July 2018, June 2019), between months (June, July), and by surface feature (LC/Eddy, Other; Table 1.2). Data normality was assessed using a Shapiro-Wilk test, and homogeneity of variance was assessed using a Levene test. If parametric assumptions were met, one-way ANOVAs and Tukey HSD post-hoc tests were used, with standardized fish density (fish per 10 kg *Sargassum*; fish per $m^2$ *Sargassum*) or CPUE (fish per 30 min.) as the dependent variable, and cruise, month, or surface feature as the predictor variable. When data did not meet parametric assumptions, a Kruskal-Wallis (KW) chi-squared test was used with Wilcoxon rank sum post-hoc tests for analysis. Effect size for parametric data was estimated using Eta squared ($\eta^2$):

$$\eta^2 = \frac{SS_{ef}}{SS_t}$$

where $SS_{ef}$ is the sum of squares for the effect, and $SS_t$ is the total sum of squares. The index, $\eta^2$, assumes values between zero and one, and is an estimate of the percent variance in the dependent variable explained by the effect when multiplied by 100 (Tomczak and Tomczak 2014). A non-parametric measure of effect size ($\eta_H^2$) was also estimated using the results of the KW chi-squared test in the following formula:

$$\eta_H^2 = \frac{H - k + 1}{n - k}$$

where *H* is the test statistic obtained from the KW test, *k* is the number of groups, and *n* is the total number of observations (Tomczak and Tomczak 2014). For both parametric and

non-parametric data, $\eta^2$ or $\eta_H^2$ values of 0.01 – 0.06 are considered to have a small effect, values 0.06 – 0.14 have a moderate effect, and values ≥ 0.14 have a large effect (Cohen 1988).

The spatial and temporal variability in fish density and CPUE was further investigated by examining the relationships between these metrics and measured environmental and biological variables: water depth (m), latitude (DD), longitude (DD), temperature (°C), salinity, depth at chlorophyll max (m), distance from shore (km), distance from the continental shelf (km), and surface chlorophyll concentration ($mg/m^3$). All environmental variables were included in separate generalized additive models (GAMs) for $\log_{10}(x)$-transformed total fish density estimates (fish per kg *Sargassum*; fish per $m^2$ *Sargassum*), $\log_{10}(x)$-transformed total fish CPUE estimates (fish per 30 min.), as well as separate $\log_{10}(x+1)$-transformed models for dominant taxa (fish per kg *Sargassum*; fish per 30 min.). GAMs allow for more flexibility in the model when multiple non-linear predictor variables are used (Hastie and Tibshirani 2014). A stepwise GAM was performed, using the *step.Gam* function in the R gam package. This stepwise method compares the Akaike's Information Criteria (AIC) of each model with and without each of the environmental variables included as either a linear term or a cubic regression spline-based smooth term (R function *s*). The model with the lowest AIC was chosen, and model parameter statistics were listed for each GAM. Model statistic values were generated using the *summary.gam* function in R, which gives an approximate significance of a Wald-type test statistic (*F*) based on the confidence interval of the smoothed parameter (Wood 2013). Significance of linear predictors in the model was also estimated using the Wald-type test statistic (*t*), which is based on the Bayesian

covariance matrix of the predictor but is similar to the frequentist covariance matrix for parametric variables (Wood 2013). Response plots of significant variables in the model with the lowest AIC were generated using the *getViz* function in the R mgcViz package. The response plots include a panel for each significant independent variable that is included in the selected GAM. The x-axis of each panel represents one of the independent variables, and the y-axis of each is the partial or additive effect of the respective variable on the response variable being analyzed. Each row in these plots is a different response variable. These plots can be interpreted as the relationship between either the linear or spline-based smooth form of each significant independent variable and the scaled response variable.

#### 1.2.3.4 Juvenile Fish Diversity

Three fish community metrics were calculated for each gear type and compared separately among cruises (July 2017, June 2018, July 2018, June 2019) and between months (June, July). Taxonomic richness (S) was expressed as number of species observed in a sample, or number of taxa when individuals were identified to genus or family. Shannon species diversity (H') was calculated using the equation:

$$H' = \frac{n\ln n - \sum f_i \ln f_i}{n}$$

where $n$ is the number of individuals in a sample and $f_i$ is the number of individuals collected in species $i$ (Zar 1999). Pielou's evenness (J') was calculated using the equation

$$J' = \frac{H'}{\ln S}$$

where H' is Shannon species diversity and $S$ is taxonomic richness, or the total number of taxa.

If parametric assumptions were met (as described above), one-way ANOVAs and Tukey HSD post-hoc tests were used, with H', S, and J' as the dependent variable, and cruise or month as the predictor variable. When data did not meet parametric assumptions, a KW chi-squared test was used with Wilcoxon rank sum post-hoc tests for analysis.

Spatial and temporal variability in diversity was further investigated using separate generalized additive models (GAMs) for H' and gear type with environmental and biological variables as predictors. As discussed above, a stepwise GAM was performed to determine which variables to include in the best model and response plots of the significant variables were generated. However, H' estimates for both neuston net and H-L sampling were not transformed as a comparison of the residual plots and model fitting parameters revealed the model with raw estimates had a better fit and more of the variability was described. For H' GAMs based on H-L data, the large number of environmental variables included in the best model constrained the smoothing terms. Smooth terms are constrained by an additive constant that is dependent on the number of parameters and observations in the model (Wood 2019). To alleviate this constraint, the knots were set to 3, the minimum number of knots allowed, for all cubic regression smoothing parameters in the model.

#### 1.2.3.5 Juvenile Fish Assemblage Structure

Juvenile fish assemblage structure was examined using a suite of multivariate analyses to assess variability among cruises (July 2017, June 2018, July 2018, June 2019) as well as the influence of environmental parameters. Variability in the fish assemblage structure was assessed by creating separate community matrices for fish collected using

neuston net and H-L sampling. These matrices were generated with the taxa as columns and samples as rows, and the raw number of individual fish of a given taxa collected from that sample given in each cell. Both community matrices were first ln(x+1) transformed, and Bray-Curtis distance matrices were then estimated and plotted using a non-metric multidimensional scaling (NMDS) plot to examine any differences in the assemblage composition coded by cruise. An analysis of similarity (ANOSIM) test was used, which tests the null hypothesis that there are no differences in the assemblages between defined groups of samples (Clarke and Gorley 2006). This test uses permutations (999 permutations used for all ANOSIMs) to determine statistical significance of the ANOSIM R test statistic, which is an indicator of whether between or within group rank dissimilarities are higher. Values closer to zero indicate that there are no differences in the assemblages between groups, and values closer to one indicate differences between groups are greater than within a group. A similarity percentages (SIMPER) test was then used to determine which species contributed most to the variability in assemblages by group. The influence of environmental and biological variables on the fish assemblage structures was investigated using the *BIOENV* function in the R vegan package (Clarke and Ainsworth 1993). This function determines which environmental variables should be included in a subset model by maximizing the rank correlation between scaled environmental variables and the community dissimilarity matrix.

For the community analysis based on neuston net collections, any identifications that were provided at the genus level were combined with the species identifications in the same genus to avoid inflating diversity metrics. For example, *Stephanolepis setifer*

and *Stephanolepis hispidus* were combined into *Stephanolepis* spp. To provide ample taxonomic information for abundant taxa instead of providing taxonomic information at only family or genus level to estimate diversity indices, the following individual fish were removed from the neuston net community matrix: one fish identified to Carangidae, one to *Caranx* spp., and two to *Seriola* spp. One *Coryphaena hippurus* that was the only fish collected in a neuston net causing an outlier value in the multivariate analysis was also removed, resulting in 1,423 individual fish included in the community analysis after removal of five individual fish mentioned. The fish collected using H-L were identified to species level, with the exception of 25 *Seriola* spp. that were released due to large sample sizes during the June 2019 cruise. These fish were removed from the community analysis, which resulted in 633 individual fish being included in the analysis.

## 1.3 Results

### 1.3.1 Sampling Effort

During the four cruises, 1,428 fish were collected in neuston nets (n=40 net tows) and 658 fish were collected during H-L sampling (n=23 sets) across 30 different *Sargassum* sampling stations (Table 1.2). Most fishes collected in neuston net samples were collected during the July 2017 cruise (58% of the total catch), followed by the June 2019 (19%), July 2019 (15%), and June 2018 (7%) cruises. The total biomass of *Sargassum* collected at each station ranged from 36.0-214.4 kg (mean=100.4 kg). The distribution of total fish catch for H-L sampling was more evenly distributed among cruises; most fishes were collected during the July 2018 cruise (37%), followed by the June 2019 (29%), July 2017 (24%), and June 2018 (10%) cruises.

### 1.3.2 Catch Composition

The neuston net collections were dominated by 10 taxa that comprised about 90% of the total catch (Table 1.3): *Balistes capriscus* (34.8%), *Abudefduf saxatilis* (13.6%), *Histrio histrio* (9.5%), *Stephanolepis* spp. (8.8%), *Aluterus monoceros* (8.5%), *Cantherhines pullus* (4.8%), *Caranx crysos* (3.4%), *Kyphosus sectatrix* (2.2%), *Lobotes surinamensis* (2.2%), and *Seriola rivoliana* (2.0%). Eighty-eight percent of the *B. capriscus* collected in neuston net samples were collected in the July 2017 cruise, as well as 37% of all *A. saxatilis*. *Histrio histrio* were most abundant (42%) in the June 2019 cruise. The most numerically dominant families collected in the neuston net were Balistidae (36% of total catch), Monocanthidae (24%), and Pomacentridae (14%). Monocanthidae and Carangidae were the most species-rich families sampled with the neuston net (n=6 species each).

Fishes collected using H-L sampling were numerically dominated by four species that made up about 90% of the total catch (Table 1.4): *S. rivoliana* (43.5%), *C. crysos* (30.4%), *Seriola dumerili* (9.7%), and *Elagatis bipinnulata* (7.3%). *Seriola rivoliana* were most abundant in the July 2018 and June 2019 cruises (each with 44% of all *S. rivoliana* collected). Most of the *C. crysos* collected (53%) were in the July 2018 cruise, followed by the July 2017 cruise (41%). The most dominant and species-rich family collected using H-L was Carangidae (98% of total catch). The next abundant family was Scombridae (1%), followed by Balistidae (0.5%).

Table 1.3 Total number of juvenile fishes collected in *Sargassum* habitats using a neuston net during four research cruises in the northern Gulf of Mexico.

| Family | Species | July 2017 | June 2018 | July 2018 | June 2019 | Total |
|---|---|---|---|---|---|---|
| Antennariidae | *Histrio histrio* | 34 | 14 | 31 | 57 | 136 |
| Balistidae | *Balistes capriscus* | 438 | 1 | 54 | 4 | 497 |
| | *Canthidermis maculata* | 8 | 0 | 0 | 0 | 8 |
| | *Canthidermis sufflamen* | 5 | 0 | 2 | 0 | 7 |
| Blenniidae | unID Bleniidae | 0 | 0 | 0 | 1 | 1 |
| Carangidae | *Caranx crysos* | 32 | 6 | 10 | 0 | 48 |
| | *Caranx ruber* | 6 | 2 | 1 | 4 | 13 |
| | *Caranx* spp. | 1 | 0 | 0 | 0 | 1 |
| | *Carangoides bartholomaei* | 5 | 1 | 1 | 7 | 14 |
| | *Elagatis bipinnulata* | 5 | 0 | 6 | 1 | 12 |
| | *Seriola dumerili* | 0 | 1 | 0 | 2 | 3 |
| | *Seriola rivoliana* | 11 | 5 | 9 | 4 | 29 |
| | *Seriola* spp. | 2 | 0 | 0 | 0 | 2 |
| | unID Carangidae | 0 | 0 | 0 | 1 | 1 |
| Coryphaenidae | *Coryphaena hippurus* | 0 | 1 | 0 | 0 | 1 |
| Diodontidae | *Diodon holocanthus* | 0 | 0 | 1 | 2 | 3 |
| Exocoetidae | *Parexocoetus brachypterus* | 1 | 0 | 0 | 0 | 1 |
| | *Prognichthys occidentalis* | 1 | 0 | 0 | 0 | 1 |
| Hemiramphidae | *Oxyporhamphus* spp. | 3 | 0 | 0 | 0 | 3 |
| | *Hemiramphus* spp. | 0 | 0 | 0 | 1 | 1 |
| Kyphosidae | *Kyphosus incisor* | 0 | 2 | 16 | 6 | 24 |
| | *Kyphosus sectatrix* | 29 | 0 | 2 | 0 | 31 |
| | *Kyphosus* spp. | 5 | 0 | 3 | 1 | 9 |
| Lobotidae | *Lobotes surinamensis* | 14 | 2 | 11 | 4 | 31 |
| Monocanthidae | *Aluterus monoceros* | 121 | 0 | 0 | 0 | 121 |
| | *Aluterus scriptus* | 6 | 0 | 1 | 3 | 10 |
| | *Aluterus* spp. | 0 | 0 | 0 | 1 | 1 |
| | *Cantherhines macrocerus* | 5 | 0 | 0 | 2 | 7 |
| | *Cantherhines pullus* | 16 | 36 | 5 | 11 | 68 |
| | *Monacanthus* spp. | 0 | 0 | 1 | 0 | 1 |
| | *Stephanolepis hispidus* | 1 | 0 | 3 | 0 | 4 |
| | *Stephanolepis setifer* | 1 | 4 | 4 | 1 | 10 |
| | *Stephanolepis* spp. | 4 | 0 | 4 | 118 | 126 |
| Nomeidae | *Psenes cyanophrys* | 0 | 0 | 0 | 1 | 1 |
| Pomacentridae | *Abudefduf saxatilis* | 71 | 28 | 50 | 45 | 194 |
| Syngnathidae | *Syngnathus pelagicus* | 7 | 0 | 0 | 1 | 8 |
| TOTAL | | **832** | **103** | **215** | **278** | **1,428** |

Table 1.4 Total number of fishes collected in *Sargassum* habitats using hook-and-line sampling during four research cruises in the northern Gulf of Mexico.

| Family | Species | July 2017 | June 2018 | July 2018 | June 2019 | Total |
|---|---|---|---|---|---|---|
| Balistidae | *Balistes capriscus* | 2 | 0 | 0 | 0 | 2 |
| | *Canthidermis sufflamen* | 1 | 0 | 0 | 0 | 1 |
| Carangidae | *Caranx crysos* | 81 | 7 | 106 | 6 | 200 |
| | *Caranx ruber* | 0 | 5 | 4 | 0 | 9 |
| | *Elagatis bipinnulata* | 44 | 1 | 3 | 0 | 48 |
| | *Seriola dumerili* | 6 | 25 | 6 | 27 | 64 |
| | *Seriola fasciata* | 1 | 4 | 1 | 6 | 12 |
| | *Seriola rivoliana* | 14 | 22 | 125 | 125 | 286 |
| | *Seriola* spp. | 0 | 0 | 0 | 25 | 25 |
| | *Selar crumenophthalmus* | 1 | 0 | 0 | 0 | 1 |
| Kyphosidae | *Kyphosus incisor* | 0 | 0 | 1 | 0 | 1 |
| Monocanthidae | *Aluterus monoceros* | 1 | 0 | 0 | 0 | 1 |
| Scombridae | *Euthynnus alletteratus* | 6 | 0 | 0 | 0 | 6 |
| | *Katsuwonus pelamis* | 1 | 0 | 0 | 0 | 1 |
| | *Thunnus atlanticus* | 1 | 0 | 0 | 0 | 1 |
| TOTAL | | **159** | **64** | **246** | **189** | **658** |

### 1.3.3 Neuston Net Standardization

No predictable relationship was observed between total number of fish and *Sargassum* biomass collected in neuston net samples (Figure 1.3a). The cubic regression spline yielding the largest $r^2$ value ($r^2 = 0.075$; $F_{3,36} = 0.97$, $p = 0.416$), followed by the second-order polynomial model ($r^2 = 0.073$; $F_{2,37} = 1.46$, $p = 0.245$), and the linear model ($r^2 = 0.009$; $F_{1,38} = 0.35$, $p = 0.560$). Though not significant and limited in sample size, a slightly stronger relationship was observed between the total number of fish collected in the neuston net and surface area towed (Figure 1.3b). The largest $r^2$ value was observed in the cubic regression spline model ($r^2 = 0.157$; $F_{3,29} = 1.80$, $p = 0.169$), followed by the second-order polynomial model ($r^2 = 0.109$; $F_{2,30} = 1.83$, $p = 0.178$), and the linear model ($r^2 = 0.063$; $F_{1,31} = 2.08$, $p = 0.160$).

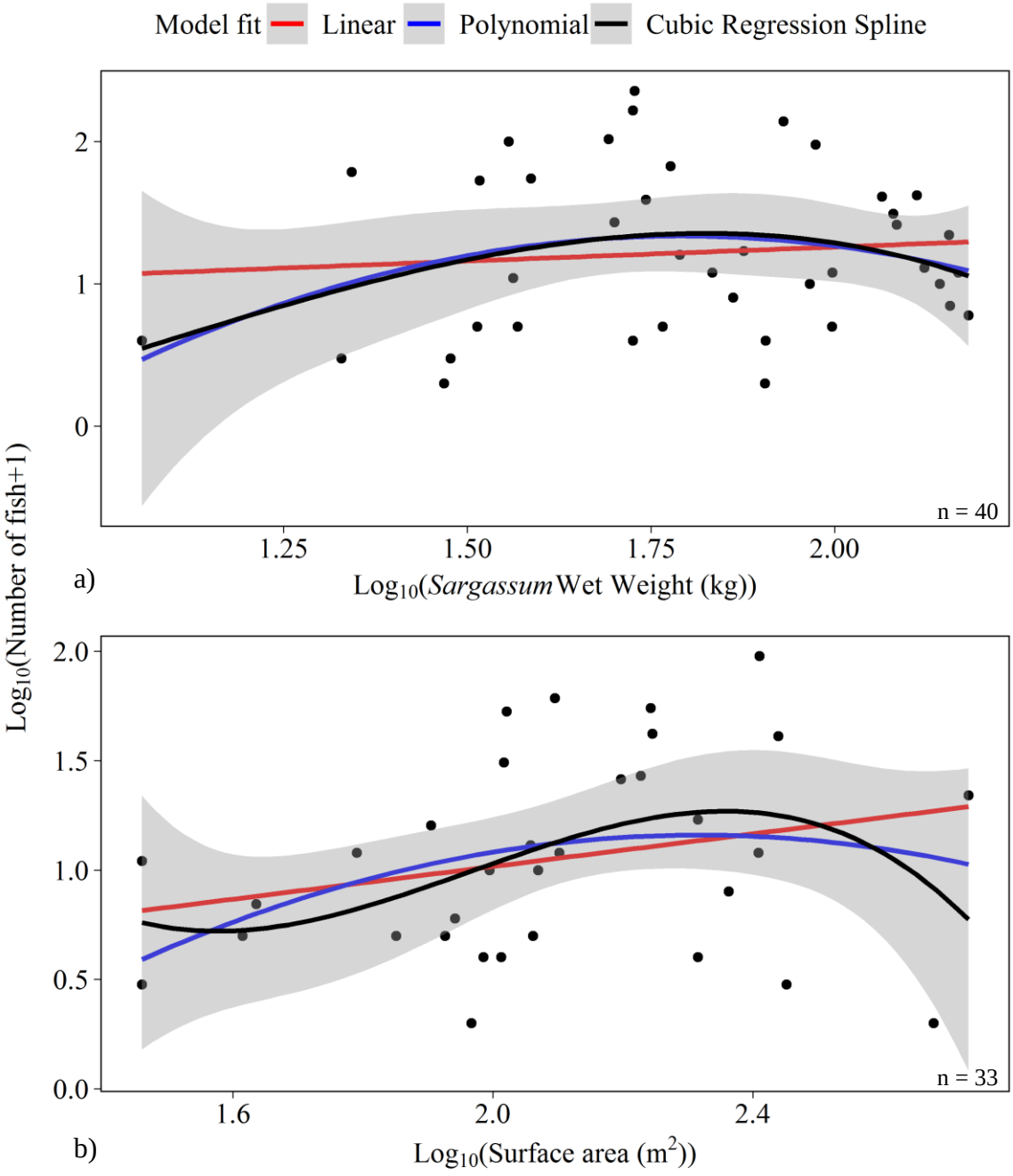


Figure 1.3 $Log_{10}(x+1)$-transformed estimates of number of individual fish and a) $log_{10}$-transformed estimates of *Sargassum* wet weight and b) surface area ($m^2$) collected in neuston nets fitted using linear (red), second-order polynomial (blue), and cubic regression spline (black) models. Gray area represents 95% confidence interval for cubic regression spline model. Note the difference in scale of x-axis and y-axis values, and the different number of observations in each panel.

No relationship was found between the two methods (biomass, surface area) of neuston net sample standardization ($r^2 = 0.0003$, $F_{1,31} = 0.01$, $p = 0.915$), indicating each method may describe different relationships when standardizing sampling effort (Figure 1.4). Therefore, the taxon-specific relationships were quantified for both standardization methods to observe any differences in fit.

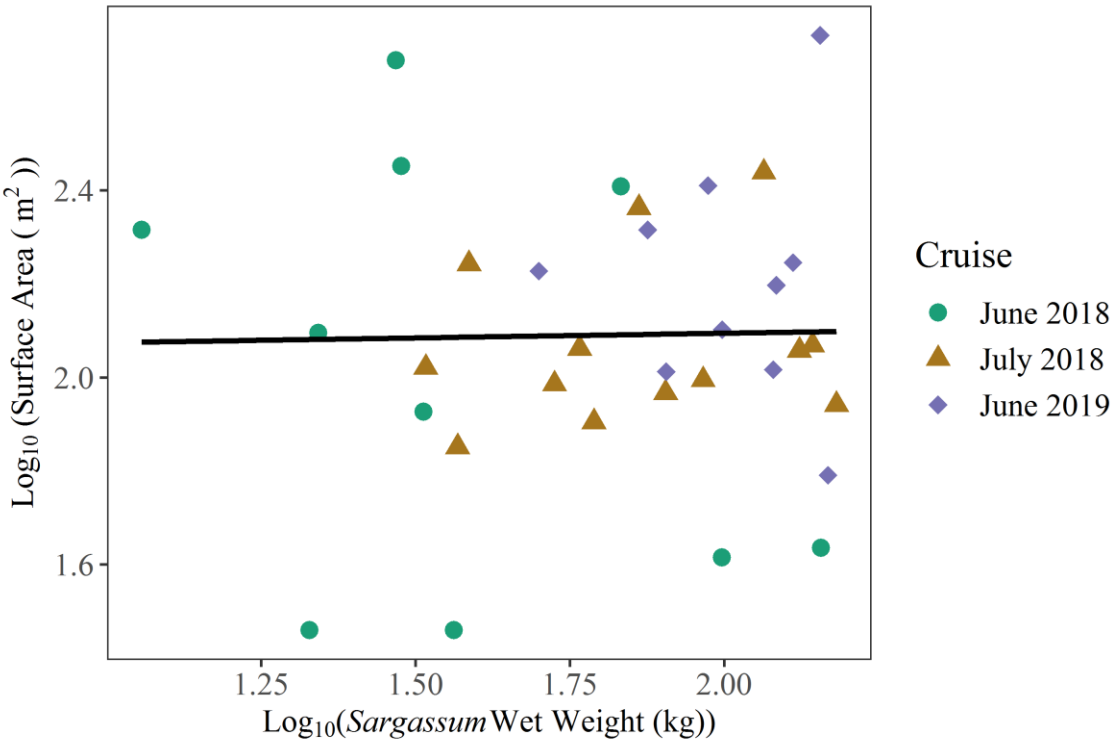


Figure 1.4 Linear relationship between $\log_{10}$-transformed estimates of surface area and *Sargassum* wet weight.

Taxon-specific relationships between fish abundances and *Sargassum* biomass collected in neuston net samples were found to be highly variable between species (Figure 1.5). Weak positive correlations were observed for *H. histrio* and *Stephanolepis* spp., and no correlations were observed for *B. capriscus* and *A. saxatilis*.

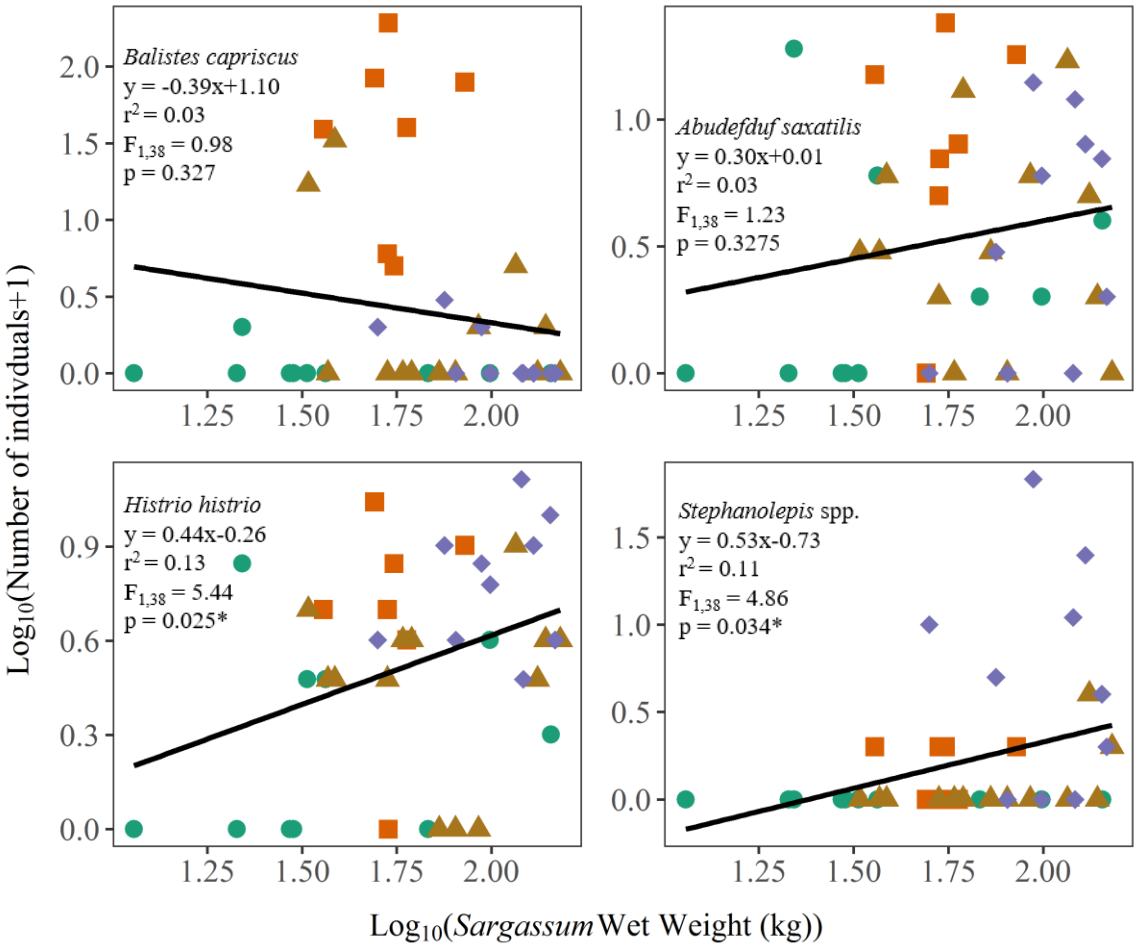


Figure 1.5 Linear relationships between $\log_{10}(x+1)$-transformed estimates of number of individual fish of the most dominant taxa collected in the neuston net and $\log_{10}$-transformed estimates of *Sargassum* wet weight. Note the differences in scale of the y-axis values.

In a reduced data set excluding the July 2017 cruise, positive significant relationships were again observed for *H. histrio* and *Stephanolepis* spp. relative to *Sargassum* biomass (Figure 1.6). However, no significant relationships were observed between the number of individuals for the four dominant taxa collected in the neuston net and *Sargassum* surface area (Figure 1.7).

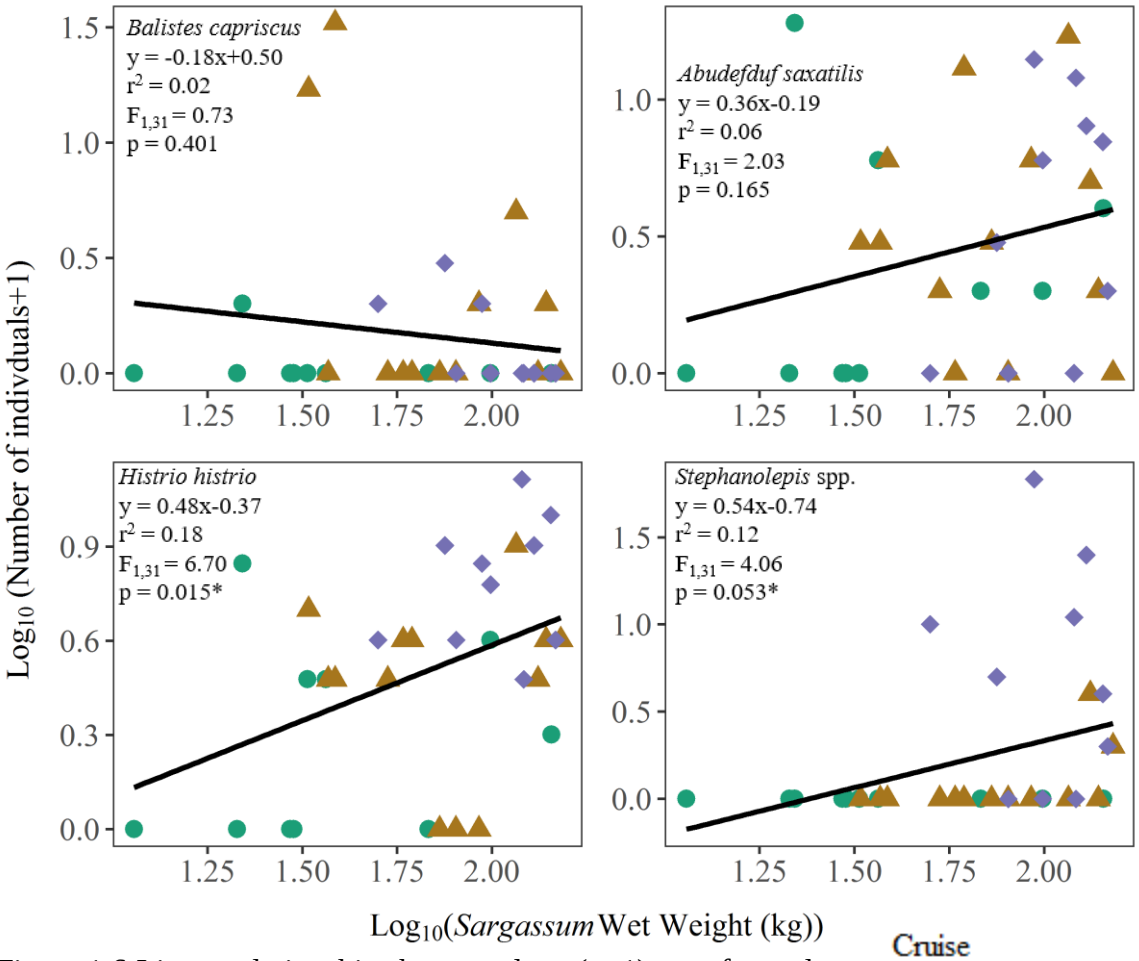


Figure 1.6 Linear relationships between $\log_{10}(x+1)$-transformed estimates of number of individual fish of the most dominant taxa collected in the neuston net and $\log_{10}$-transformed estimates of *Sargassum* wet weight from 2018-2019 cruises. Note the differences in scale of the y-axis values.

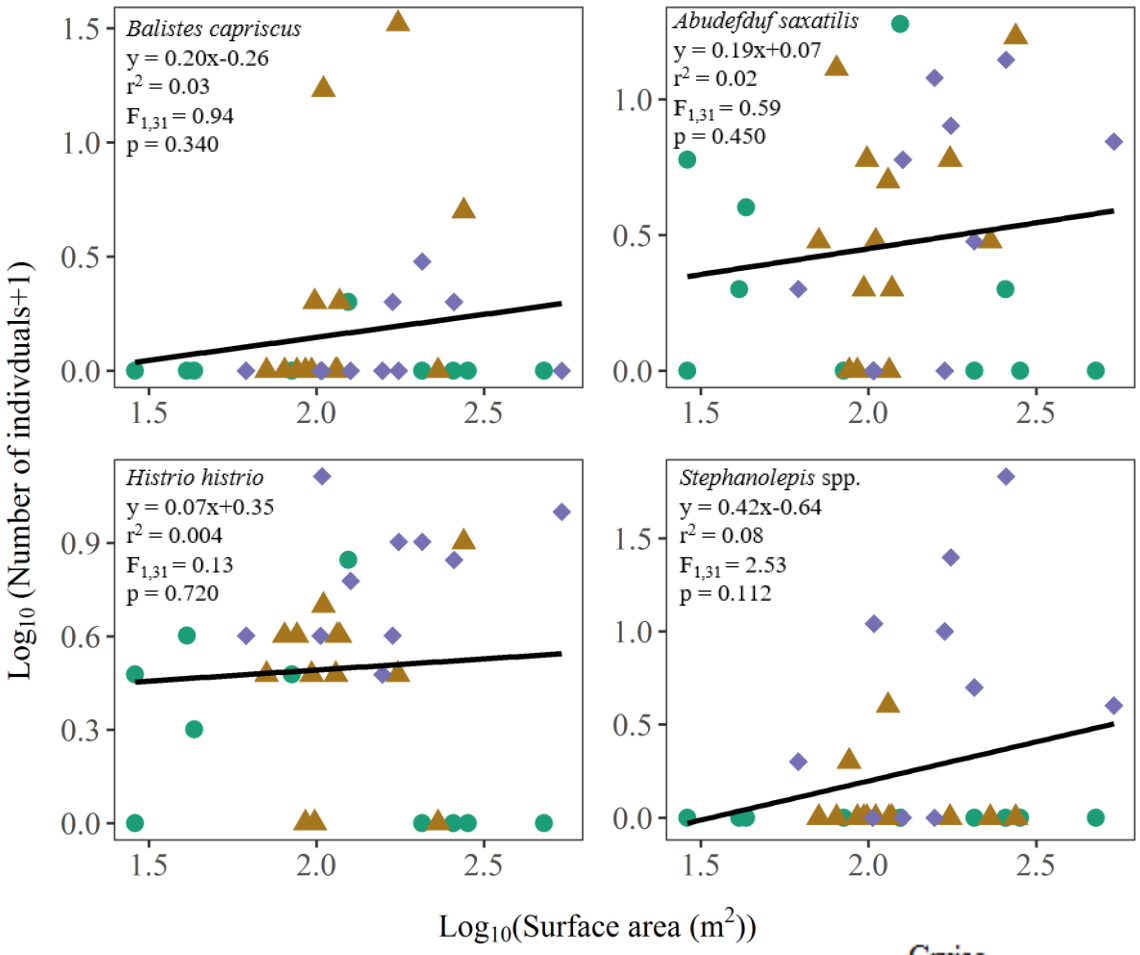


Figure 1.7 Linear relationships between $\log_{10}(x+1)$-transformed estimates of number of individual fish of the most dominant taxa collected in the neuston net and $\log_{10}$-transformed estimates of surface area from 2018-2019 cruises. Note the differences in scale of the y-axis values.

### 1.3.4 Juvenile Fish Abundance

#### 1.3.4.1 Size Distribution

Although sample sizes were generally small for most species, gear size-selectivity was observed during this study, with generally wider size range and larger juvenile fishes collected using H-L sampling relative to neuston net sampling (Figure 1.8). *Caranx crysos* collected using the H-L gear type had a significantly different length distribution (two-sample K-S test, $D = 0.96$, $p < 0.001$) and larger individuals. *C. crysos* in H-L collections ranged from 56.0 – 320.0 mm SL, and those collected in the neuston net ranged from 11.5 – 75.0 mm SL. Sample sizes were smaller for *Caranx ruber*, but the length distributions were still significantly different ($D = 1.00$, $p < 0.001$). The H-L fish ranged between 61.3 – 119.0 mm SL and neuston net fish ranged only between 29.0 – 57.0 mm SL. Both *Seriola* species were more abundant in the H-L collections, and the size frequency distribution differed for each species between gears. *Seriola dumerili* collected using H-L had a significantly larger size frequency distribution than those collected in the neuston net ($D = 0.97$, $p = 0.009$). Individuals collected using H-L ranged from 61.1 – 215.0 mm SL, and those in the neuston net collections ranged from 21.8 – 64.5 mm SL. Similarly, *S. rivoliana* collected using H-L had a significantly larger size frequency distribution than those collected in the neuston net ($D = 0.92$, $p < 0.001$). *Seriola rivoliana* individuals collected using H-L ranged in size from 44.4 – 287.0 mm SL and the individuals collected in the neuston net ranged in size from 15.6 – 120.0 mm SL.

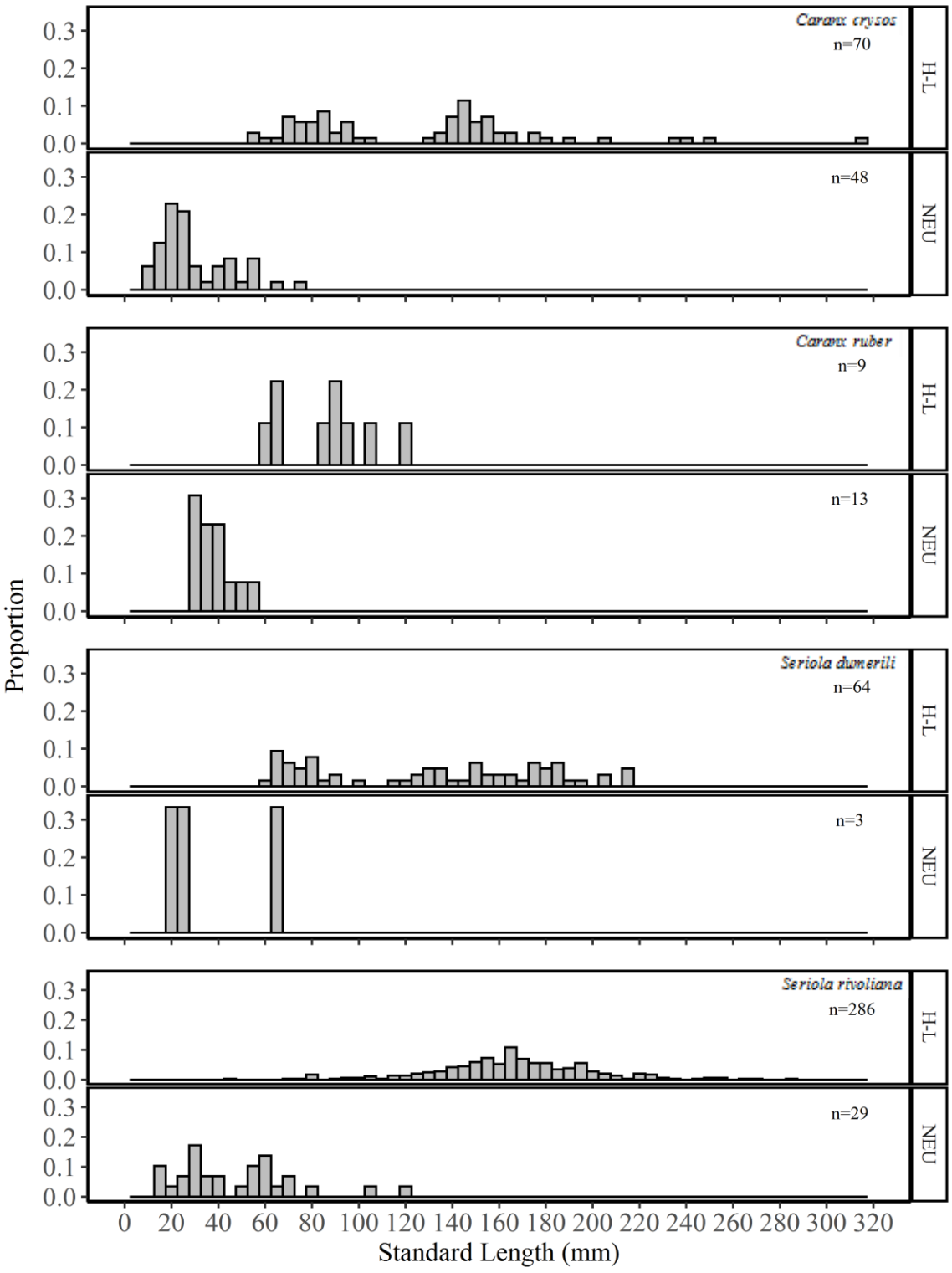


Figure 1.8 Length frequency distributions (standard length) for *Caranx crysos*, *C. ruber*, *Seriola dumerili*, and *S. rivoliana* collected in both hook-and-line (H-L) and neuston net (NEU) samples. Number of individuals of each species collected in each gear denoted by "n" in respective panel. Length frequency distributions were generated using 5 mm size bins.

### 1.3.4.2 Neuston Net Sampling

Standardized (biomass, surface area) fish densities from neuston net collections were not normally distributed (Shapiro-Wilk tests: $p<0.001$), therefore non-parametric tests were used. When standardized by biomass (per 10 kg *Sargassum*), juvenile fish density was found to be higher in July relative to June (Figure 1.9a), although a small effect size was observed ($H = 1.35$, $df = 1$, $p = 0.250$, $\eta_H^2 = 0.009$). Among cruises, juvenile fish density was significantly higher during the July 2017 cruise compared to all other cruises (Figure 1.9b; $H = 15.48$, $df = 3$, $p = 0.001$, $\eta_H^2 = 0.347$). When standardized by surface area sampled (per $m^2$ *Sargassum*), juvenile fish density was not different between months (Figure A.1a; $H = 0.11$, $df = 1$, $p = 0.740$, $\eta_H^2 = -0.029$). Among cruises (excluding July 2017), juvenile fish density also did not differ (Figure A.1b; $H = 2.10$, $df = 2$, $p = 0.350$, $\eta_H^2 = 0.003$).

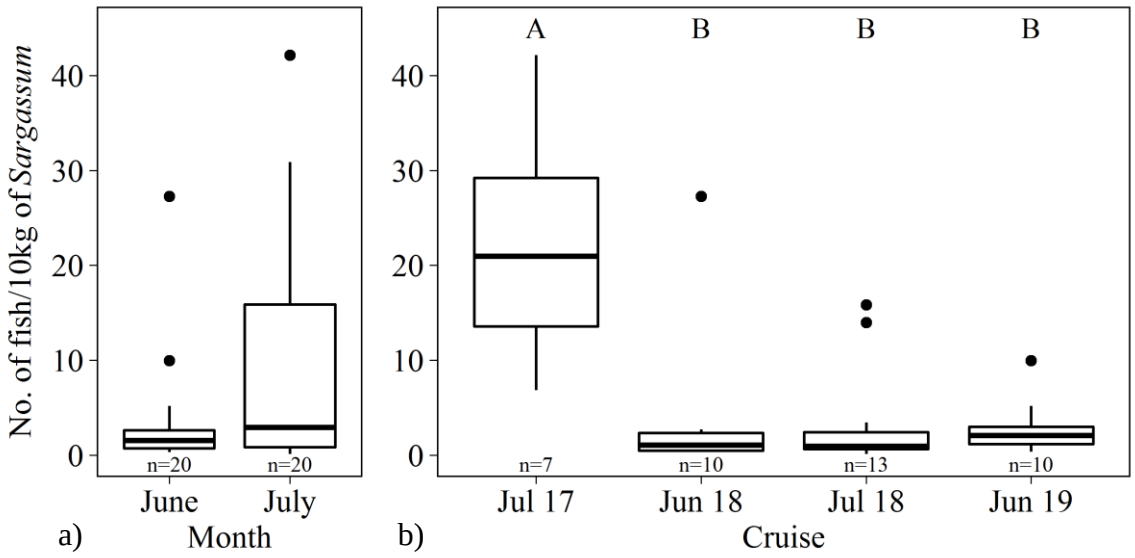


Figure 1.9 Boxplots of number of fish collected in neuston nets per 10 kg of *Sargassum* by a) month, and b) cruise. In boxplots, outside bars represent first and third quartiles and dark bar inside boxes represent median. Sample sizes are presented for each sample group and letters indicate statistical significance among cruises as determined by a Kruskal-Wallis test and Wilcoxon rank sum pairwise test.

Neuston net total fish density, when standardized by biomass (per 10 kg *Sargassum*) was found to be similar whether the sample was collected within the LC/Eddy or Other features (Figure 1.10; H = 2.71, df = 1, p = 0.100, $\eta_H^2$ = 0.045). There were no differences observed with surface feature and fish density standardized by biomass for *B. capriscus* (Figure 1.11a; H = 2.77, df = 1, p = 0.096, $\eta_H^2$ = 0.047), *A. saxatilis* (Figure 1.11b; H = 3.07, df = 1, p = 0.080, $\eta_H^2$ = 0.055), or *Stephanolepis* spp. (Figure 1.11d; H = 0.04, df = 1, p = 0.838, $\eta_H^2$ = -0.025). However, standardized fish density of *H. histrio* was found to be significantly lower in samples collected within the LC/Eddy compared to the Other sampling stations (Figure 1.11c; H = 5.74, df = 1, p = 0.017, $\eta_H^2$ = 0.125).

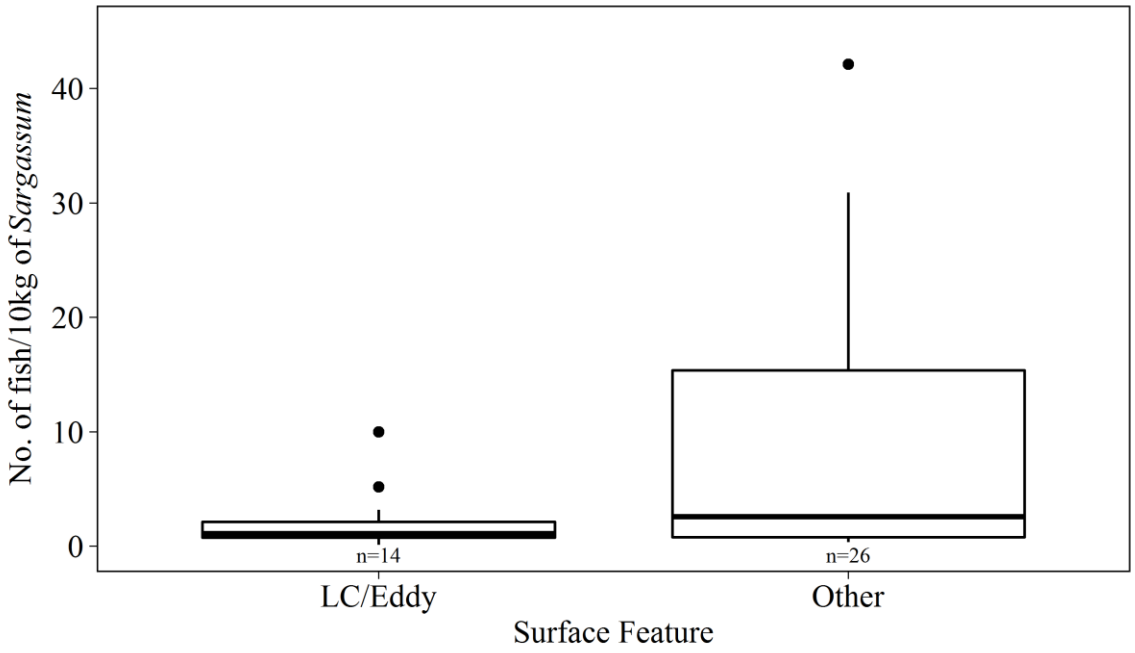


Figure 1.10 Boxplot of total number of fish collected in neuston nets per 10 kg of *Sargassum* by surface feature. In boxplots, outside bars represent first and third quartiles and dark bar inside boxes represent median. Sample sizes are presented for each sample group.

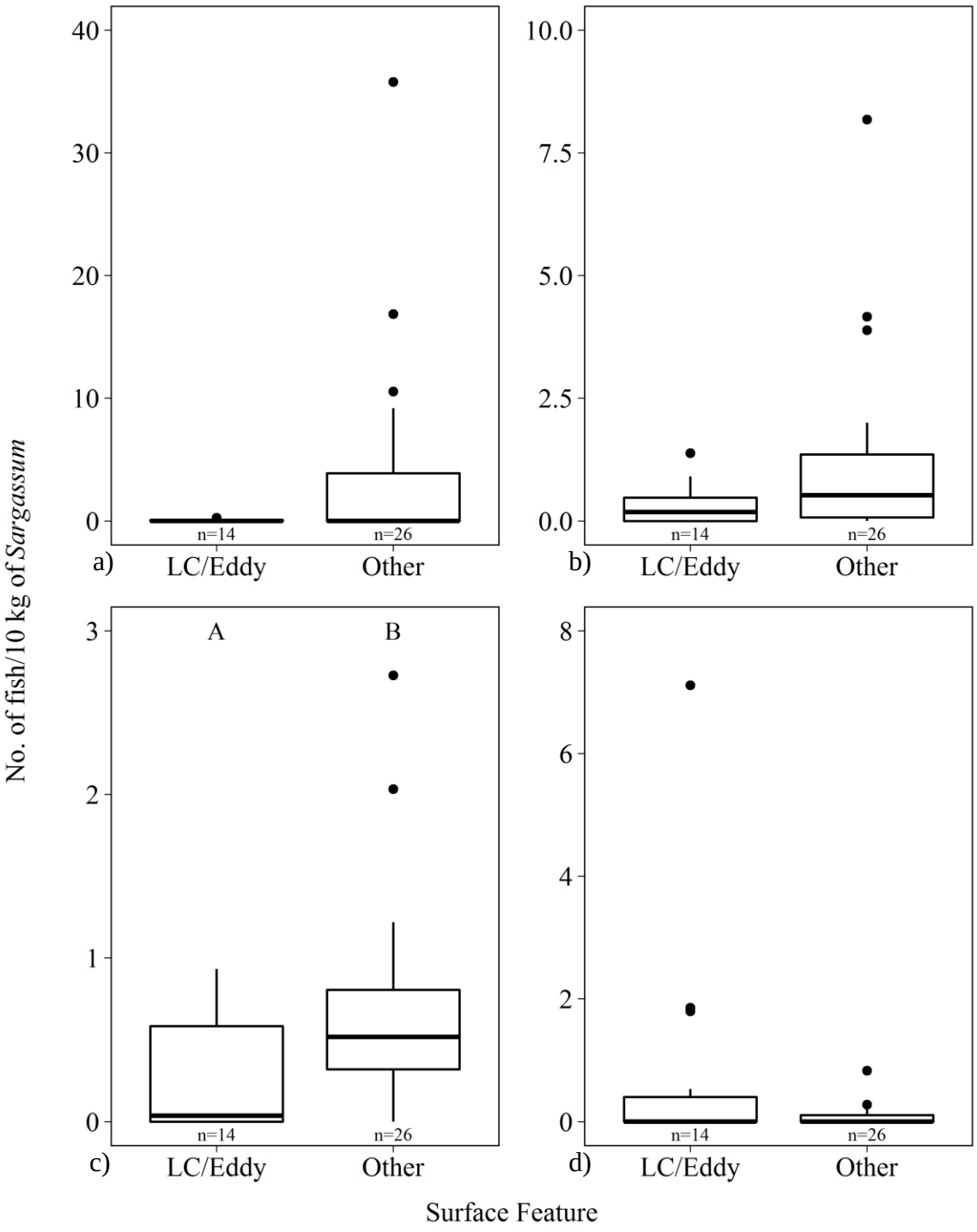


Figure 1.11 Boxplots of number of fish collected in neuston nets per 10 kg of *Sargassum* by surface feature for dominant taxa: a) *Balistes capriscus*, b) *Abudefduf saxatilis*, c) *Histrio histrio*, and d) *Stephanolepis* spp. In boxplots, outside bars represent first and third quartiles and dark bar inside boxes represent median. Sample sizes are presented for each sample group and letters indicate statistical significance among cruises as determined by a Kruskal-Wallis test and Wilcoxon rank sum pairwise test. Note the differences in y-axis values.

When standardized by surface area (fish per $m^2$ *Sargassum*), total fish density was also found to be similar whether associated with either surface feature (Figure A.2; H = 1.28, df = 1, p = 0.259, $\eta_H^2$ = 0.009). No differences were observed between surface feature and fish density standardized by surface area for *B. capriscus* (Figure A.3a; H = 0.02, df = 1, p = 0.889, $\eta_H^2$ = -0.032), *A. saxatilis* (Figure A.3b; H = 0.79, df = 1, p = 0.373, $\eta_H^2$ = -0.007), or *Stephanolepis* spp. (Figure A.3d; H = 0.22, df = 1, p = 0.643, $\eta_H^2$ = -0.025). For *H. histrio*, fish density standardized by surface area was significantly lower within the LC/Eddy features compared to Other stations (Figure A.3c; H = 9.61, df = 1, p = 0.002, $\eta_H^2$ = 0.278).

A stepwise GAM examining the influence of environmental variables on total juvenile fish density (per kg of *Sargassum*) resulted in a best model including salinity and surface chlorophyll (chl) concentration as linear parameters, and depth at chlorophyll max and distance from shelf break as smooth parameters (Table 1.5). Total neuston net fish density was found to increase with increasing salinity, was highest at low and intermediate values of depth at chlorophyll max, and was highest at samples collected about 50 km from the shelf break (Figure 1.12a). This pattern was driven by the relatively high total fish density collected during the July 2017 cruise (Figure A.4).

The best model for standardized juvenile *B. capriscus* density included longitude and distance from shore as linear coefficients, and latitude, water depth, temperature, salinity, and surface chl as smoothed coefficients (Table 1.5). Due to the large number of environmental variables included in the best model for *B. capriscus*, it resulted in a constraint on the smoothing terms. So, the knots were set to three for all cubic regression smoothing parameters in the model to alleviate this constraint. The highest standardized

densities of *B. capriscus*, the most numerically dominant taxon in the neuston net collections, were observed at intermediate values of water depth and surface chl, the two significant predictors in the model (Figure 1.12b). Again, this pattern was driven by the relatively high density of *B. capriscus* collected during the July 2017 cruise (Figure A.5).

The best model for *A. saxatilis* standardized density was determined to have one linear predictor, distance from shore, though a very low correlation value was observed (Table 1.5). A non-significant negative linear relationship was observed between standardized fish density and distance from shore, observed in the distribution of the species with highest density near shore (Figure A.6). Standardized fish density of *H. histrio* was best explained by a model with distance from shelf break as a linear predictor and surface chl as a smoothed parameter (Table 1.5). A significant negative linear relationship was observed with distance from shelf break, and highest densities were observed at low and intermediate values of surface chl (Figure 1.12c). In general, the lowest density of *H. histrio* was observed in *Sargassum* collected furthest offshore, with high densities observed throughout the northern sampling stations (Figure A.7). The best model for *Stephanolepis* spp. standardized density was determined to have salinity as a linear predictor and latitude and distance from shore as smoothed predictors (Table 1.5). A significant positive linear relationship was observed with salinity, and highest densities were generally observed at stations relatively far from shore, though driven by the high densities observed in the June 2019 cruise (Figure 1.12d; Figure A.8).

Table 1.5 Results of GAMs for total and taxon-specific fish density estimates for most abundant taxa based on neuston net collections (fish per kg *Sargassum*). Each model's Akaike's Information Criteria (AIC), deviance explained (DE), $r^2$, and sample size (n) provided above parameter significance values. Parameter (Par.) type given: If linear, a Wald-type 't' statistic value provided, if smooth a Wald-type 'F' statistic value provided. Significance values (p) provided for all statistics. Asterisks indicate statistically significant p-values at alpha-level of 0.05.

| | **Model AIC = 54.4** | **DE = 70.2%** | **$r^2$ = 0.60** | **n = 40** | |
|---|---|---|---|---|---|
| Response Variable | Environmental Variable | Par. type | t | F | p |
| **No. total fish per kg of *Sargassum*** | Salinity | linear | 3.59 | - | 0.001* |
| | Surface chl concentration | linear | 1.45 | - | 0.159 |
| | Depth at chlorophyll max | smooth | - | 2.49 | 0.049* |
| | Distance from shelf break | smooth | - | 5.85 | 0.001* |
| | **Model AIC = -84.7** | **DE = 80.2%** | **$r^2$= 0.74** | **n = 40** | |
| Response Variable | Environmental Variable | Par. type | t | F | p |
| **No. *Balistes capriscus* per kg of *Sargassum*** | Longitude | linear | -0.99 | - | 0.332 |
| | Distance from shore | linear | 1.90 | - | 0.068 |
| | Latitude | smooth | - | 1.86 | 0.208 |
| | Water depth | smooth | - | 3.40 | 0.036* |
| | Temperature | smooth | - | 1.29 | 0.264 |
| | Salinity | smooth | - | 2.87 | 0.168 |
| | Surface chl concentration | smooth | - | 28.81 | <0.001* |
| | **Model AIC = -122.0** | **DE = 7.8%** | **$r^2$= 0.05** | **n = 40** | |
| Response Variable | Environmental Variable | Par. type | t | F | p |
| **No. *Abudefduf saxatilis* per kg of *Sargassum*** | Distance from shore | linear | -1.80 | - | 0.080 |
| | **Model AIC = -203.4** | **DE = 46.5%** | **$r^2$= 0.38** | **n = 40** | |
| Response Variable | Environmental Variable | Par. type | t | F | p |
| **No. *Histrio histrio* per kg of *Sargassum*** | Distance from shelf break | linear | -3.65 | - | 0.001* |
| | Surface chl concentration | smooth | - | 2.64 | 0.040* |
| | **Model AIC = -257.1** | **DE = 97.7%** | **$r^2$= 0.96** | **n = 40** | |
| Response Variable | Environmental Variable | Par. type | t | F | p |
| **No. *Stephanolepis* spp. per kg of *Sargassum*** | Salinity | linear | 6.48 | - | <0.001* |
| | Latitude | smooth | - | 41.53 | <0.001* |
| | Distance from shore | smooth | - | 76.62 | <0.001* |

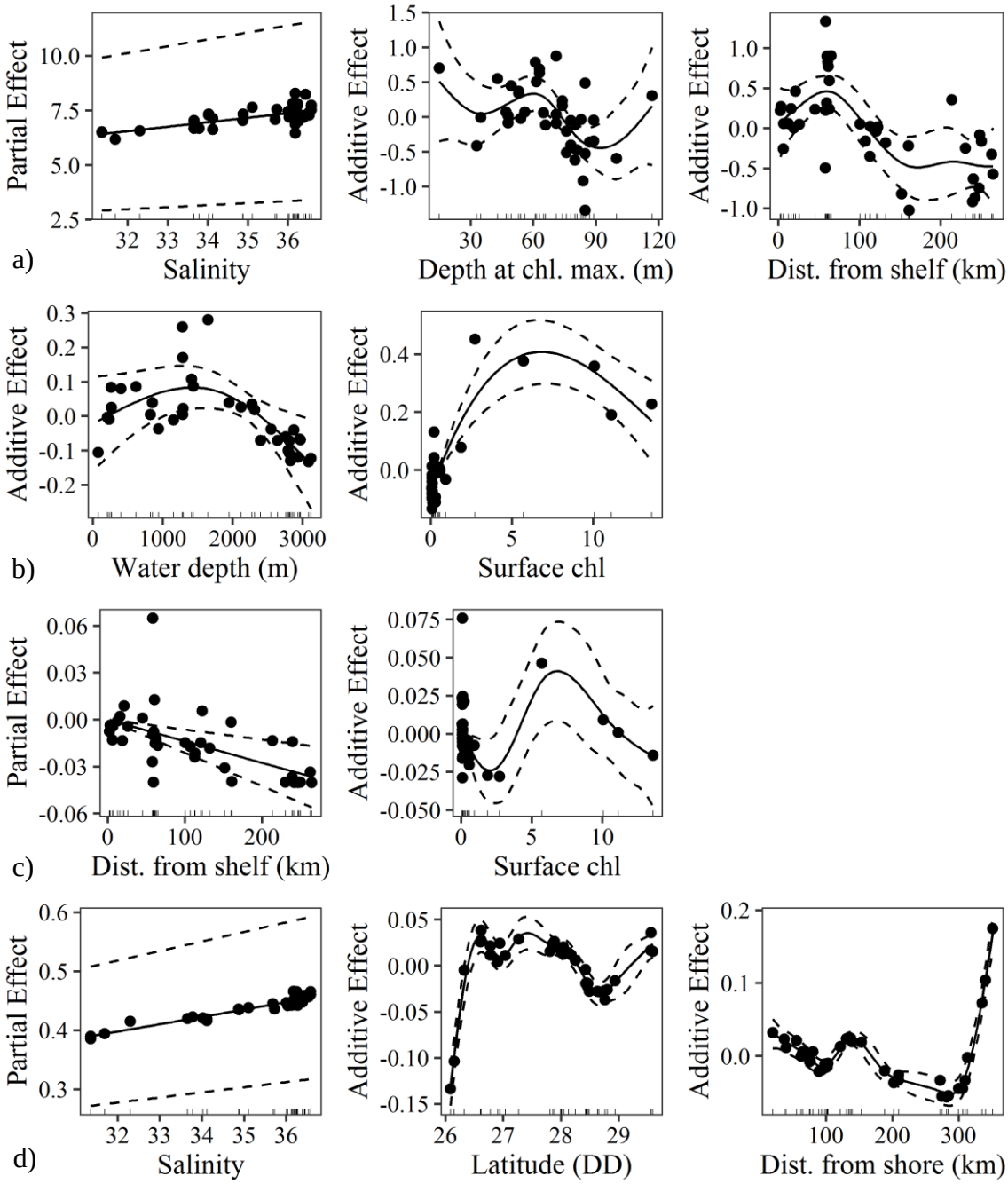


Figure 1.12 Plots of $\log_{10}(x)$-transformed estimates of a) total number of fish per kg *Sargassum*, and $\log_{10}(x+1)$-transformed estimates of number of b) *Balistes capriscus* c) *Histrio histrio* d) *Stephanolepis* spp. per kg *Sargassum* as a response to significant environmental variables in GAMs with the lowest AIC. Solid lines represent linear or smoothed estimates and dashed lines represent 95% confidence intervals. Y-axes represent partial effects for linear variables and additive effects for smoothed variables.

A stepwise GAM (excluding the July 2017 cruise) examining the influence of environmental variables on total juvenile fish density (per $m^2$ *Sargassum* surface area) resulted in a best model including water depth and distance from shore as non-significant linear predictors, and temperature as a significant smoothed predictor (Table A.1). Fish density was highest at end members of the observed range of temperatures, and lowest at about 29°C (Figures A.9 and A.10).

**1.3.4.3 Hook-and-Line Sampling**

Juvenile fish CPUE estimated from H-L sampling were not normally distributed (Shapiro-Wilk test: $p<0.001$), therefore non-parametric tests were used. For all species combined, CPUE did not differ between months (Figure 1.13a; $H = 0.28$, $df = 1$, $p = 0.598$, $\eta_H^2 = -0.034$). Juvenile fish CPUE was relatively higher during the July 2018 and June 2019 cruises compared to the July 2017 and June 2018 cruises, however effect size was small, with one notable outlier during the July 2017 cruise (Figure 1.13b; $H = 2.11$, $df = 3$, $p = 0.550$, $\eta_H^2 = -0.047$). There was no differences found between CPUE estimates for samples collected within or outside of surface features (Figure 1.14; $H = 1.00$, $df = 1$, $p = 0.317$, $\eta_H^2 < 0.001$).

Hook-and-line CPUE was analyzed using GAMs for total estimates and the most abundant taxa collected, with knots set to three for smoothing parameters in the dominant taxa models to alleviate constraints. The best model to describe total H-L CPUE had temperature and distance from shelf break as linear parameters, and depth at chlorophyll max and distance from shore as smoothed parameters (Table 1.6). There was a significant negative relationship with distance from shelf break for H-L collections (Figure 1.15a). Fish CPUE peaked at about 80m chlorophyll max depth, and was highest at further from

shore sampling stations. Total CPUE was generally highest in lower latitude sampling stations, except for some samples collected near the continental shelf in the June 2019 cruise yielding higher CPUE off the Florida continental shelf and near the Louisiana Birdfoot Delta (Figure A.11).

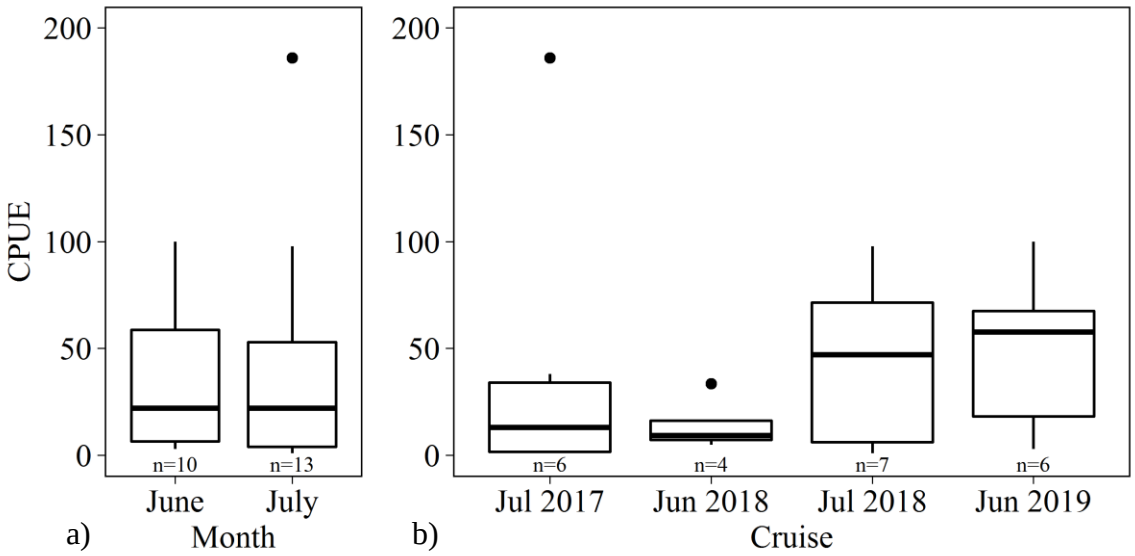


Figure 1.13 Boxplots of number of fish collected per 30 minute fishing period during hook-and-line sampling by a) month, and b) cruise. In boxplots, outside bars represent first and third quartiles and dark bar inside boxes represent median. Sample sizes are presented for each sample group.

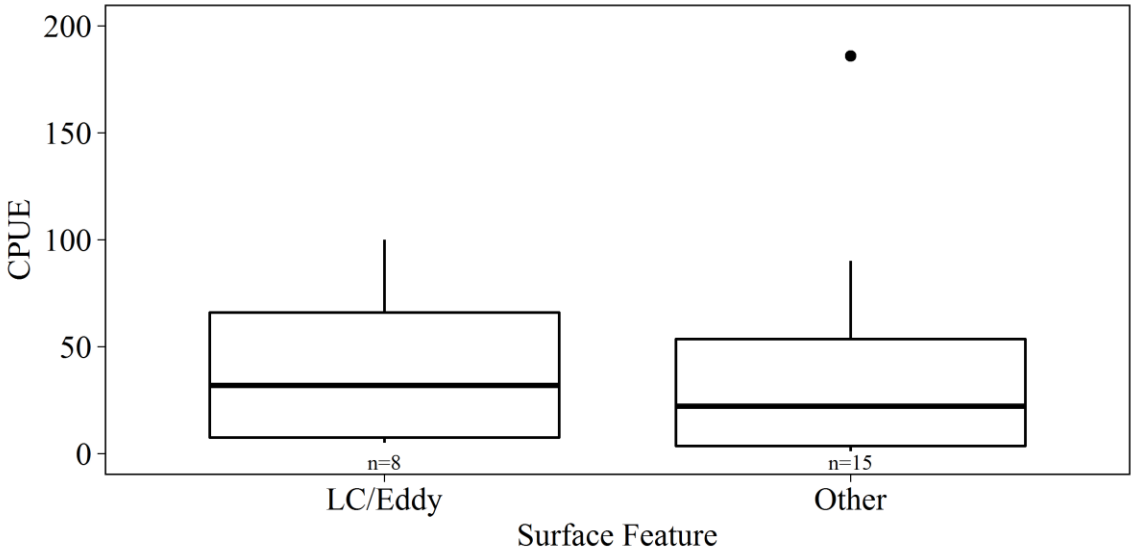


Figure 1.14 Boxplot of number of fish collected per 30 minute fishing period during hook-and-line sampling by surface feature. In boxplots, outside bars represent first and third quartiles and dark bar inside boxes represent median. Sample sizes are presented for each sample group.

The CPUE of the most dominant species, *S. rivoliana*, was found to have eight parameters in the best model, all as smoothing predictors except for longitude, salinity, and depth at chlorophyll max (Table 1.6). A significant negative linear relationship was found between CPUE and longitude, and the highest CPUE of this species was observed at higher latitudes and further distances from shore (Figure 1.15b; Figure A.12). *Caranx crysos* CPUE was found to have a model with seven parameters, all as smoothers excluding latitude, longitude, and salinity (Table 1.6). No predictors were found to be significant in the model and a low $r^2$ value was observed, but the highest CPUE were observed closer to shore and at eastern sampling stations (Figure A.13). CPUE of *S. dumerili* was found to be best described with a model of seven predictors, all as smoothers except for longitude and water depth (Table 1.6). A significant negative linear relationship was observed between CPUE of this species and longitude (Figure 1.15c). Highest CPUEs were observed at mid-latitudes of the sampling area, lower temperatures, further distances from shore, and low surface chlorophyll concentrations (Figure 1.15c; Figure A.14).

Table 1.6 Results of GAMs for total and taxon-specific CPUE estimates for most abundant taxa based on hook-and-line collections (fish per 30 min.). Each model's Akaike's Information Criteria (AIC), deviance explained (DE), $r^2$, and sample size (n) provided above parameter significance values. Parameter (Par.) type given If linear, a Wald-type 't' statistic value provided, if smooth a Wald-type 'F' statistic value provided. Significance values (p) provided for all statistics. Asterisks indicate significant p-values at alpha-level 0.05.

| | **Model AIC = 17.4** | **DE = 91.6%** | **$r^2$ = 0.83** | | **n = 23** |
|---|---|---|---|---|---|
| Response Variable | Environmental Variable | Par. type | t | F | p |
| **No. total fish per 30 min.** | Temperature | linear | -1.58 | - | 0.143 |
| | Distance from shelf break | linear | -4.34 | - | 0.001* |
| | Depth at chlorophyll max | smooth | - | 5.20 | 0.009* |
| | Distance from shore | smooth | - | 9.08 | 0.001* |
| | **Model AIC = 33.3** | **DE = 80.1%** | **$r^2$= 0.63** | | **n = 23** |
| Response Variable | Environmental Variable | Par. type | t | F | p |
| **No. *Seriola rivoliana* per 30 min.** | Longitude | linear | -3.25 | - | 0.007* |
| | Salinity | linear | 1.52 | - | 0.155 |
| | Depth at chlorophyll max | linear | 1.83 | - | 0.093 |
| | Latitude | smooth | - | 10.22 | 0.007* |
| | Temperature | smooth | - | 1.42 | 0.291 |
| | Distance from shore | smooth | - | 5.52 | 0.016* |
| | Distance from shelf break | smooth | - | 0.20 | 0.666 |
| | Surface chl concentration | smooth | - | 2.35 | 0.153 |
| | **Model AIC = 46.0** | **DE = 46.9%** | **$r^2$= 0.19** | | **n = 23** |
| Response Variable | Environmental Variable | Par. type | t | F | p |
| **No. *Caranx crysos* per 30 min.** | Latitude | linear | -1.67 | - | 0.117 |
| | Longitude | linear | 1.85 | - | 0.086 |
| | Salinity | linear | 0.51 | - | 0.618 |
| | Temperature | smooth | - | 2.92 | 0.155 |
| | Distance from shore | smooth | - | 0.72 | 0.411 |
| | Distance from shelf break | smooth | - | 0.19 | 0.671 |
| | Surface chl concentration | smooth | - | 0.40 | 0.535 |
| | **Model AIC = 3.3** | **DE = 85.5%** | **$r^2$= 0.72** | | **n = 23** |
| Response Variable | Environmental Variable | Par. type | t | F | p |
| **No. *Seriola dumerili* per 30 min.** | Longitude | linear | -3.13 | - | 0.009* |
| | Water depth | linear | -1.37 | - | 0.196 |
| | Latitude | smooth | - | 7.56 | 0.009* |
| | Temperature | smooth | - | 9.97 | 0.008* |
| | Depth at chlorophyll max | smooth | - | 2.01 | 0.163 |
| | Distance from shore | smooth | - | 10.48 | 0.002* |
| | Surface chl concentration | smooth | - | 7.08 | 0.011* |

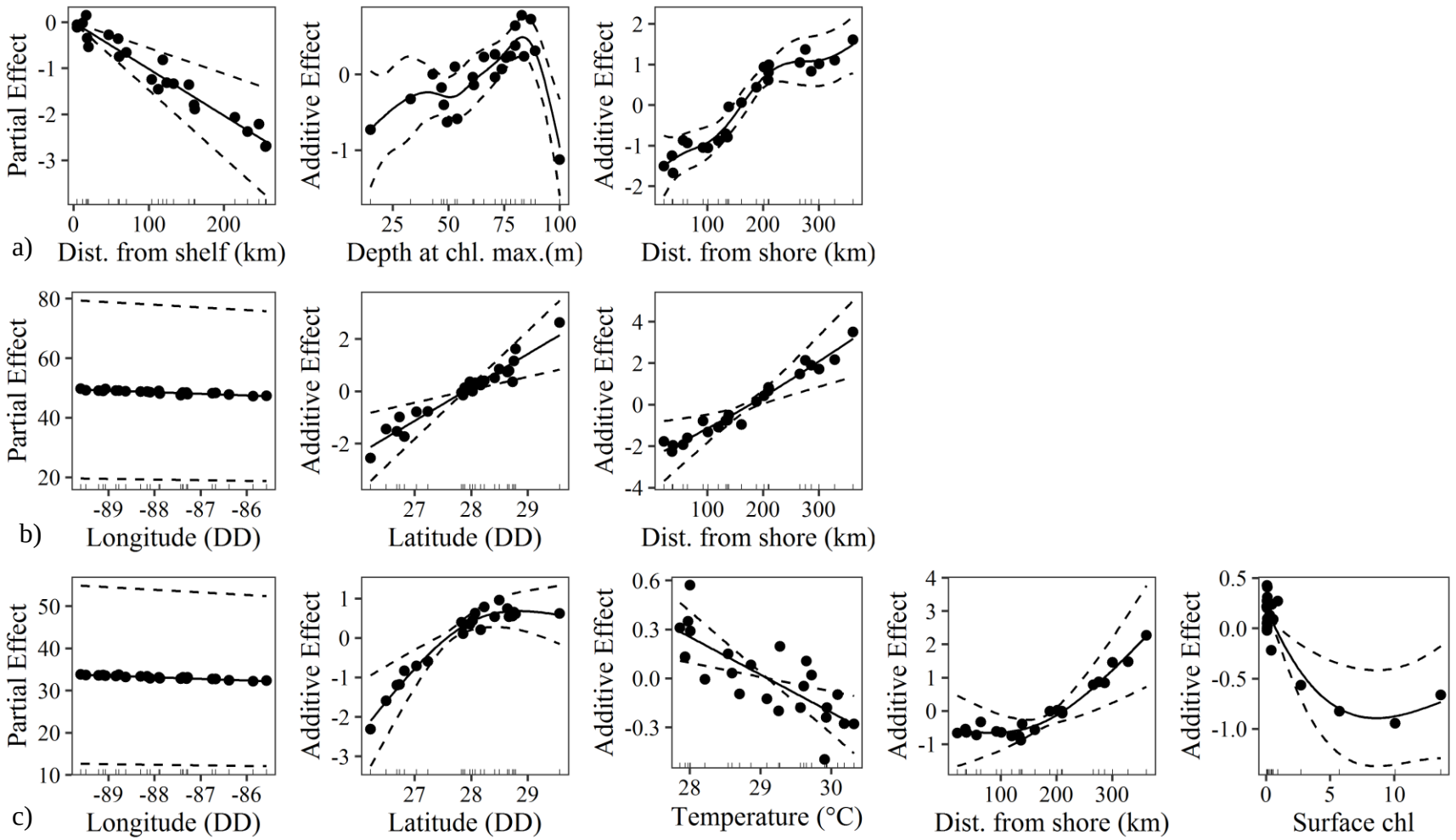


Figure 1.15 Plots of $\log_{10}(x)$-transformed estimates of a) CPUE and $\log_{10}(x+1)$-transformed estimates of b) *Seriola rivoliana* and c) *Seriola dumerili* CPUE as a response to significant environmental variables in GAMs with lowest AIC. Solid lines represent linear or smoothed estimates and dashed lines represent 95% confidence intervals. Y-axes represent partial effects for linear variables and additive effects for smoothed variables.

### 1.3.5 Juvenile Fish Diversity

Shannon diversity (H') based on fishes collected in the neuston net was found to have a normal distribution (Shapiro-Wilk test: $p = 0.444$) and homogeneity of variance with cruise and month as factors (Levene test: $p > 0.300$), so parametric pairwise tests were used. Taxonomic richness (S) and Pielou's evenness (J') in neuston net samples were not normally distributed (Shapiro-Wilk test: $p < 0.01$), however, and non-parametric pairwise tests were used to determine significance. Estimates of H', S, and J' based on neuston net collections were largely similar between months and among cruises (Figure 1.16). Shannon diversity was not found to be different between cruises, with the lowest diversity observed in June 2018 ($F_{3,35} = 1.08$, $p = 0.372$, $\eta^2 = 0.084$), and H' was slightly higher in July, with a small effect size observed ($F_{1,37} = 0.09$, $p = 0.764$, $\eta^2 = 0.002$). Taxonomic richness was found to be significantly different between cruises ($H = 13.01$, $df = 3$, $p = 0.005$, $\eta_H^2 = 0.286$), and larger estimates of S were observed in July with a small effect size ($H = 1.66$, $p = 0.198$, $df = 1$, $\eta_H^2 = 0.018$). Pielou's evenness was found to be significantly lower in the July 2017 cruise compared to all other cruises ($H = 14.98$, $df = 3$, $p = 0.002$, $\eta_H^2 = 0.342$). This resulted in a slightly lower J' observed in July compared to June, though not significantly different and a small effect size was found ($H = 2.40$, $df = 1$, $p = 0.121$, $\eta_H^2 = 0.038$).

Shannon diversity (H') and taxonomic richness (S) based on H-L samples were both found to have a normal distribution (Shapiro-Wilk test: $p > 0.060$) and homogeneity of variance with cruise and month as factors (Levene test: $p > 0.200$), so parametric tests were used for H' and S. Pielou's evenness (J') was not normally distributed (Shapiro-Wilk test: $p = 0.029$), and non-parametric tests were used to determine statistical

significance. Estimates of H', S, and J' based on H-L sampling were not found to have any significant differences among cruise or month (Figure 1.17). Shannon diversity was highest in the June 2018 cruise with a large effect size ($F_{3,19}$ = 1.26, p = 0.317, $\eta^2$ = 0.166). A higher maximum H' was observed in June samples (1.52) compared to July (1.07), but mean H' was similar ($F_{1,21}$ = 0.88, p = 0.358, $\eta^2$ = 0.040). Taxonomic richness was not significantly different among cruises, but was the lowest in July 2018 ($F_{3,19}$ = 0.40, p = 0.752, $\eta^2$ = 0.060). There was also no statistical difference in S by month, with lower values observed in July ($F_{1,21}$ = 0.07, p = 0.791, $\eta^2$ = 0.003). Pielou's evenness was also not different by cruise but the lowest value was observed in June 2019 (H = 1.61, df = 3, p = 0.656, $\eta_H^2$ = -0.073). Month also had a small to no effect on J' estimates, and mean values were very similar (H = 0.24, df = 1, p = 0.624, $\eta_H^2$ = -0.036).

Patterns in the estimates of H' based on neuston net collections were best explained by water depth, distance from shore, and distance from shelf break as linear predictors, and temperature, salinity, and depth at chlorophyll max as smoothed predictors (Table 1.7). Patterns in the estimates of H' based on hook-and-line sampling were best explained by a model with eight parameters (Table 1.7). Significant relationships were observed with salinity and surface chlorophyll concentration, with highest H' observed at higher salinities (about 36 psu) and both low (about 0.1 mg/$m^3$) and high (about 13 mg/$m^3$) values of surface chlorophyll (Figure 1.18).

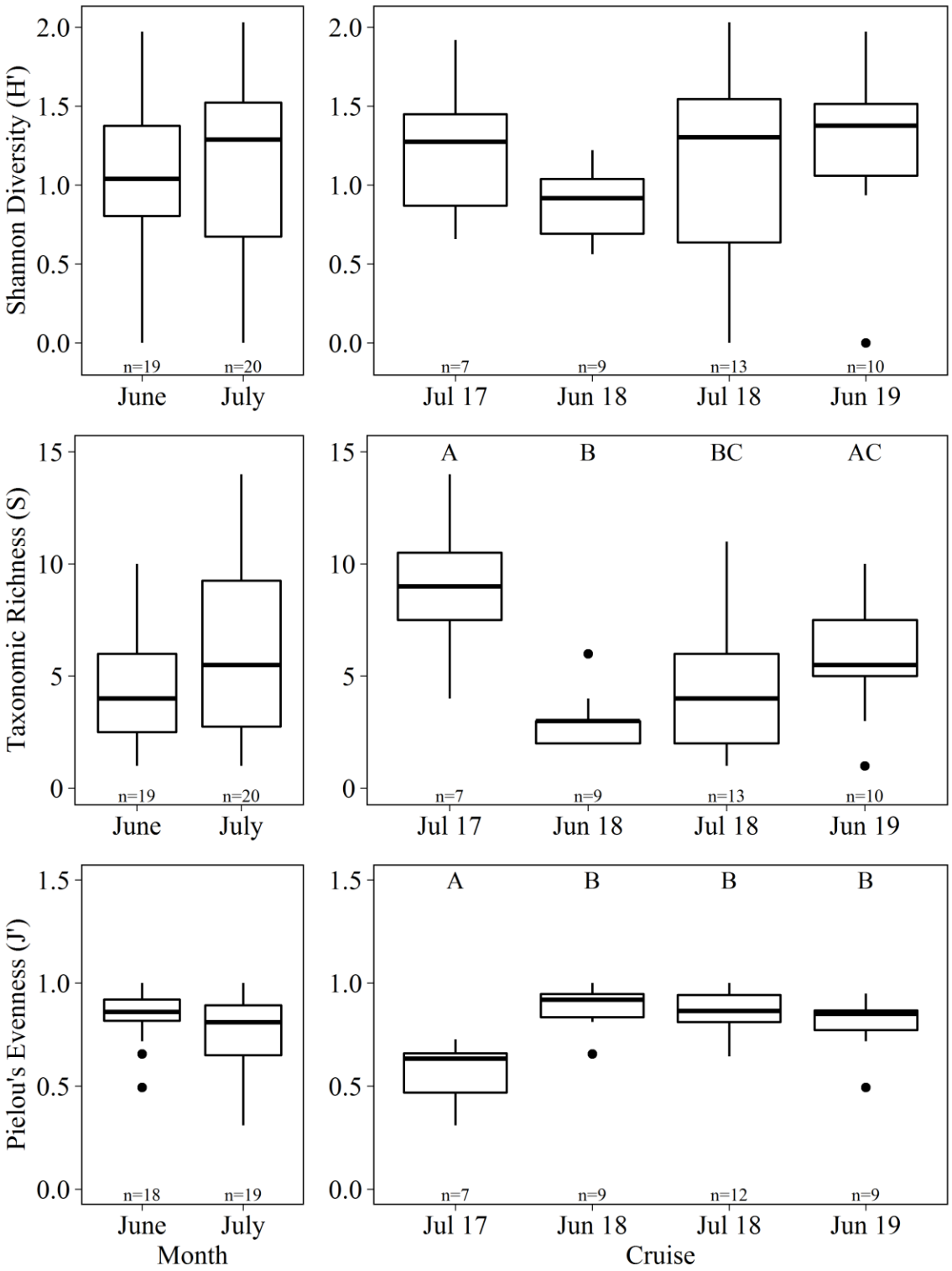


Figure 1.16 Boxplots of diversity indices derived from neuston net samples by month and cruise. In boxplots, outside bars represent first and third quartiles and dark bar inside boxes represent median. Letters indicate significant difference as determined by Kruskal-Wallis test and sample sizes are presented for each sample group.

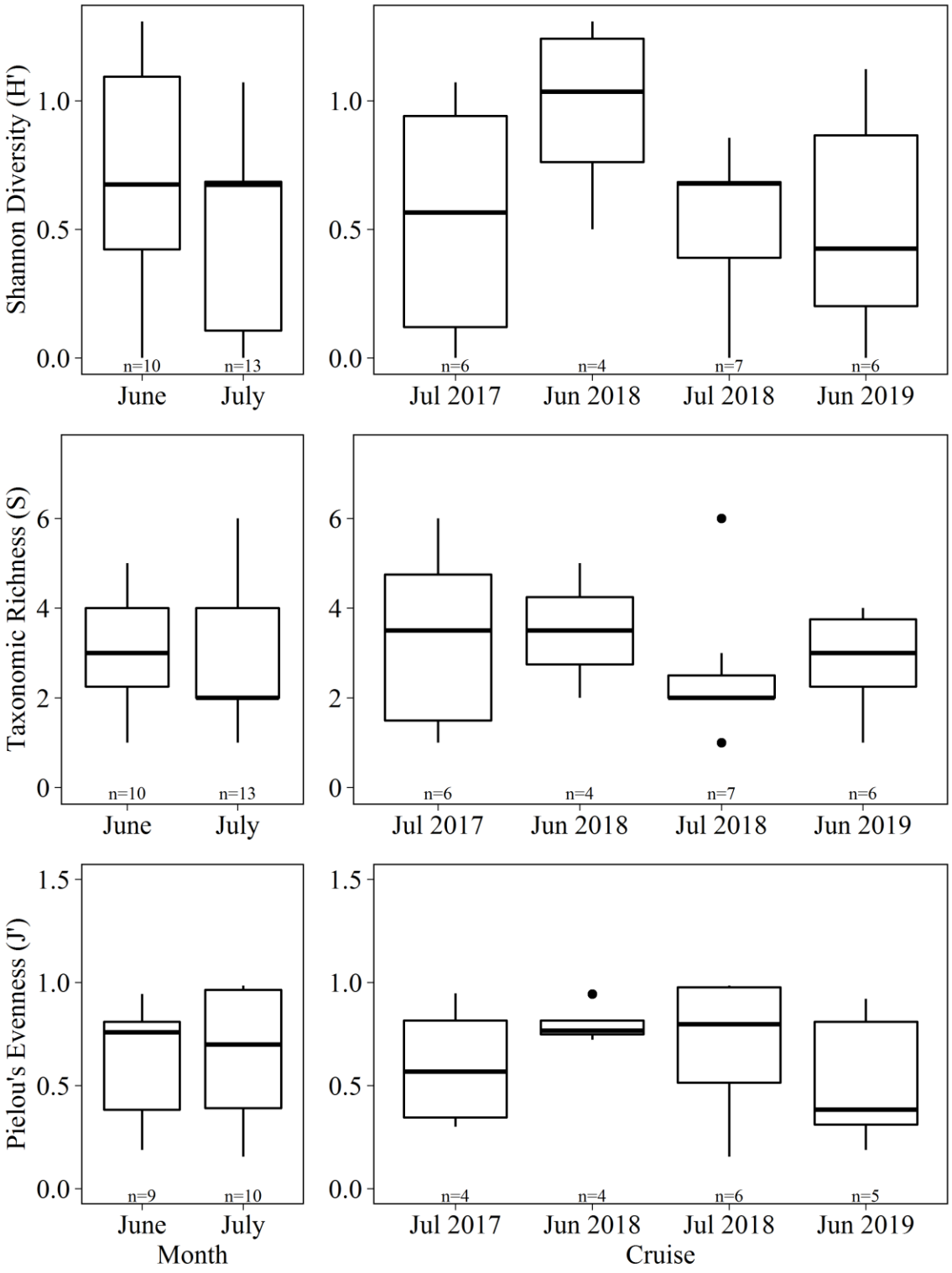


Figure 1.17 Boxplots of diversity indices derived from hook-and-line samples by month and cruise. In boxplots, outside bars represent first and third quartiles and dark bar inside boxes represent median. Sample sizes are presented for each sample group.

Table 1.7 Results of GAMs Shannon diversity estimates based on neuston net and hook-and-line sampling. Each model's Akaike's Information Criteria (AIC), deviance explained (DE), $r^2$, and sample size (n) provided above parameter significance values. Parameter (Par.) type given If linear, a Wald-type 't' statistic value provided, if smooth a Wald-type 'F' statistic value provided. Significance values (p) provided for all statistics. Asterisks indicate significant p-values at an alpha-level of 0.05.

| | **Model AIC = 45.0** | **DE = 69.4%** | **$r^2$= 0.48** | | **n = 39** |
|---|---|---|---|---|---|
| Response Variable | Environmental Variable | Par. type | t | F | p |
| **Shannon diversity Neuston net sampling** | | | | | |
| | Water depth | linear | -1.03 | - | 0.315 |
| | Distance from shore | linear | -1.72 | - | 0.100 |
| | Distance from shelf break | linear | 1.58 | - | 0.127 |
| | Temperature | smooth | - | 1.92 | 0.115 |
| | Salinity | smooth | - | 1.60 | 0.232 |
| | Depth at chlorophyll max | smooth | - | 2.03 | 0.103 |
| | **Model AIC = 25.2** | **DE = 67.1%** | **$r^2$= 0.33** | | **n = 23** |
| Response Variable | Environmental Variable | Par. type | t | F | p |
| **Shannon diversity Hook-and-line sampling** | | | | | |
| | Latitude | linear | 1.99 | - | 0.073 |
| | Depth at chlorophyll max | linear | -0.41 | - | 0.690 |
| | Distance from shelf break | linear | 1.29 | - | 0.224 |
| | Water depth | smooth | - | 3.10 | 0.086 |
| | Temperature | smooth | - | 1.28 | 0.427 |
| | Salinity | smooth | - | 6.41 | 0.028* |
| | Distance from shore | smooth | - | 2.51 | 0.124 |
| | Surface chl concentration | smooth | - | 5.43 | 0.024* |

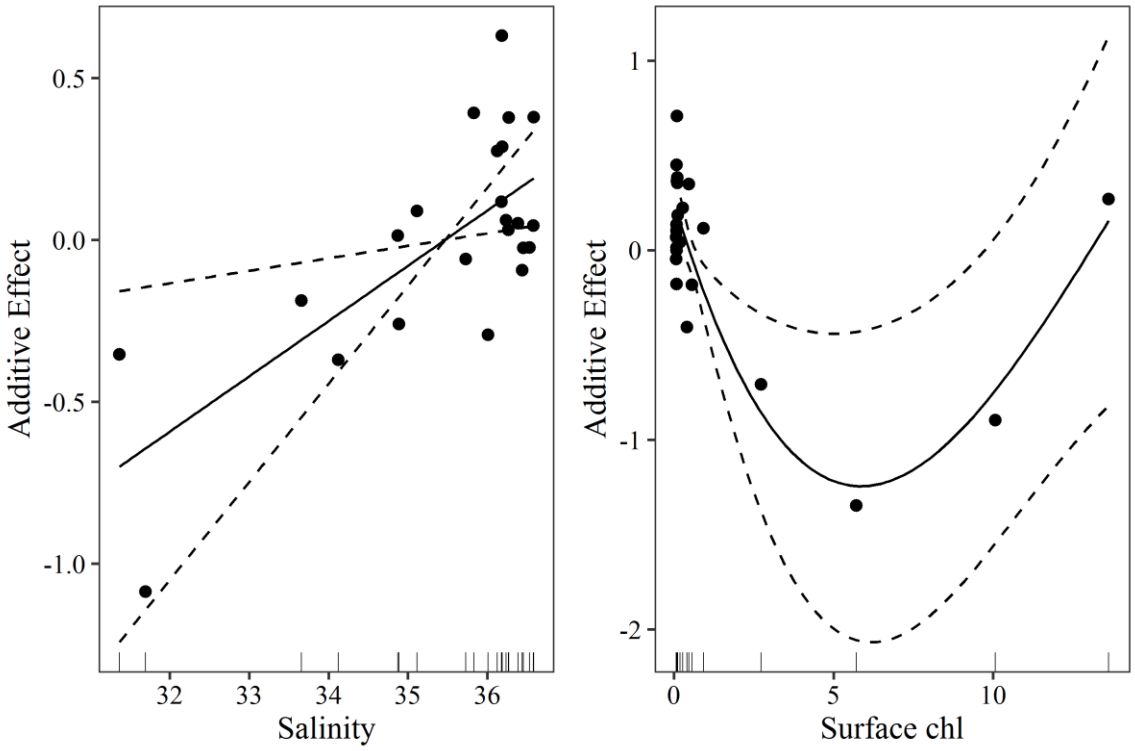


Figure 1.18 Plots of raw estimates of Shannon diversity in hook-and-line samples as a response to significant environmental variables in GAM with lowest AIC. Solid lines represent smoothed estimates and dashed lines represent 95% confidence intervals. Y-axis represents additive effects of smoothed variables on the response variable.

### 1.3.6 Juvenile Fish Assemblage Structure

The community assemblage based on neuston net sampling was found to have a high degree of overlap when grouped by cruise (Figure 1.19; 2D stress = 0.16, ANOSIM R = 0.17, p = 0.001). There was some separation in the assemblages between the July 2017 and June 2019 cruises, with Gray Triggerfish driving the differences in the former where that species was highly abundant (Table A.2). The juvenile fish assemblage collected using H-L sampling also had a high degree of overlap by cruise (Figure 1.20; 2D stress = 0.13, ANOSIM R = 0.11, p = 0.07).

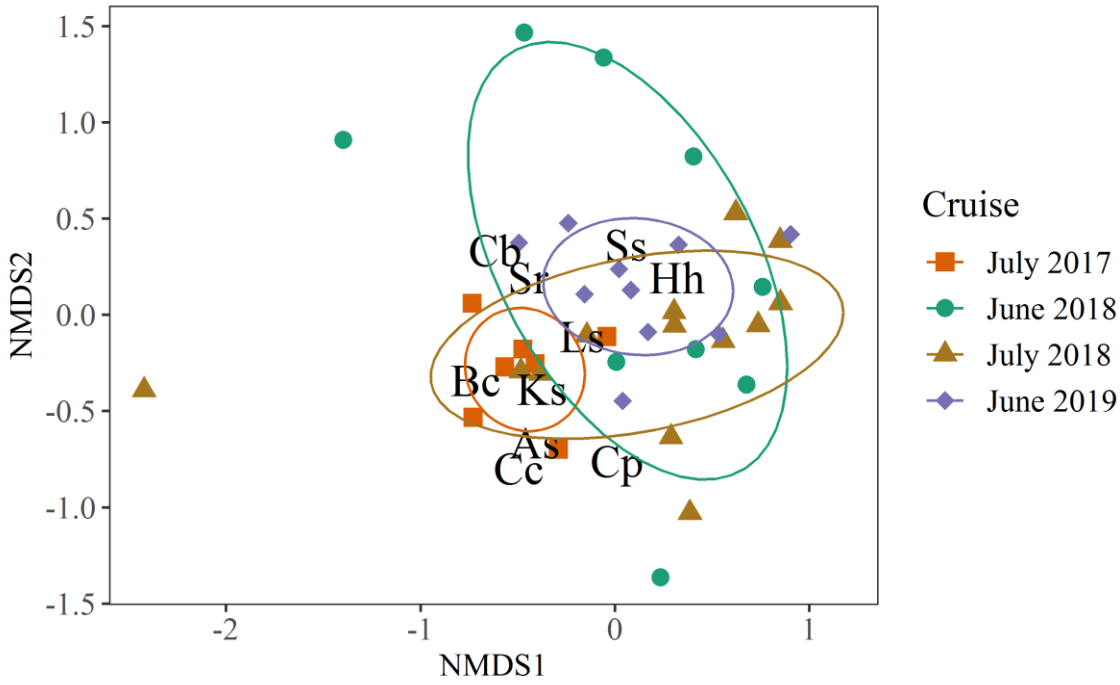


Figure 1.19 NMDS plot of community assemblage based on neuston net sampling coded by cruise. Ellipses denote 50% confidence intervals of each cruise and letters indicate which species are driving differences as determined by a SIMPER analysis. As – *Aluterus* spp., Bc – *Balistes capriscus*, Cb – *Carangoides bartholomaei*, Cc – *Caranx crysos*, Cp – *Cantherhines pullus*, Hh – *Histrio histrio*, Ks – *Kyphosus* spp., Ls – *Lobotes surinamensis*, Sr – *Seriola rivoliana*, Ss – *Stephanolepis* spp.

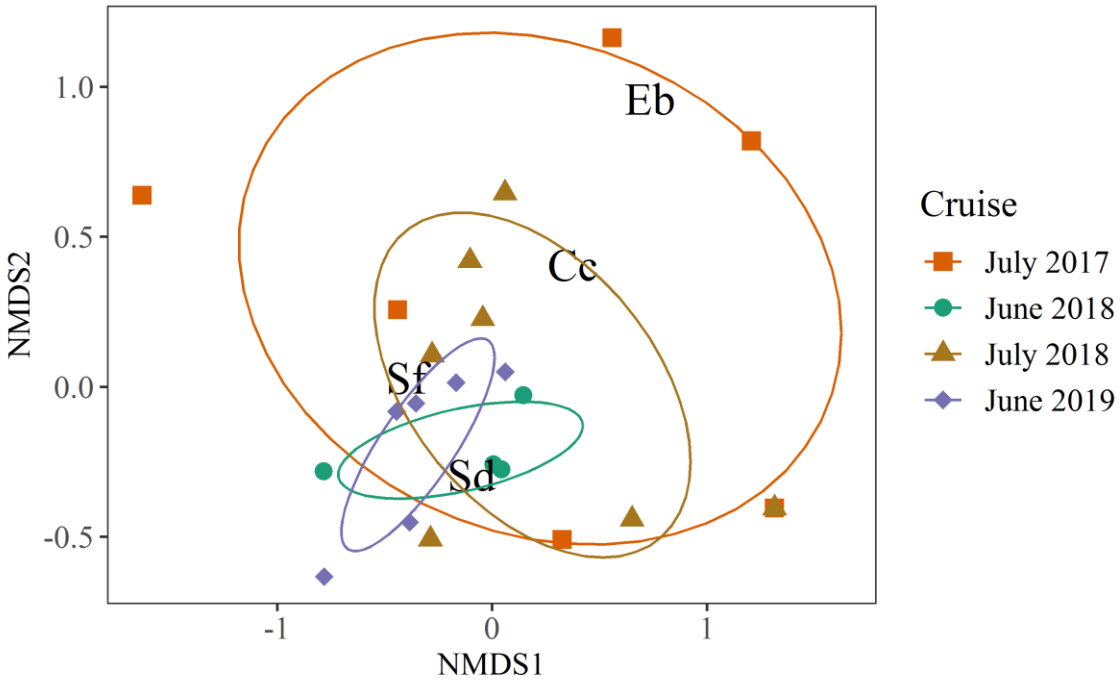


Figure 1.20 NMDS plot of community assemblage based on hook-and-line sampling coded by cruise. Ellipses denote 50% confidence intervals of each cruise and letters indicate which species are driving differences as determined by a SIMPER analysis. Cc – *Caranx crysos*, Eb – *Elagatis bipinnulata*, Sd – *Seriola dumerili*, Sf – *Seriola fasciata*.

The results of the BIOENV analysis determined the best model to describe the assemblage derived from neuston net sampling included only distance from shore, though a low and non-significant correlation was observed (Spearman's $\rho = 0.20$, $p = 0.994$). As determined by a separate BIOENV analysis, the best model for describing the assemblage derived from H-L sampling was determined to include only surface chlorophyll concentration (Spearman's $\rho = 0.38$, $p = 0.429$).

**1.4 Discussion**

In my study, 2,086 total fish were collected using hook-and-line and neuston net sampling methods. Comparisons to previous studies is difficult, as multi-gear approaches are commonly used. For neuston net samples, using *Sargassum* biomass to standardize fish abundances has been the most common method, and positive linear relationships have been observed between numbers of fish and biomass (Casazza and Ross 2008; Kramer 2014). However, I did not observe this linear relationship. Likewise, my attempt to standardize total fish abundances by surface area sampled resulted in relatively weak relationships. At the level of individual taxa, *H. histrio* (Sargassumfish) and *Stephanolepis* spp. (filefish) had significant positive linear relationships with *Sargassum* biomass but not with surface area. There may be several reasons why relationships between fish abundance and *Sargassum* biomass or surface area were highly variable, and not predictable. First, the variability may be related to how fish use the habitat, which may vary by species, ontogeny, or space. The "thickness" or how dense *Sargassum* is aggregated varies, and may be influential in species' use of *Sargassum*. For example, Sargassumfish are ambush predators living "within" the *Sargassum* fronds; these fish display more sedentary behaviors to capture prey (Pietsch and Grobecker 1990) and thus

the biomass of *Sargassum* may be relatively important for foraging. A positive correlation (r = 0.31) between Sargassumfish and *Sargassum* biomass was also observed in purse seine sampling in the Atlantic Ocean (Dooley 1972). The biomass of *Sargassum* may also be important for filefish, which have been observed within or in very close proximity to *Sargassum* in video observations (Casazza and Ross 2008). In contrast, other fishes (e.g., carangids) school just below the canopy of the *Sargassum*, therefore surface area (rather than the thickness of the mat) may be more relevant. The complexity of the *Sargassum* habitat and the associated juvenile fishes may not be fully captured by the sampling efforts that have been done within the habitat, and future research should be focused on quantifying this complexity. Studies have used biomass (Dooley 1972; Cassaza and Ross 2008; Kramer 2014; current study), mat volume (Wells and Rooker 2004), and surface area (current study), but future research should aim to quantify the depth of *Sargassum* in the water column and the structure of the habitat. Fish abundance and species richness has been found to increase with rugosity of artificial reefs in the Caribbean (Gratwicke and Speight 2005), and quantifying the rugosity or structure of *Sargassum* habitats could be valuable. Though the ephemeral nature of *Sargassum* would make such a study difficult, the species-specific relationships with the habitat could be better understood by quantifying *Sargassum* structure and complexity.

For several species collected using both the neuston net and H-L sampling, it was apparent that the gears were size selective. In general, individuals of the same species were found to have a smaller size range when collected in the neuston net than those collected using H-L. Previous *Sargassum* studies combined gears when estimating fish abundance and diversity, but analyses conducted in this study were separated by gear to

acknowledge the gear bias. Regardless of gear type, little temporal variability was observed in fish density, CPUE, and diversity, as month did not have a significant effect on these estimates. Some interannual variability was observed, a result of higher fish densities observed in the July 2017 cruise. Our results differ from previous studies in that relative abundances of fishes and diversity metrics have been found to vary between months, with a decrease in relative abundance and an increase in diversity metrics from late spring months through the summer months (Wells and Rooker 2004). I likely did not observe a strong temporal effect on juvenile fish assemblages because sampling for this study only took place during two months, whereas Wells and Rooker (2004) sampled in four months, and sampling in the current study did not always occur in the exact same region each month. Though it would be difficult to observe temporal differences with our sampling methodology, spatial variables were often found to be driving differences in fish density, CPUE, and diversity. Spatial differences have also been observed in other *Sargassum* studies (Bortone et al. 1977; Wells and Rooker 2004; Kramer 2014). For example, when observing sampling zones in the Florida shelf waters, the number of species were found to increase from inshore to offshore waters and from NW to SE sampling zones, and H' was found to decrease from NW to SE zones (Bortone et al. 1977). Sampling efforts in a inshore north, offshore north, and offshore south zones of Texas waters also found that relative abundance of fishes and diversity measures were significantly different between these zones (Wells and Rooker 2004). Finally, in the northern GOM, distance from shore was found to be the main driver of structure of juvenile fish assemblages (Kramer 2014).

Spatial variability in juvenile fish density, CPUE, and diversity was taxon-specific. Fish density generally decreased as samples were collected further from shore (with the exception of *Stephanolepis* spp.) and CPUE increased from inshore to offshore. These relationships varied by taxon, indicating it is important to determine which factors are driving variability for different species. In the northwestern GOM, *B. capriscus* and *Stephanolepis* [reported as *Monacanthus*] *hispidus* were found to have significantly higher relative abundances in offshore sampling zones compared to inshore (Wells and Rooker 2003). Though I found the same relationship with *Stephanolepis* spp., I did not observe this for *B. capriscus*. This could be a result of sampling different regions of the GOM, but our sampling stations ranged about 20 – 367 km from shore, whereas the samples designated as offshore in the Wells and Rooker (2003) study were in waters [24 – 112 km] from shore and the inshore samples were less than [24 km] from shore.

Since our sampling efforts ranged much further offshore, the highly variable oceanographic conditions of the central and northern GOM must be considered. In this study, the highest surface chlorophyll estimates were observed near the Birdfoot Delta (5.7 – 13.6 mg/$m^3$), and further offshore waters (generally South of 28.4° N) had surface chlorophyll estimates below 0.5 mg/$m^3$. The further offshore stations were not only depleted in surface chlorophyll, but were often influenced by surface features such as the Loop Current and associated eddies in the June 2018, July 2018, and June 2019 cruises. Fish density or CPUE in this study was not found to be different between stations influenced by such features and those stations that were not. There was, however, lower density of Sargassumfish observed in samples collected at stations influenced by the Loop Current or eddies, compared to those not influenced by such features. This could be

a result of lower productivity observed in offshore waters influenced by the Loop Current or eddies, or this could be an artifact of new *Sargassum* growth advected into the GOM from the Caribbean.

Recent large blooms of *Sargassum* in the Caribbean have resulted in the introduction of new growth to the GOM, via the Loop Current (Wang et al. 2019). If the new growth introduced to the GOM also has a relatively new community of associated juvenile fishes, this could be why a lower density of Sargassumfish was observed in samples influenced by the Loop Current or associated eddies. The types of macrofauna associated with *Sargassum* in the northwest Atlantic Ocean have been found to vary with age of the algae, as determined by observing the epiphyte coverage and color of the algae (Stoner and Greening 1984). Further, higher epiphyte coverage has been observed in *Sargassum* collected in the Gulf of Mexico compared to *Sargassum* from the Turks and Caicos Islands (Shadle et al. 2019), which has implications for different macrofaunal communities being observed in these two regions. To determine the source of *Sargassum* and the influence the age of the algae has on the associated community in different regions, direct measurements of both *Sargassum* age and associated macrofauna should be taken in the Gulf of Mexico, Caribbean, and the North Atlantic. This would facilitate an understanding of the direct impact that the introduction of *Sargassum* from large blooms in the Caribbean to the Gulf of Mexico has on the *Sargassum*-associated communities. There also is value in determining the direct role of surface features (e.g., Loop Current or eddies) on the *Sargassum*-associated juvenile fishes. While this study is the first to observe the role of these features on the density/abundance of *Sargassum*-associated fishes, future research could benefit from quantifying the invertebrate

community within *Sargassum* in areas influenced by different surface features. This would provide evidence of what changes to the *Sargassum*-associated macrofaunal community as a whole can be observed when influenced by different surface features. There is value in understanding this relationship, as we can better predict future impacts that large *Sargassum* blooms have on the resources the habitat provides to juvenile fishes.

Surface chlorophyll was found to be a significant driver of the spatial variability in juvenile fish density, CPUE, and diversity. Some outliers were observed, but *B. capriscus* and *H. histrio* densities were found to increase with surface chlorophyll until a peak at about 5 mg/m$^3$, and fish densities slightly decreased following that peak. A different trend was found for CPUE of *S. dumerili* with highest CPUE associated with low values of surface chlorophyll (< 1 mg/m$^3$). Peak density of *B. capriscus* observed at surface chlorophyll estimates of 5 mg/m$^3$ is likely related to the high productivity of waters near the Louisiana Birdfoot Delta, where high *B. capriscus* density was also observed (Figure A.5). The Mississippi River supplies large amounts of nitrogen to the northern GOM, which promotes phytoplankton growth in the coastal nutrient-rich surface waters (Dagg and Breed 2003). High phytoplankton productivity then supports the subsequent trophic levels (e.g., zooplankton, juvenile and larval fish). Evidence of elevated ichthyoplankton abundance and chlorophyll has been found in waters associated with the Mississippi River plume front (Grimes and Finucane 1991). Our observations of peak fish density of *B. capriscus* and *H. histrio* at elevated surface chlorophyll estimates is likely a result of the highly productive coastal waters they reside in. This could indicate that food/nutrient availability could be an important driver of fish distributions associated with *Sargassum*.

### 1.4.1 Conclusion

The community of fishes collected in this study was consistent with other studies in the region (Table 1.8), but I found that fish abundance was highly variable in relation to *Sargassum* wet weight or surface area coverage. Other methods of standardization should be investigated to incorporate factors such as rugosity, depth in the water column, and "patchiness" of *Sargassum* at the surface to better understand the importance of the structure of the habitat to the associated juvenile fishes. There was little temporal variability in fish assemblages, fish density, CPUE, and diversity, however spatial variables (e.g., distance from shelf) and chlorophyll concentration were found to be significant drivers of variability. The influence of surface features (Loop Current, eddies) was found to be significant for only one species (*H. histrio*). The results of this chapter can be used to characterize fish relationships with *Sargassum*, which combined with remote sensing estimates of *Sargassum* biomass, may serve as a predictor of juvenile abundance, a critical component of assessment models.

Table 1.8 *Sargassum*-associated fish assemblage metrics estimated from previous Gulf of Mexico literature and current study, adapted from Table 5 in Kramer 2014. H-L = hook and line sampling. H' = Shannon diversity, J' = Pielou's evenness, S = species/taxa richness.

| | Bortone et al. (1977) | Wells and Rooker (2004) | Hoffmayer et al. (2006) | Kramer (2014) | This Study (Neuston) | This Study (H-L) |
|---|---|---|---|---|---|---|
| Top families | Monacanthidae | Monacanthidae | Balistidae | Carangidae | Balistidae | Carangidae |
| | Carangidae | Carangidae | Monacanthidae | Monacanthidae | Monacanthidae | Scombridae |
| | Antennariidae | Balistidae | Carangidae | Kyphosidae | Pomacentridae | Balistidae |
| No. families | 16 | 17 | 12 | 21 | 13 | 5 |
| No. taxa (S) | 40 | 36 | 27 | 35 | 26 | 14 |
| No. individuals | 2,857 | 10,518 | 350 | 1,585 | 1,423 | 658 |
| H' mean | 0.81 | | | 1.15 | 1.11 | 0.61 |
| H' range | 0.28 - 1.92 | 0.44 - 0.60 | | 0.23 - 1.72 | 0 - 2.03 | 0 - 1.52 |
| J' mean | 0.22 | | | 0.76 | 0.80 | 0.65 |
| J' range | 0.13 - 0.83 | 0.52 - 0.73 | | 0.34 - 1.00 | 0.31 - 1.00 | 0.15 - 0.99 |
| No. samples | 62 | 25 | 23 | 50 | 39 | 23 |
| Gear | Dip net, few neustons | Purse seine | Neuston | Dip net, neuston, and purse seine | Neuston | Hook-and-line |

# CHAPTER II – SPATIAL AND TEMPORAL VARIABILITY IN THE DIETS OF *SARGASSUM*-ASSOCIATED JUVENILE FISHES

## 2.1 Introduction

### 2.1.1 Background and Significance

*Sargassum* is a genus of holopelagic brown algae that is comprised of two species, *S. natans* and *S. fluitans*, and is found floating at the surface of the ocean, with its primary distribution in the Atlantic Ocean and the Gulf of Mexico (GOM) (Dooley 1972). Pelagic *Sargassum* is also distributed throughout the Pacific and Indian Oceans, as well as the Caribbean Sea and the Red Sea. Wind and ocean currents transport *Sargassum* throughout its distribution range, and cause it to form large mats and weedlines. Aggregations of *Sargassum* provide feeding and refuge opportunities for a diverse community of invertebrates and fishes. Carangids and monacanthids are the numerically dominant taxa observed in the GOM in fish collections, and as many as 40 taxa representing as many as 21 families have been recorded in association with *Sargassum* (Bortone et al. 1977; Wells and Rooker 2004; Hoffmayer et al. 2005; Kramer 2014; current study). *Sargassum* also supports diverse invertebrate assemblages, including attached epizoans, as well as mobile shrimp (*Leander tenuicornis* and *Latreutes fucorum*), swimming crabs (*Portunus* spp.), and molluscs (Coston-Clements et al. 1991).

*Sargassum* has been designated an Essential Fish Habitat because it supports a diverse assemblage of fishes (SAFMC 2002). In addition, high abundances of juvenile fishes suggest *Sargassum* may serve as a nursery habitat, particularly for managed species. For example, Casazza and Ross (2008) observed that species collected in *Sargassum* and adjacent open water off the coast of North Carolina were generally larger

in size and significantly higher in abundance in the *Sargassum* habitats. In addition, the diets of *Sargassum*-associated individuals included a higher diversity of prey and larger prey volume (Casazza 2008). Collectively these observations support the hypothesis that *Sargassum* may provide survival advantages to associated juvenile fishes.

### 2.1.2 Diet Analysis

Trophic relationships of *Sargassum*-associated fishes have been studied in the GOM, primarily using natural biomarkers, such as stable isotopes and fatty acids (Kramer 2014; Rooker et al. 2006; Turner and Rooker 2006; Wells and Rooker 2009). These analyses provide long term indicators of which prey resources are contributing to the diet of an individual predator or forager, which can be used to make generalizations regarding nutritional sources for fishes. For example, Rooker et al. (2006) observed enriched nitrogen isotope values for *S. natans* and *S. fluitans* relative to particulate organic matter (POM) and epiphytic algae (*Cladophora* sp.). Using a 2-source mixing model of carbon, the majority of the carbon was found to be derived from POM, suggesting the primary food supplied to consumers in *Sargassum* habitats is in the form of POM rather than *Sargassum*. With respect to consumer trophic levels, *Sargassum* was found to contribute more to the diets of lower level consumers (e.g., *Balistes capriscus*) relative to higher level consumers (e.g., *Euthynnus alletteratus*) (Rooker et al. 2006; Wells and Rooker 2009). In contrast, Kramer (2014) found evidence to support *Sargassum* as a primary source of carbon in the *Sargassum* food webs off the coast of Alabama. Unlike Rooker et al. (2006), Kramer (2014) applied a lipid correction in the mixing model calculations, which may explain the discrepancy, as lipids are depleted in $^{13}C$. The results from these studies are equivocal, and suggest the role of *Sargassum* at the base of the food web and

the diets of associated organisms varies spatially and temporally, though the cause of the variability remains unknown.

Gut content analysis is a useful tool to characterize fish diets and inform food web models. In contrast to natural biomarkers described above, the stomach contents provide a "snapshot" of recent feeding, although multiple individuals need to be examined to capture the variance associated with diet. Analyzing stomach contents of sub-groups of fishes within a fish population can be used to determine the nutritional status of those sub-groups in relation to the whole fish community (Hyslop 1980). The seasonal variability in diet can be determined by sampling the same population repeatedly over time. Ontogenetic shifts in diet can also be determined when individuals of the same species are collected at different size ranges (Werner and Gilliam 1984).

Stomach content analysis of fishes associated with *Sargassum* has been compared to fishes collected in open water habitats during sampling efforts conducted off the coast of North Carolina (Casazza 2008). The dominant prey items of all fishes analyzed in the study were fish, copepods, and crustaceans. Taxonomic richness in the diets of *Sargassum*-associated fishes was evident as 55 prey items were unique to those collected within the *Sargassum* and only eight prey items were unique to those collected in open water. Casazza (2008) concluded that the high diversity and concentration of prey items within *Sargassum* highlighted the importance of *Sargassum* for juvenile fishes as nursery habitat.

Various methods are available to quantify gut contents, depending on the hypothesis being addressed. The methods vary in their data requirements, although most require the enumeration and identification of prey. The results can be presented as

percent frequency of occurrence (%F), which is the number of individual guts that contain at least one prey item in a specific prey category as a percent of the total number of (not empty) guts analyzed. A value for %F can be provided for each prey taxonomic group. Gut contents can also be expressed as percent by number (%N), or the total number of individual prey items within a prey group of an individual stomach as a percent of the total number of prey items within all stomachs analyzed. Volume and weight (dry or wet) of prey items can also be measured. Numerical and volumetric methods are often combined into one index of relative importance (IRI) to determine the overall contribution of a specific prey item to an individual fish's diet. The IRI method has been criticized for being redundant in providing data for the importance of a specific prey item (Macdonald and Green 1983), as well as not being as robust as each individual metric that is combined in the index being observed separately (Cortés 1997). The use of count data and measurements of volume and weight of prey items is commonly included in diet studies, but the digestion of prey items can be problematic in using such metrics (Baker et al. 2014). Therefore, %F may be a preferred measure of diet composition, as it is a more robust measure with fewer observational uncertainties (i.e., only presence/absence of prey items is required).

One of the proposed nursery role functions of *Sargassum* is that it provides a foraging area for the juvenile stages of many fish species (Casazza and Ross 2008; Kramer 2014). Among these are managed fisheries species, including Gray Triggerfish (*Balistes capriscus*), Greater Amberjack (*Seriola dumerili*), Lesser Amberjack (*Seriola fasciata*), Almaco Jack (*Seriola rivoliana*), and Tripletail (*Lobotes surinamensis*) (Waters et al. 2017; Farmer et al. 2016; Mickle et al. 2016). Gray Triggerfish, a recreationally-

and commercially-managed fishery species, is one of the most abundant juvenile species associated with *Sargassum* in the GOM (Kramer 2014; Wells and Rooker 2004; this study). Gray Triggerfish associated with *Sargassum* have been estimated to have a relatively low trophic level of 1.7 using stable isotope analysis and were thought to predominantly rely on *Sargassum* for nutrition (Rooker et al. 2006). Gray Triggerfish (9 – 75 mm standard length, SL) associated with *Sargassum* have been observed feeding on epifauna of the *Sargassum* and zooplankton in the GOM, and organic material and copepods in the Atlantic Ocean (Ballard and Rakocinski 2012; Casazza 2008). Diet studies of Amberjack spp. (Greater Amberjack, Lesser Amberjack, Almaco Jack) are largely limited to the adult stages, with relatively few observations from the GOM or non-captive fishes (Barreiros et al. 2003; Hamasaki et al. 2009; Manooch, III and Haimovici 1983). Juvenile Almaco Jack (12-64 mm SL) collected in *Sargassum* off the coast of North Carolina were observed feeding on calanoid copepods and crustaceans during the day and shrimp at night (Casazza 2008). Juvenile Greater Amberjack (25 – 297 mm SL) collected in the Gulf of Castellammare off the coast of Sicily fed on zooplankton until reaching about 120 mm SL and then shifted to a more diverse feeding strategy, including benthic fish and marine arthropods (Badalamenti et al. 1995). Tripletail is a recreational fishery species in the GOM, and diet studies are limited to adult specimens collected from anglers and seafood markets (Franks et al. 2003; Strelcheck et al. 2004). Diet studies of these managed fishery species are limited to other oceanic regions or larger size classes of juveniles or adults, and diet information is lacking for individuals of these species collected within *Sargassum*, where it is presumed the juveniles are relying on the habitat for feeding.

### 2.1.3 Objectives

The objective of this chapter is to characterize the trophic ecology of *Sargassum*-associated juvenile Gray Triggerfish, Greater Amberjack, Lesser Amberjack, Almaco Jack, and Tripletail using gut content analyses. An understanding of how these species feed in association with *Sargassum* will establish a baseline for comparative diet studies, and provide support for the role of *Sargassum* as a nursery habitat for juvenile fishes. By estimating the variability in the resource use and nursery-role of *Sargassum*, the results can be used to inform fisheries management. In this chapter I will also describe the spatial and temporal variability in diet for each species, as well as the environmental and biological variables influencing these differences. Ontogenetic shifts in diet were analyzed for Greater Amberjack and Almaco Jack and, lastly, diet overlap among the species was determined.

## 2.2 Methods

### 2.2.1 Fish Collection

Fishes were collected during four research cruises on the *R/V Point Sur* in 2017, 2018, and 2019 (Figure 1.1; Table 1.1). Some sampling stations were associated with the Loop Current or an anticyclonic eddy feature (Figure 1.2). Fishes for diet analysis were primarily collected with a 1x2 m neuston net (505 µm mesh) towed through *Sargassum*, and during 30-minute hook-and-line fishing periods using Sabiki rigs (Table 1.2). A few additional fish specimens were collected using the following methods: 1) a larval purse seine deployed around *Sargassum* mats (n=4 fish collected 7/16/2018 and 6/4/2019); 2) opportunistic dipnetting along the edge of *Sargassum* (n=7 fish collected 7/27/2017,

7/16/2018, and 5/28/2019); and 3) opportunistic hook-and-line fishing (n=2 fish collected 7/27/2017). All fishes were either preserved in 95% ethanol or frozen after collection.

### 2.2.2 Diet Analysis

All fish were identified, weighed (to the nearest 0.1 g), and measured (standard length, SL, or total length, TL, to the nearest 0.1 mm). All guts were removed from preserved fishes, weighed (to the nearest 0.0001 g), and gut contents were analyzed under a dissecting microscope. For Gray Triggerfish, there is a general lack of distinction in the external morphology of the stomach and intestine for small individuals, therefore the entire gut tract was analyzed for gut contents. For Greater Amberjack, Lesser Amberjack, Almaco Jack, and Tripletail, only the stomach contents were analyzed. Prey items were removed from guts and identified to the lowest possible taxonomic level. When certain prey items were difficult to quantify (e.g., fragments of bryozoan epiphytes), only presence/absence was noted. Taxonomic resolution in prey identification was highly variable, in part because many prey items were partially digested. Therefore prey categories were lumped at the most confident level of identification into the following groups: Algae, Amphipods, Barnacles, Calanoid copepods, *Cerataspis*, Chaetognaths, Cladocerans, Crabs, Decapod larvae, Epiphytes on *Sargassum*, Euphausiids, Fish, Fish Eggs, Foraminifera, Harpacticoid copepods, Invertebrate eggs, Isopods, *Latreutes fucorum* (Slender Sargassum Shrimp), *Leander tenuicornis* (Brown Grass Shrimp), Larvaceans, Molluscs, Ostracods, Other Copepods (excluding Calanoid and Harpacticoid), Other Shrimp, Polychaetes, *Sargassum*, and Stomatopods. Frequency of occurrence (%F) was calculated for a particular prey item as the number of guts

containing that prey item expressed as a percentage of the total number of guts found with prey items present for each species (Hyslop 1980).

### 2.2.3 Data Analysis

Percent frequency of occurrence was calculated for each species (with a minimum sample size of five specimens) by cruise and for all cruises combined. Temporal variability in %F was examined using separate NMDS plots for each species coded by cruise. NMDS plots were generated using a presence or absence matrix of 0's and 1's to estimate a Jaccard distance matrix. Each column in this matrix was a prey item and each row was an individual fish. An analysis of similarity (ANOSIM) was then used, which determined whether %F differed by cruise (Clarke and Gorley 2006). The ANOSIM test uses permutations to estimate between and within group rank dissimilarities, and determine which is higher. For all ANOSIMs, 999 permutations were used. The ANOSIM R test statistic ranges from zero to one, and values closer to zero indicate no differences in diet between groups. Values closer to one indicate differences in diet between the groups. A separate NMDS plot was generated for each species and coded by surface feature: Loop Current or eddy-associated (LC/Eddy) or "Other" (Figure 1.2; Table 1.2), and an ANOSIM was used to determine whether diet was different between these two groups (LC/Eddy and Other).

The vessel's navigation instrumentation package was used to record water depth (m) and location (latitude and longitude, decimal degrees) at each station. A SBE 09 Plus CTD (SBE 11 deck box) was used to collect water temperature (°C) and salinity near the surface (4.5 m depth), as well as the depth of maximum chlorophyll concentration (m). The proximity tool in ArcGIS was used to estimate distance from shore (km) and distance

from the continental shelf (km), which calculates the distance between a sampling coordinate and either the 200 m isobath line (continental shelf) or the nearest continental border (shore). This method accounts for earth's curvature and estimates the closest point-to-line distance in any direction. Remote sensing products were used by collaborators at the University of South Florida's Optical Oceanography lab to estimate sea surface chlorophyll concentration ($mg/m^3$). The *BIOENV* function in the R vegan package was used to determine whether the environmental or spatial variables mentioned above influenced differences in diet (Clarke and Ainsworth 1993). This function is used to determine which of the environmental variables should be included in the "best" model that aims to maximize the rank correlation between the scaled environmental variables and the presence/absence community matrix. The variables determined to be in the "best" model were shown using vectors overlaid on the NMDS plots to observe the magnitude (length) and direction of that variable's influence. The significance of the environmental variables was assessed using the *envfit* function in R. The following variables were included in each *BIOENV* analysis: water depth (m), latitude (DD), longitude (DD), temperature (°C), salinity, depth at chlorophyll max (m), distance from shore (km), distance from the continental shelf (km), and surface chlorophyll concentration ($mg/m^3$).

Ontogenetic diet shifts were analyzed for Greater Amberjack and Almaco Jack by first transforming %F into proportional estimates of occurrence:

$$Proportion\ diet\ item\ a = (\frac{FO_a}{100}) / \sum(\frac{FO_{a-z}}{100}),$$

where $FO_a$ is the %F of diet item *a*, and $FO_{a\text{-}z}$ is the %F for all diet items of that species.

These proportions were then used to calculate the Schoener Index (Schoener 1970) to observe diet overlap between size classes of the same species, using the following formula:

$$C = 1 - 0.5 \times \left(\sum_{i=1}^{n} \left| P_{xi} - P_{yi} \right|\right),$$

where $P_{xi}$ and $P_{yi}$ are the proportional occurrences of prey *i* in the diet of groups *x* and *y*, which are groups of defined size classes. The values of this index range from 0 to 1, with increasing values indicating higher diet overlap, and values greater than 0.6 indicate a biologically significant overlap (Wallace 1981). Size classes (50-mm bins) were based on total length (TL) for both species. One individual Almaco Jack was missing a TL measurement, so TL was estimated using the relationship between TL and standard length (SL) in mm for all other Almaco Jack individuals (TL = 1.27*SL – 2.91; $r^2$ = 0.98).

The biologically significant overlap (Schoener Index > 0.6) in diet between species was estimated with the Schoener Index using raw %F values for each prey item (Wallace 1981). NMDS plots of diets coded by species were generated to examine diet differences, and an ANOSIM test was used to determine whether diet was different between each species, which would be indicated by an R statistic value closer to 1.

## 2.3 Results

### 2.3.1 Gray Triggerfish

A total of 149 out of 162 Gray Triggerfish (14.2 – 112.0 mm SL) examined had gut contents and were available for analysis (Table 2.1). The most frequently occurring prey observed in fishes collected during both July cruises were copepods, shrimp, and

molluscs (Figure 2.1). Epiphytes were more frequently consumed in July 2017 relative to July 2018, and molluscs became more frequent in the July 2018 gut contents. Some variability in Gray Triggerfish diet was observed between these two cruises in the NMDS plot, though there was still a high degree of overlap (Figure 2.2; 2D stress = 0.17; ANOSIM $R = 0.16$, $p = 0.001$). The best model as determined by the *BIOENV* was found to have salinity ($p = 0.001$) and distance from shelf break ($p = 0.083$) as the two parameters influencing variability (Spearman's $\rho = 0.27$).

Table 2.1 Percent frequency of occurrence (%F) for *Balistes capriscus* prey items for each cruise and for all cruises combined (Total). The n-values denote number of fish guts examined for diet analysis.

| Prey Item | July 2017 | June 2018 | July 2018 | Total |
|---|---|---|---|---|
| | **n = 104** | **n = 1** | **n = 44** | **n = 149** |
| **ANNELIDA** | | | | |
| Polychaete | 34.6 | 100.0 | 6.8 | 26.8 |
| **ARTHROPODA** | | | | |
| Amphipod | 27.9 | 0.0 | 22.7 | 26.2 |
| Calanoid | 43.3 | 0.0 | 54.5 | 46.3 |
| Harpacticoid | 34.6 | 0.0 | 18.2 | 29.5 |
| Other Copepods | 60.6 | 0.0 | 75.0 | 64.4 |
| *L. fucorum* | 27.9 | 0.0 | 6.8 | 21.5 |
| *L. tenuicornis* | 2.9 | 0.0 | 0.0 | 2.0 |
| Other Shrimp | 58.7 | 0.0 | 31.8 | 50.3 |
| Crabs | 19.2 | 100.0 | 13.6 | 18.1 |
| Decapod larvae | 3.8 | 0.0 | 0.0 | 2.7 |
| Isopod | 6.7 | 0.0 | 11.4 | 8.1 |
| Barnacle | 1.9 | 0.0 | 0.0 | 1.3 |
| Cladoceran | 1.0 | 0.0 | 0.0 | 0.7 |
| Ostracod | 1.0 | 0.0 | 0.0 | 0.7 |
| **MOLLUSCA** | | | | |
| Molluscs | 37.5 | 0.0 | 65.9 | 45.6 |
| **OCHROPHYTA** | | | | |
| *Sargassum* | 44.2 | 100.0 | 18.2 | 36.9 |
| **TUNICATA** | | | | |
| Larvacean | 1.0 | 0.0 | 2.3 | 1.3 |
| **CHORDATA** | | | | |
| Fish | 16.3 | 0.0 | 13.6 | 15.4 |
| Fish Eggs | 33.7 | 0.0 | 2.3 | 24.2 |
| **OTHER** | | | | |
| Algae | 0.0 | 100.0 | 0.0 | 0.7 |
| Epiphytes | 55.8 | 0.0 | 9.1 | 41.6 |
| Foraminifera | 1.9 | 0.0 | 0.0 | 1.3 |
| Invertebrate eggs | 6.7 | 0.0 | 0.0 | 4.7 |
| Plant | 1.9 | 0.0 | 0.0 | 1.3 |

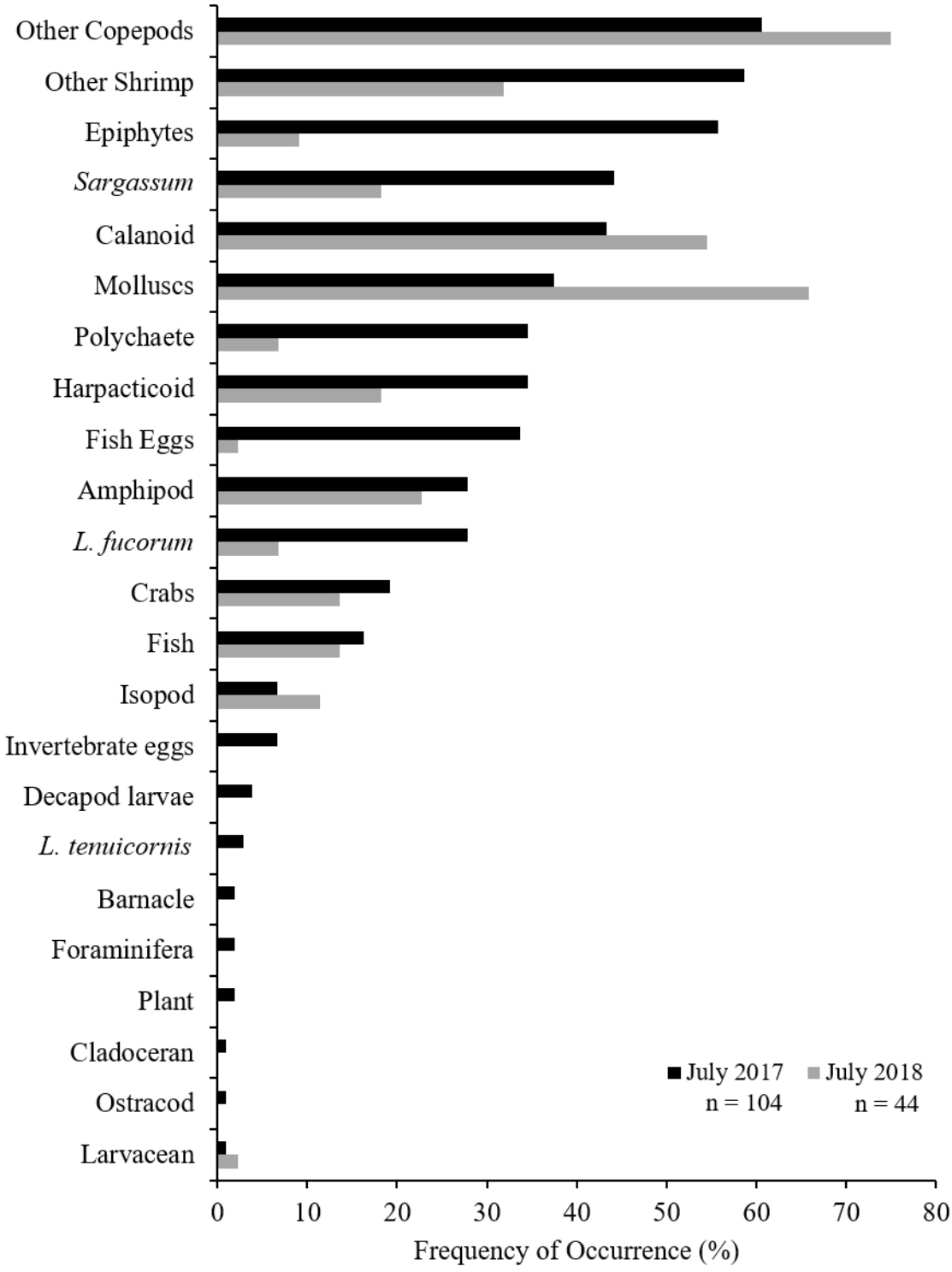


Figure 2.1 Frequency of occurrence (%) of *Balistes capriscus* prey items for fishes collected in July 2017 and July 2018. The n-values denote the number fish guts examined for diet analysis.

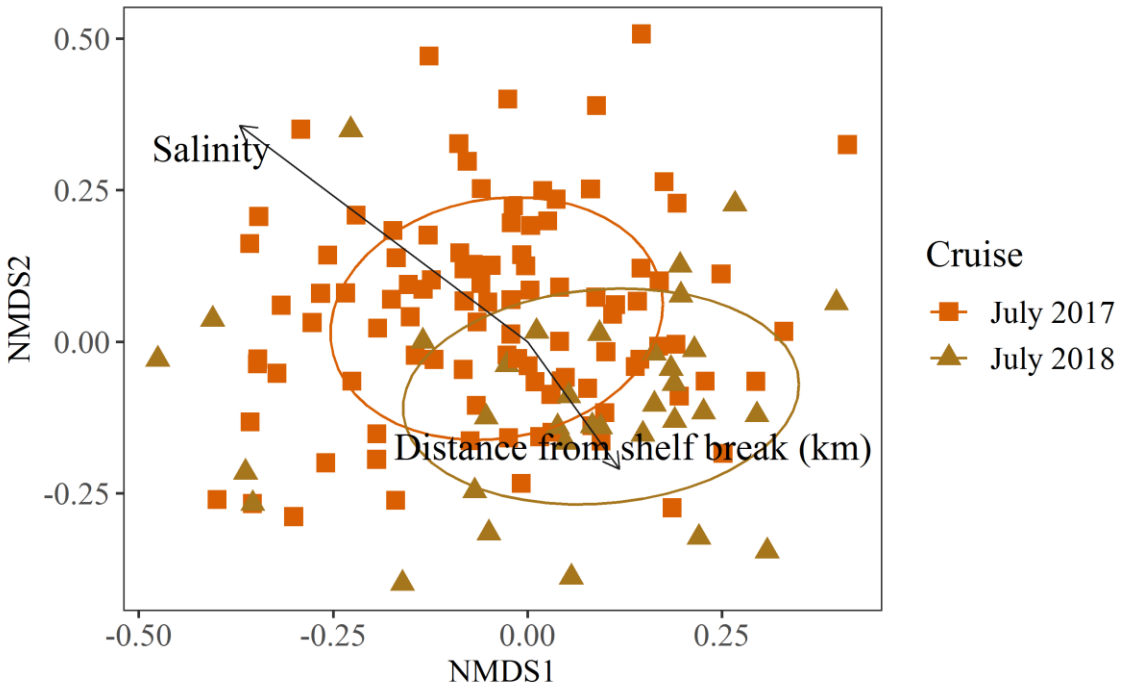


Figure 2.2 NMDS plot of *Balistes capriscus* diet by cruise (July 2017 and July 2018). Direction and magnitude of vectors denote relative influence of environmental factors. Ellipses denote 50% confidence intervals of each cruise and vectors included for environmental variables determined to be in best model using a BIOENV analysis. Cruise sample sizes: July 2017 (n = 104), July 2018 (n = 44).

### 2.3.2 Greater Amberjack

A total of 61 out of 73 Greater Amberjack (25.1 – 269.0 mm TL) examined had stomach contents and were available to analyze (Table 2.2). In most cruises, fish, crabs, and the two species of shrimp endemic to *Sargassum* were important prey in terms of %F (Figure 2.3). Fish were most frequently consumed in July 2017 and the two species of shrimp were found to be consumed most frequently in July 2018. Decapod larvae were a dominant prey item in July 2018, but were consumed much less frequently in the other cruises. Relatively little temporal variability was observed in Greater Amberjack diet, with the most separation between the two July cruises (Figure 2.4; 2D stress = 0.13; ANOSIM R = 0.02, p = 0.315). The results of the *BIOENV* analysis determined that the best model had distance from shelf break (p = 0.025) and latitude (p = 0.527) as the

parameters, though a relatively low correlation value was observed (Spearman's $\rho$ = 0.17). Greater Amberjack diet was found to have little variability between surface feature type (Figure 2.5; 2D stress = 0.13; ANOSIM R = 0.19, p = 0.037).

Table 2.2 Percent frequency of occurrence (%F) for *Seriola dumerili* prey items for each cruise and for all cruises combined (Total). The n-values denote number of fish guts examined for diet analysis.

| Prey Item | July 2017 **n = 8** | June 2018 **n = 21** | July 2018 **n = 6** | June 2019 **n = 26** | Total **n = 61** |
|---|---|---|---|---|---|
| **ANNELIDA** | | | | | |
| Polychaete | 0.0 | 0.0 | 16.7 | 3.8 | 3.3 |
| **ARTHROPODA** | | | | | |
| Amphipod | 0.0 | 0.0 | 16.7 | 11.5 | 6.6 |
| Calanoid | 12.5 | 4.8 | 16.7 | 3.8 | 6.6 |
| Other Copepods | 0.0 | 23.8 | 16.7 | 23.1 | 19.7 |
| *L. fucorum* | 50.0 | 42.9 | 66.7 | 30.8 | 41.0 |
| *L. tenuicornis* | 25.0 | 14.3 | 50.0 | 30.8 | 26.2 |
| Other Shrimp | 50.0 | 85.7 | 66.7 | 46.2 | 62.3 |
| Crabs | 25.0 | 28.6 | 66.7 | 26.9 | 31.1 |
| Decapod larvae | 0.0 | 4.8 | 50.0 | 23.1 | 16.4 |
| Isopod | 0.0 | 14.3 | 0.0 | 7.7 | 8.2 |
| Stomatopod | 0.0 | 0.0 | 33.3 | 15.4 | 9.8 |
| **CHAETOGNATHA** | | | | | |
| Chaetognath | 0.0 | 4.8 | 16.7 | 7.7 | 6.6 |
| **MOLLUSCA** | | | | | |
| Molluscs | 0.0 | 4.8 | 0.0 | 0.0 | 1.6 |
| **OCHROPHYTA** | | | | | |
| *Sargassum* | 25.0 | 9.5 | 50.0 | 26.9 | 23.0 |
| **CHORDATA** | | | | | |
| Fish | 75.0 | 28.6 | 50.0 | 26.9 | 36.1 |
| Fish Eggs | 0.0 | 4.8 | 0.0 | 3.8 | 3.3 |
| **OTHER** | | | | | |
| Invertebrate Eggs | 0.0 | 4.8 | 0.0 | 3.8 | 3.3 |

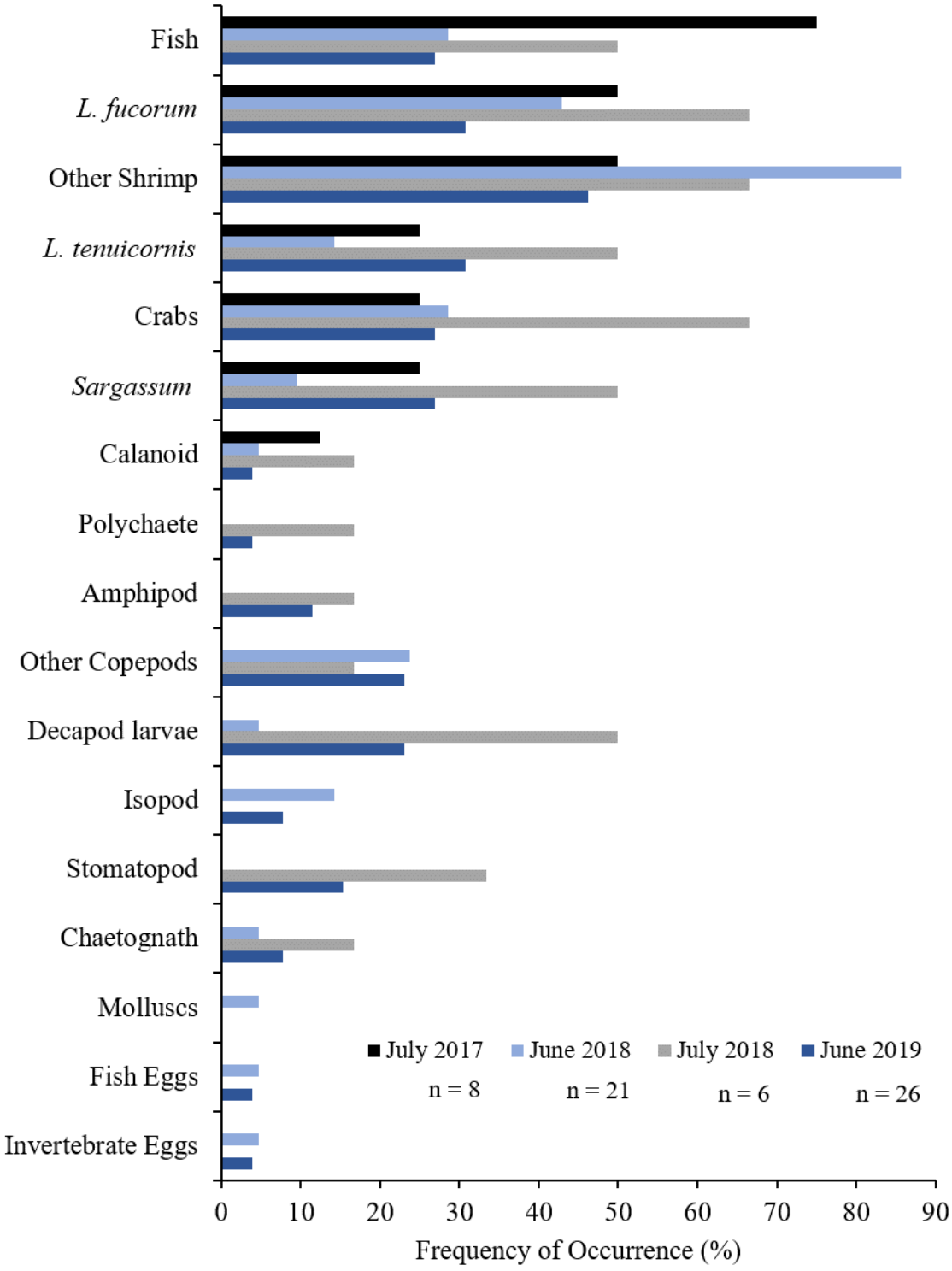


Figure 2.3 Frequency of occurrence (%) of *Seriola dumerili* prey items for fishes collected in July 2017, June 2018, July 2018, and June 2019. The n-values denote the number fish guts examined for diet analysis.

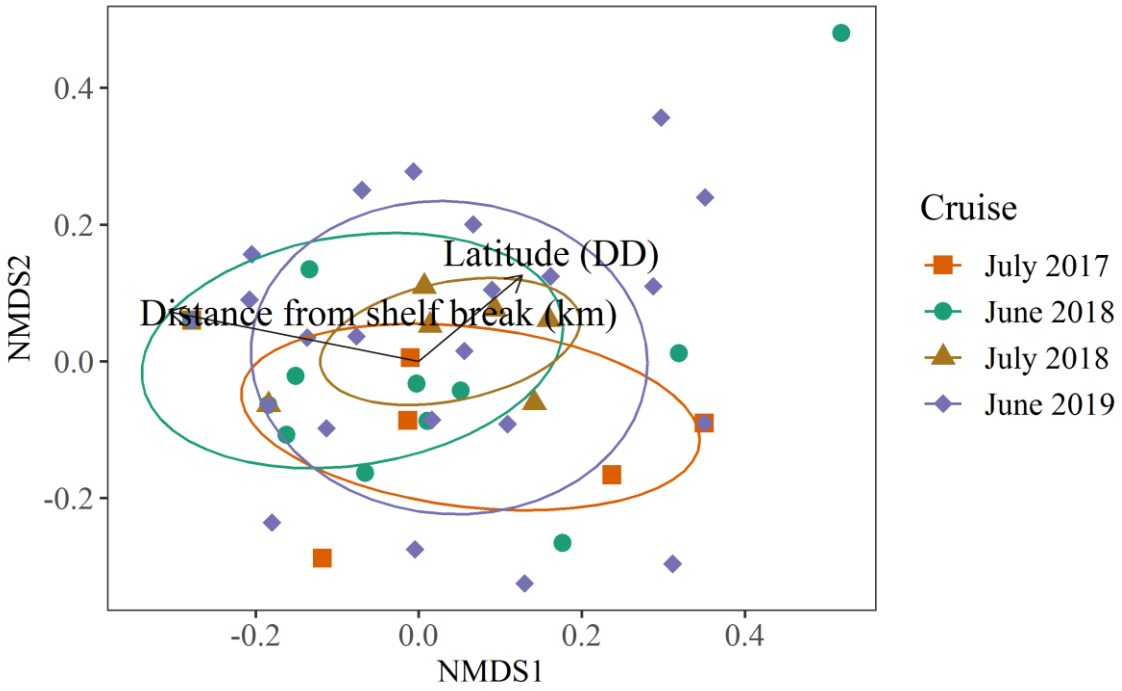


Figure 2.4 NMDS plot of *Seriola dumerili* diet by cruise. Direction and magnitude of vectors denote relative influence of environmental factors. Ellipses denote 50% confidence intervals of each cruise and vectors included for environmental variables determined to be in best model using a BIOENV analysis. Cruise sample sizes: July 2017 (n = 8), June 2018 (n = 21), July 2018 (n = 6), June 2019 (n = 26).

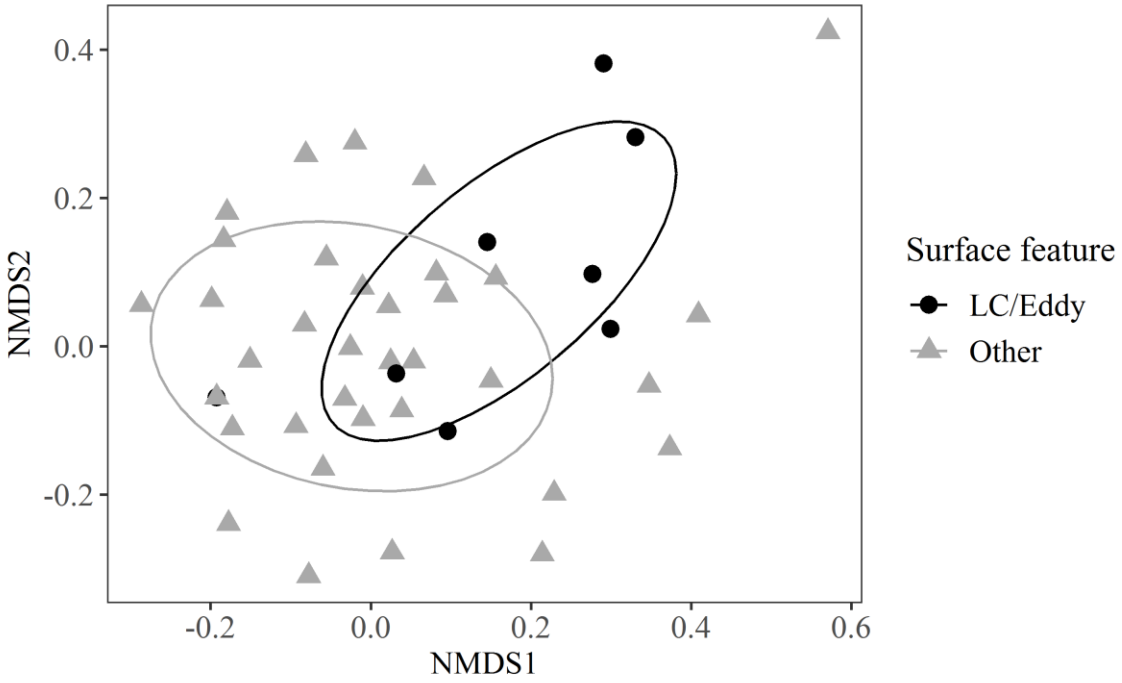


Figure 2.5 NMDS plot of *Seriola dumerili* diet coded by surface feature. Ellipses denote 50% confidence intervals of each surface feature type. Sample sizes: LC/Eddy (n = 8), Other (n = 53).

Some differences were observed between 50 mm TL size classes of Greater Amberjack (Figure 2.6). There was biologically significant overlap in diet between the 50-100 and 100 – 150 mm TL size classes, as well as the 150 – 200 and 200 – 250 mm TL size classes based on the Schoener Index values (Table 2.3). The Slender Sargassum Shrimp and other copepods were found to be a large proportion of the diet of the smallest size class, and other shrimp became more important in the 50 – 100 mm TL size class. The 50-100 and 100 – 150 mm TL size classes were similar in that crabs, fish, and other shrimp were in similar proportions of the diet. The next two size classes (150 – 200 and 200 – 250 mm TL) had a much more diverse diet, with new prey items found such as amphipods, decapod larvae, Brown Grass Shrimp, and stomatopods being consumed in similar proportions, which had biologically significant overlap. The largest size class (250 – 300 mm TL) was predominantly feeding on the two species of shrimp, invertebrate eggs, and crabs.

Table 2.3 Schoener indices of diet overlap for pairwise comparisons of 50-mm size classes of *Seriola dumerili.* Cells with values >0.60 (highlighted in bold) denote biologically significant overlap between size classes.

| | **0-50** | **50-100** | **100-150** | **150-200** | **200-250** | **250-300** |
|---|---|---|---|---|---|---|
| **0-50** | - | | | | | |
| **50-100** | 0.22 | - | | | | |
| **100-150** | 0.25 | **0.68** | - | | | |
| **150-200** | 0.23 | 0.58 | 0.54 | - | | |
| **200-250** | 0.13 | 0.56 | 0.46 | **0.75** | - | |
| **250-300** | 0.22 | 0.56 | 0.60 | 0.50 | 0.56 | - |

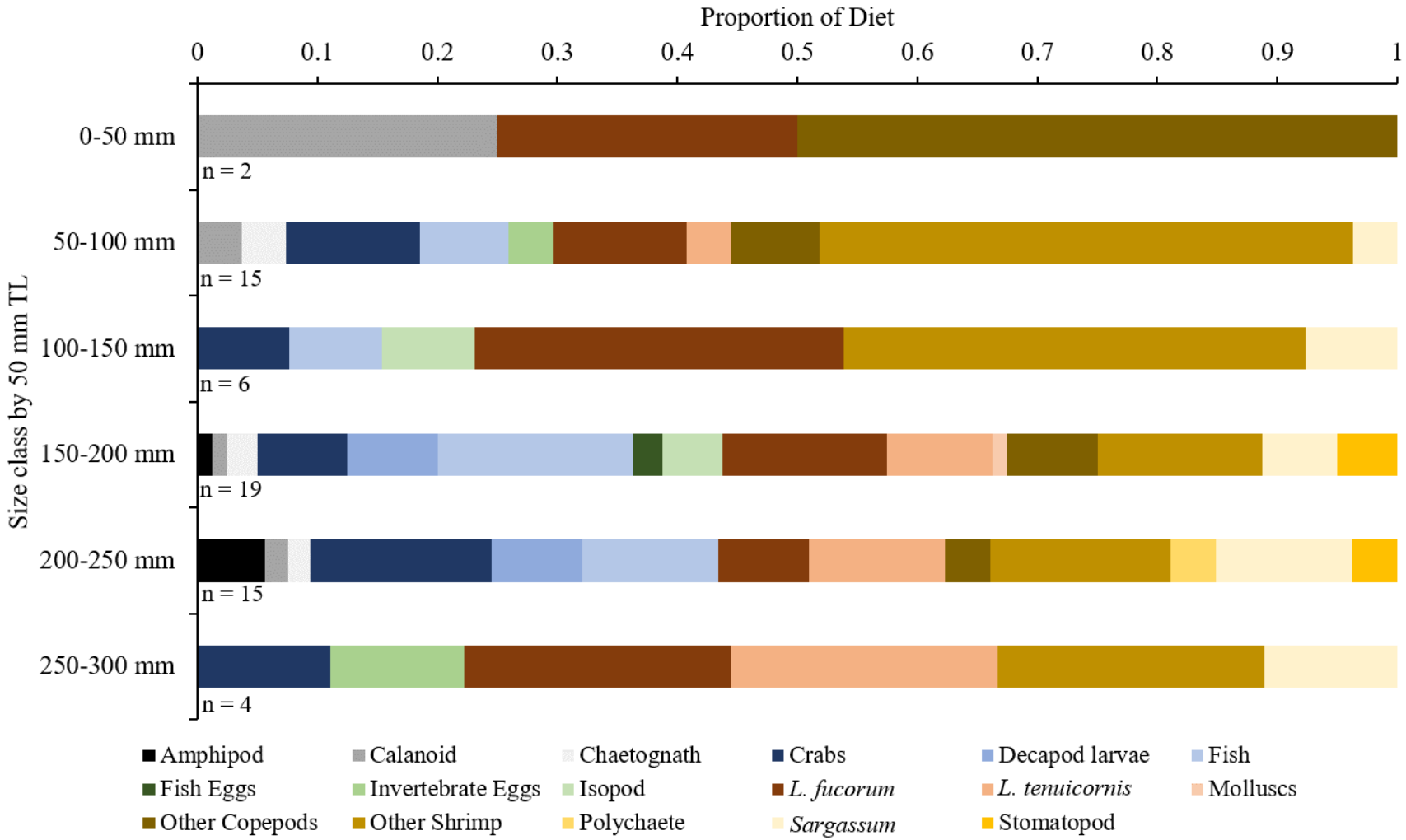


Figure 2.6 Relative abundance (standardized proportion) of prey for 50-mm size classes of *Seriola dumerili.*

### 2.3.3 Lesser Amberjack

A total of 11 of 12 Lesser Amberjack (91.4 to 191.0 mm TL) examined had stomach contents and were available for analysis (Table 2.4). Lesser Amberjack most frequently consumed amphipods, calanoid copepods, Slender Sargassum Shrimp, and fish. As there was insufficient sample sizes to compare Lesser Amberjack by cruise, the NMDS plot was presented with only vectors of important environmental variables (Figure 2.7; 2D stress = 0.02). The best model using a *BIOENV* analysis determined that water depth ($p = 0.060$), temperature ($p = 0.270$), and salinity ($p = 0.220$) best described diet variability (Spearman's $\rho = 0.47$). There was good separation in Lesser Amberjack diet between the surface feature type (Figure 2.8; 2D stress = 0.02; ANOSIM $R = 0.62$, $p = 0.003$).

Table 2.4 Percent frequency of occurrence (%F) for *Seriola fasciata* prey items for all cruises combined (Total). Number of fish guts examined for diet analysis: n = 11.

| Prey Item | Total |
|---|---|
| **ARTHROPODA** | |
| Amphipod | 45.5 |
| Calanoid | 45.5 |
| Other Copepods | 9.1 |
| *L. fucorum* | 45.5 |
| *L. tenuicornis* | 36.4 |
| Other Shrimp | 36.4 |
| Crabs | 18.2 |
| Decapod larvae | 36.4 |
| Stomatopod | 9.1 |
| **CHAETOGNATHA** | |
| Chaetognath | 9.1 |
| **MOLLUSCA** | |
| Molluscs | 9.1 |
| **OCHROPHYTA** | |
| *Sargassum* | 18.2 |
| **CHORDATA** | |
| Fish | 45.5 |

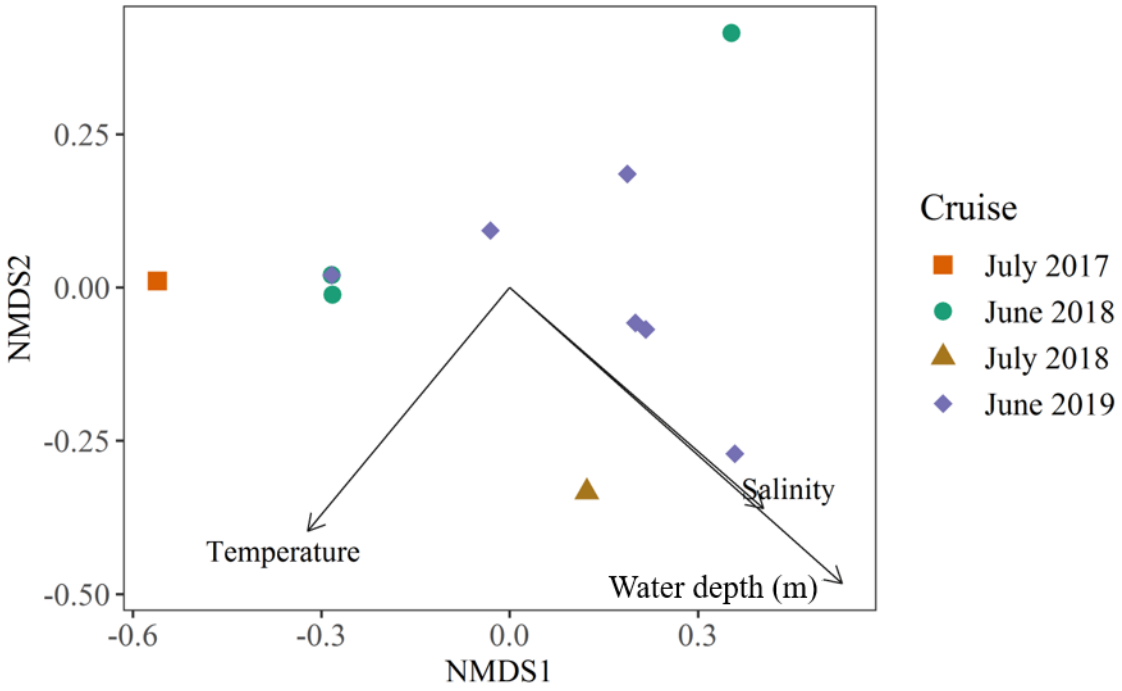


Figure 2.7 NMDS plot of *Seriola fasciata* diet by cruise. Direction and magnitude of vectors denote relative influence of environmental factors. Vectors included for environmental variables determined to be in best model using a BIOENV analysis. Cruise sample sizes: July 2017 (n = 1), June 2018 (n = 3), July 2018 (n = 1), June 2019 (n = 6).

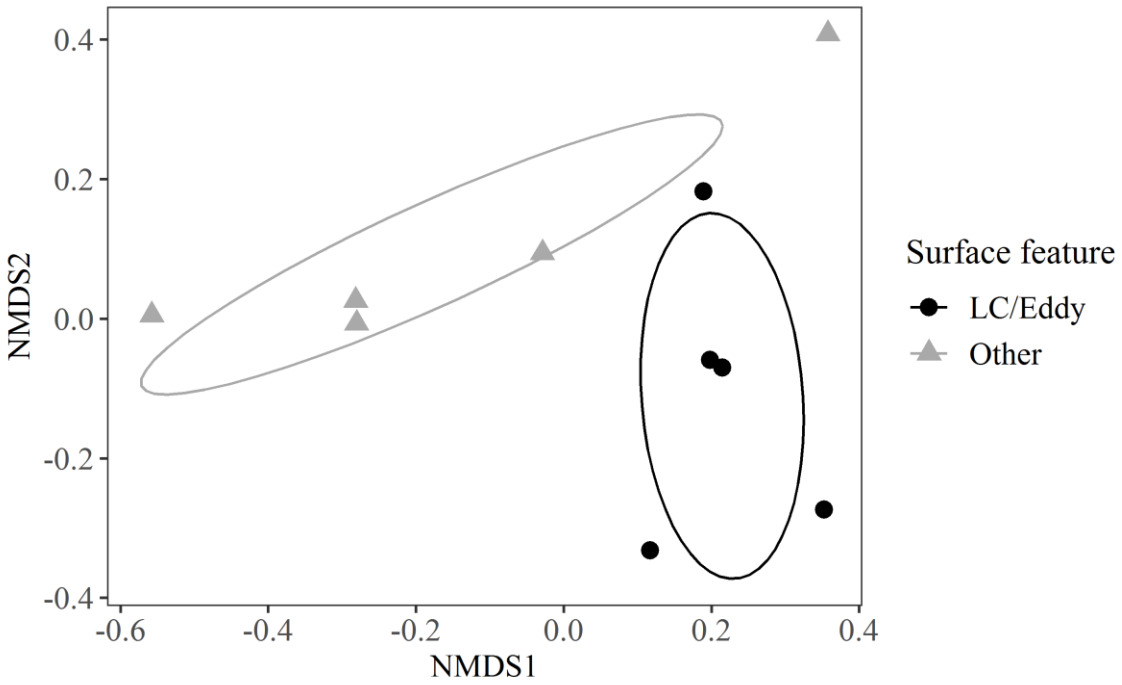


Figure 2.8 NMDS plot of *Seriola fasciata* diet coded by surface feature. Ellipses denote 50% confidence intervals of each surface feature type. Sample sizes: LC/Eddy (n = 5), Other (n = 6).

### 2.3.4 Almaco Jack

A total of 215 out of 218 Almaco Jack (19.2 to 355.0 mm TL) examined had stomach contents and were available to be analyzed (Table 2.5). Almaco Jack frequently consumed the Slender Sargassum Shrimp, Brown Grass Shrimp, and other shrimp in all cruises (Figure 2.9). Fish were most frequently consumed in July 2018 and June 2019, and chaetognaths, amphipods, decapod larvae, stomatopods, and molluscs were more frequently consumed in June 2019. Though there were some differences in %F of different prey items by cruise, there was still high overlap between cruises in the NMDS plot of Almaco Jack diets (Figure 2.10; 2D stress = 0.21; ANOSIM $R = 0.11$, $p = 0.001$). The *BIOENV* analysis found that distance from shelf break ($p = 0.001$) and surface chlorophyll ($p = 0.001$) were included in the best model (Spearman's $\rho = 0.17$). There was also a high degree of overlap of Almaco Jack diet between surface feature type (Figure 2.11; 2D stress = 0.21; ANOSIM $R = 0.14$, $p = 0.001$).

Table 2.5 Percent frequency of occurrence (%F) for *Seriola rivoliana* prey items for each cruise and for all cruises combined (Total). The n-values denote number of fish guts examined for diet analysis.

| Prey Item | July 2017 **n = 25** | June 2018 **n = 26** | July 2018 **n = 87** | June 2019 **n = 77** | Total **n = 215** |
|---|---|---|---|---|---|
| **ANNELIDA** | | | | | |
| Polychaete | 0.0 | 0.0 | 2.3 | 3.9 | 2.3 |
| **ARTHROPODA** | | | | | |
| Amphipod | 0.0 | 7.7 | 17.2 | 33.8 | 20.0 |
| Calanoid | 28.0 | 38.5 | 26.4 | 28.6 | 28.8 |
| Harpacticoid | 0.0 | 3.8 | 3.4 | 0.0 | 1.9 |
| Other Copepods | 20.0 | 34.6 | 34.5 | 14.3 | 25.6 |
| *L. fucorum* | 56.0 | 57.7 | 52.9 | 46.8 | 51.6 |
| *L. tenuicornis* | 40.0 | 23.1 | 37.9 | 32.5 | 34.4 |
| Other Shrimp | 76.0 | 76.9 | 74.7 | 68.8 | 73.0 |
| *Cerataspis* | 0.0 | 0.0 | 0.0 | 2.6 | 0.9 |
| Crabs | 12.0 | 0.0 | 46.0 | 11.7 | 24.2 |
| Decapod larvae | 0.0 | 23.1 | 29.9 | 46.8 | 31.6 |
| Euphausiid | 0.0 | 0.0 | 2.3 | 0.0 | 0.9 |
| Isopod | 4.0 | 7.7 | 19.5 | 2.6 | 10.2 |
| Ostracod | 0.0 | 0.0 | 0.0 | 2.6 | 0.9 |
| Stomatopod | 0.0 | 0.0 | 10.3 | 33.8 | 16.3 |
| **CHAETOGNATHA** | | | | | |
| Chaetognath | 4.0 | 19.2 | 31.0 | 44.2 | 31.2 |
| **MOLLUSCA** | | | | | |
| Molluscs | 0.0 | 7.7 | 16.1 | 31.2 | 18.6 |
| **OCHROPHYTA** | | | | | |
| *Sargassum* | 24.0 | 3.8 | 51.7 | 45.5 | 40.5 |
| **CHORDATA** | | | | | |
| Fish | 16.0 | 46.2 | 62.1 | 61.0 | 54.4 |
| Fish Eggs | 24.0 | 3.8 | 1.1 | 1.3 | 4.2 |
| **OTHER** | | | | | |
| Epiphytes | 4.0 | 0.0 | 2.3 | 2.6 | 2.3 |
| Foraminifera | 0.0 | 0.0 | 1.1 | 0.0 | 0.5 |
| Invertebrate Eggs | 4.0 | 0.0 | 0.0 | 0.0 | 0.5 |

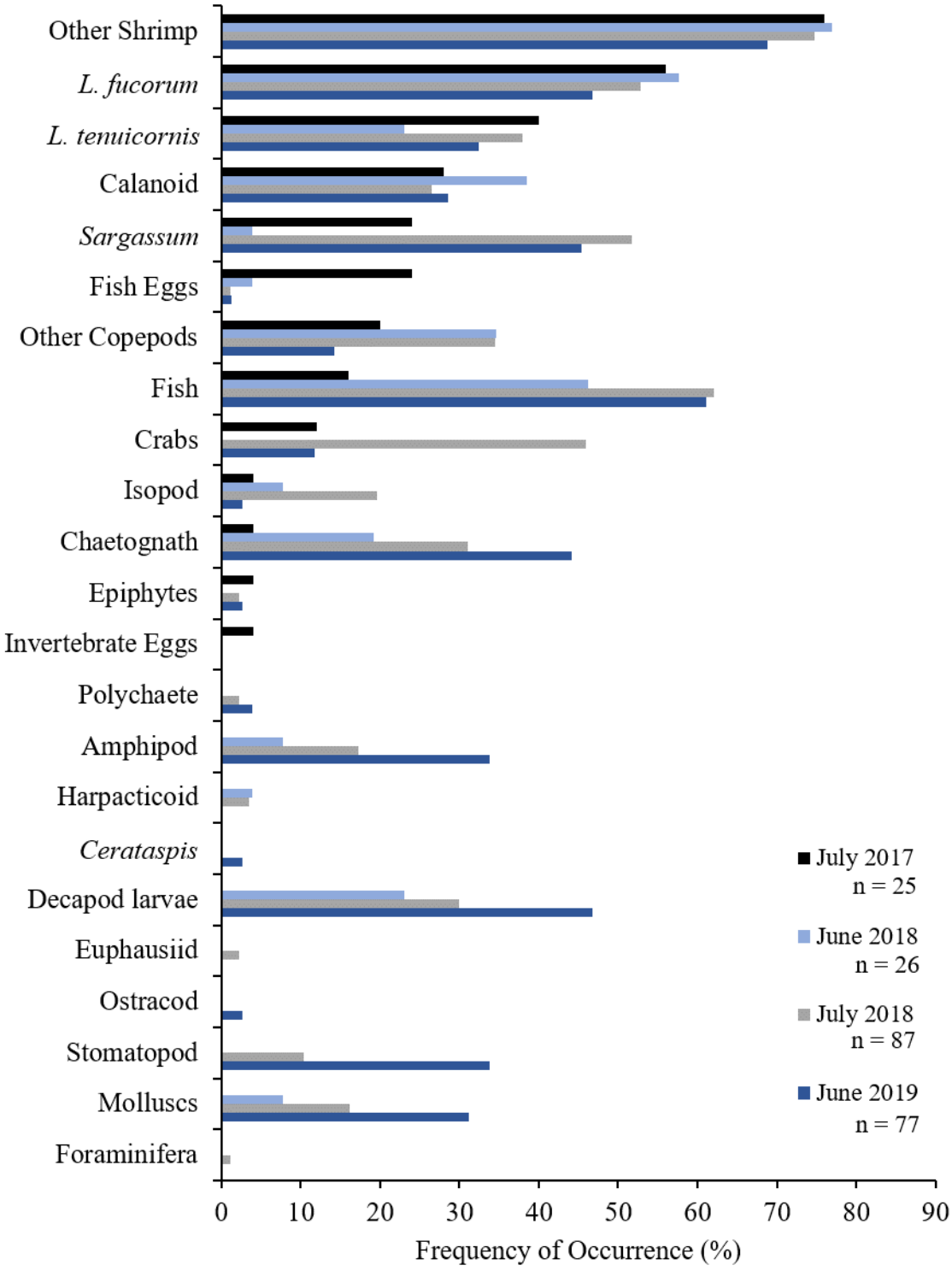


Figure 2.9 Frequency of occurrence (%) of *Seriola rivoliana* prey items for fishes collected in July 2017, June 2018, July 2018, and June 2019. The n-values denote the number fish guts examined for diet analysis.

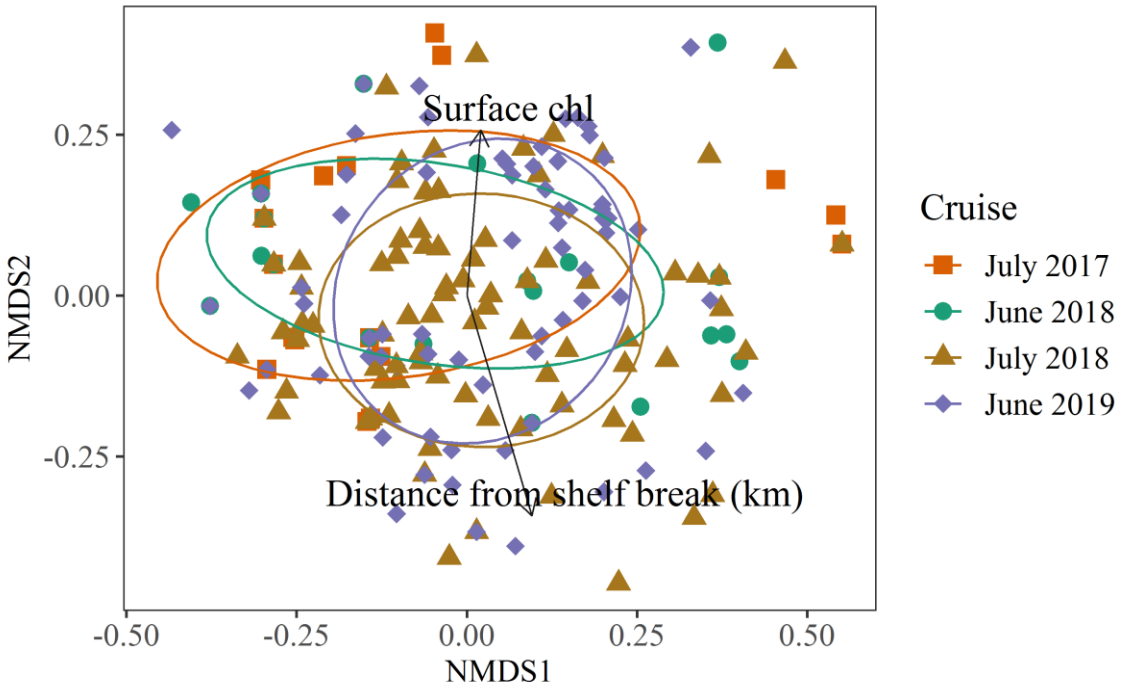


Figure 2.10 NMDS plot of *Seriola rivoliana* diet by cruise. Direction and magnitude of vectors denote relative influence of environmental factors. Ellipses denote 50% confidence intervals of each cruise and vectors included for environmental variables determined to be in best model using a BIOENV analysis. Cruise sample sizes: July 2017 (n = 24), June 2018 (n = 26), July 2018 (n = 87), June 2019 (n = 77).

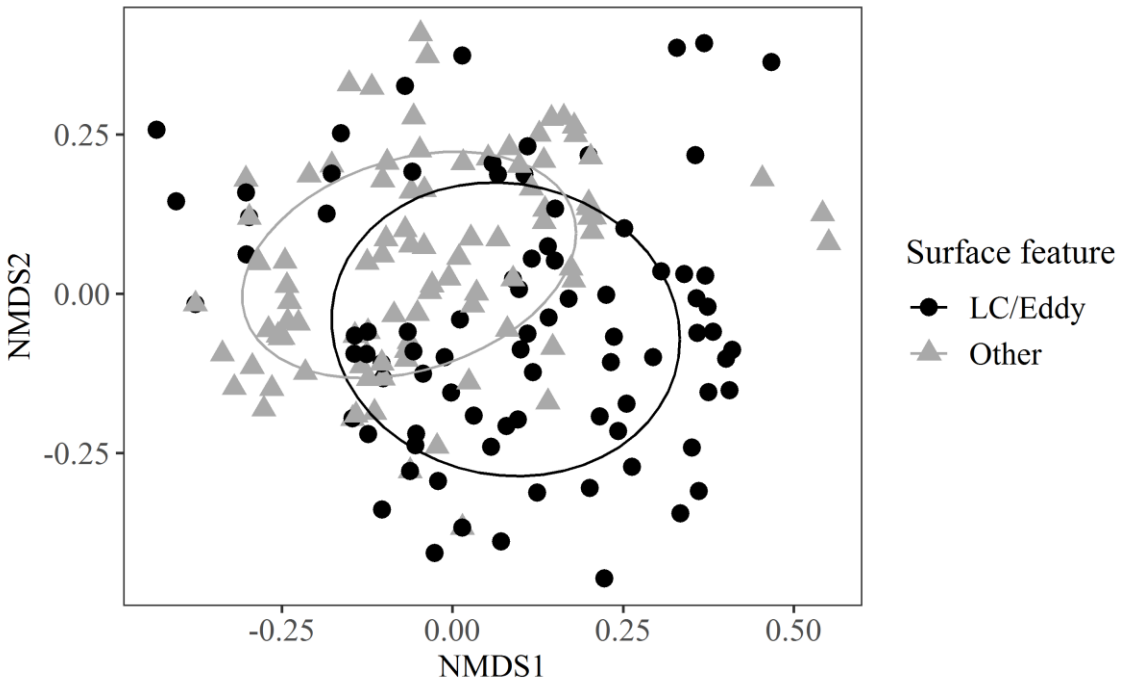


Figure 2.11 NMDS plot of *Seriola rivoliana* diet coded by surface feature. Ellipses denote 50% confidence intervals of each surface feature type. Sample sizes: LC/Eddy (n = 96), Other (n = 118).

Some ontogenetic diet shifts were observed for Almaco Jack (Figure 2.12; Table 2.6). The 0-50 mm and 50-100 mm size classes had biologically significant overlap, and fishes from both size classes had similar proportions of Slender Sargassum Shrimp, other shrimp, and fish eggs in their diets. The 50 – 100 mm size class also overlapped with the 100 – 150 mm TL size class, and both size classes consumed Brown Grass Shrimp, fish, chaetognaths, and calanoid copepods in similar proportions. The four size classes from 100 – 300 mm TL were all found to have biologically significant overlap with each other. Individuals of these size classes had a very diverse diet, and were the only size classes of this species observed feeding on amphipods. Almaco Jack of these size classes also consumed decapod larvae, molluscs, and stomatopods. The largest size class (300+ mm TL) was found to not have biologically significant overlap with any of the other smaller size classes. At this size, Slender Sargassum Shrimp, other shrimp, and fish were a large proportion of the diet, and were also found feeding on *Cerataspis* which were not observed in any other size class. Individuals in this size class were also found feeding on epiphytes and *Sargassum* more than in any other size classes.

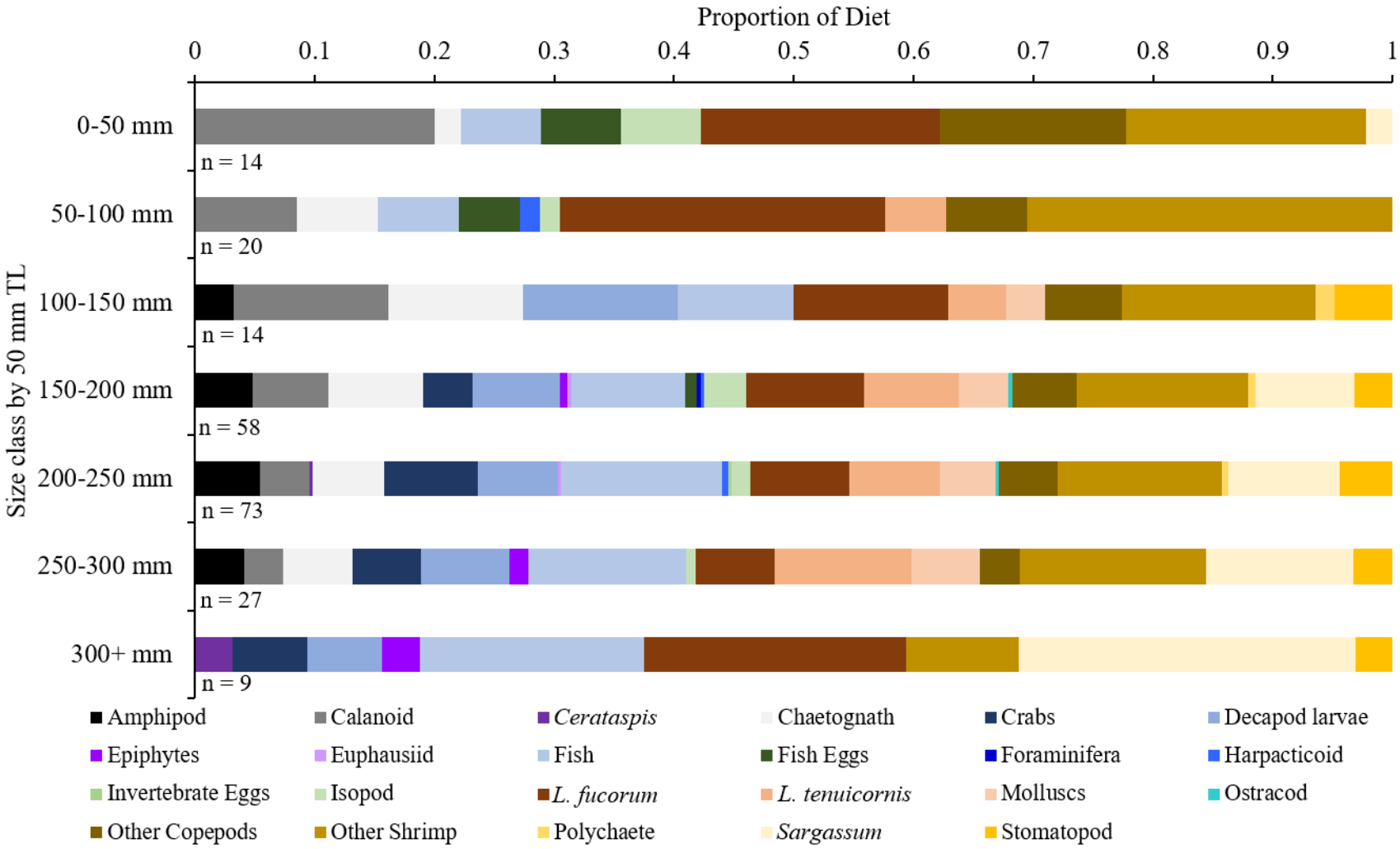


Figure 2.12 Relative abundance (standardized proportion) of prey for 50-mm size classes of *Seriola rivoliana*.

Table 2.6 Schoener indices of diet overlap for pairwise comparisons of 50-mm size classes of *Seriola rivoliana.* Cells with values >0.60 (highlighted in bold) denote biologically significant overlap between size classes.

| | **0-50** | **50-100** | **100-150** | **150-200** | **200-250** | **250-300** | **300+** |
|---|---|---|---|---|---|---|---|
| **0-50** | - | | | | | | |
| **50-100** | **0.71** | - | | | | | |
| **100-150** | 0.57 | **0.62** | - | | | | |
| **150-200** | 0.51 | 0.57 | **0.76** | - | | | |
| **200-250** | 0.44 | 0.51 | **0.70** | **0.88** | - | | |
| **250-300** | 0.41 | 0.47 | **0.66** | **0.83** | **0.88** | - | |
| **300+** | 0.38 | 0.38 | 0.41 | 0.51 | 0.56 | 0.58 | - |

### 2.3.5 Tripletail

A total of 34 out of 35 Tripletail (16.7 to 214.0 mm TL) had stomach contents and were available for analysis (Table 2.7). There was some differences observed in %F of diet items between cruises, but Tripletail frequently consumed Slender Sargassum Shrimp and other shrimp in July 2017, July 2018, and June 2019 (Figure 2.13). In June 2019, Slender Sargassum Shrimp, Brown Grass Shrimp, and *Sargassum* were observed to have higher %F than the other cruises. In the two July cruises, harpacticoid copepods, isopods, and molluscs were found in the diet, which were not observed in the diet in June 2019. There was relatively little temporal variability observed in Tripletail diet, with the most overlap between the July cruises (Figure 2.14; 2D stress = 0.17; ANOSIM R = 0.002, p = 0.407). The *BIOENV* analysis determined that the best model had salinity (p = 0.105) and water depth (p = 0.147) included, though a very low correlation value was observed (Spearman's $\rho = 0.05$). There was also high degree of overlap in Tripletail diet between surface feature type (Figure 2.15; 2D stress = 0.17; ANOSIM R = 0.09, p = 0.161).

Table 2.7 Percent frequency of occurrence (%F) for *Lobotes surinamensis* prey items for each cruise and for all cruises combined (Total). The n-values denote number of fish guts examined for diet analysis.

| Prey Item | July 2017 **n = 12** | June 2018 **n = 2** | July 2018 **n = 12** | June 2019 **n = 8** | Total **n = 34** |
|---|---|---|---|---|---|
| **ANNELIDA** | | | | | |
| Polychaete | 8.3 | 0.0 | 0.0 | 0.0 | 2.9 |
| **ARTHROPODA** | | | | | |
| Calanoid | 25.0 | 0.0 | 33.3 | 12.5 | 23.5 |
| Harpacticoid | 16.7 | 0.0 | 8.3 | 0.0 | 8.8 |
| Other Copepods | 16.7 | 0.0 | 33.3 | 0.0 | 17.6 |
| *L. fucorum* | 83.3 | 100.0 | 66.7 | 100.0 | 82.4 |
| *L. tenuicornis* | 25.0 | 100.0 | 25.0 | 50.0 | 35.3 |
| Other Shrimp | 100.0 | 100.0 | 91.7 | 75.0 | 91.2 |
| Crabs | 25.0 | 100.0 | 0.0 | 12.5 | 17.6 |
| Isopod | 8.3 | 100.0 | 8.3 | 0.0 | 11.8 |
| **MOLLUSCA** | | | | | |
| Molluscs | 8.3 | 50.0 | 8.3 | 0.0 | 8.8 |
| **OCHROPHYTA** | | | | | |
| *Sargassum* | 16.7 | 100.0 | 8.3 | 50.0 | 26.5 |
| **CHORDATA** | | | | | |
| Fish | 16.7 | 50.0 | 8.3 | 12.5 | 14.7 |
| **OTHER** | | | | | |
| Invertebrate Eggs | 16.7 | 0.0 | 0.0 | 0.0 | 5.9 |

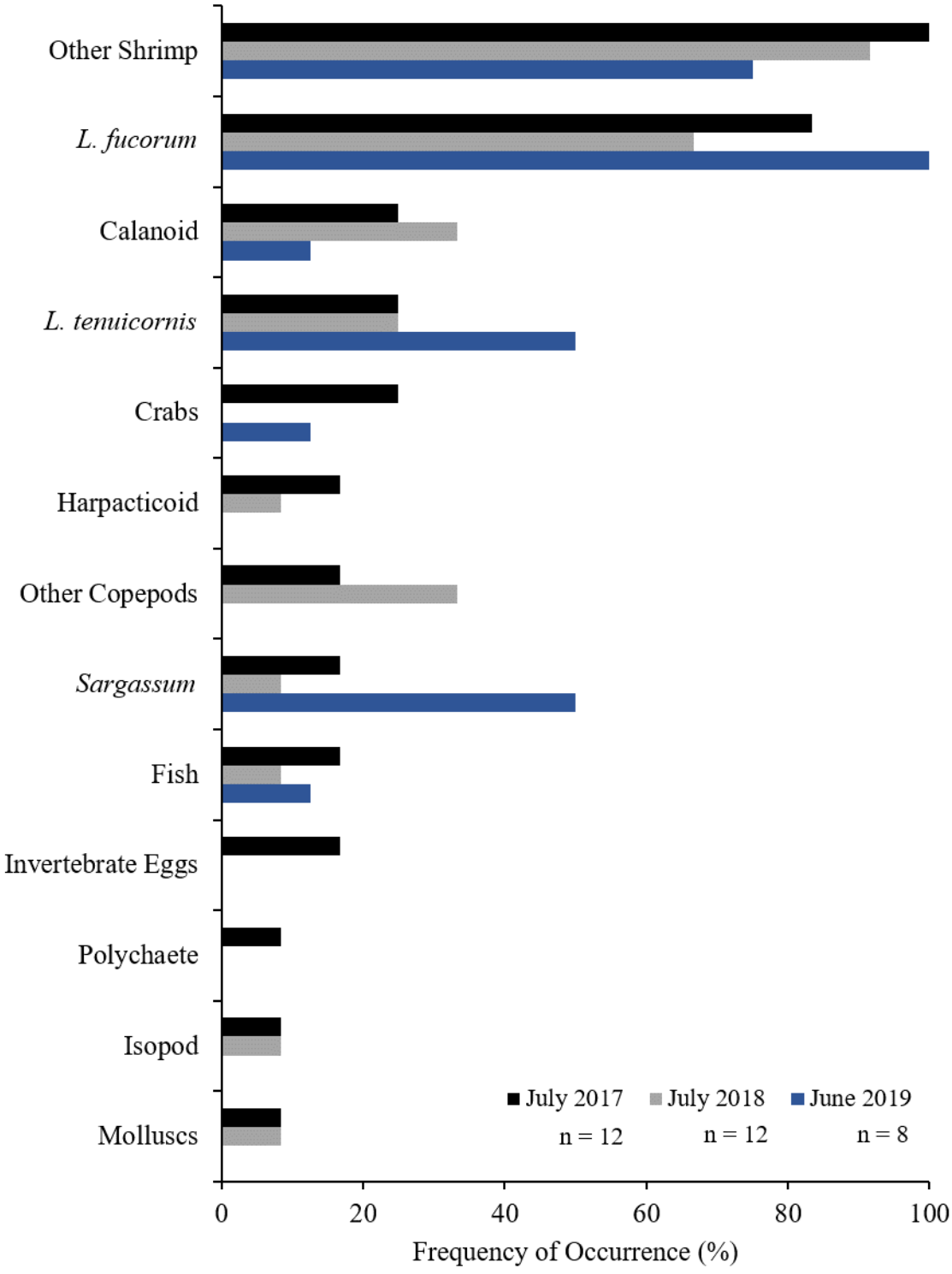


Figure 2.13 Frequency of occurrence (%) of *Lobotes surianmensis* prey items for fishes collected in July 2017, July 2018, and June 2019. The n-values denote the number fish guts examined for diet analysis.

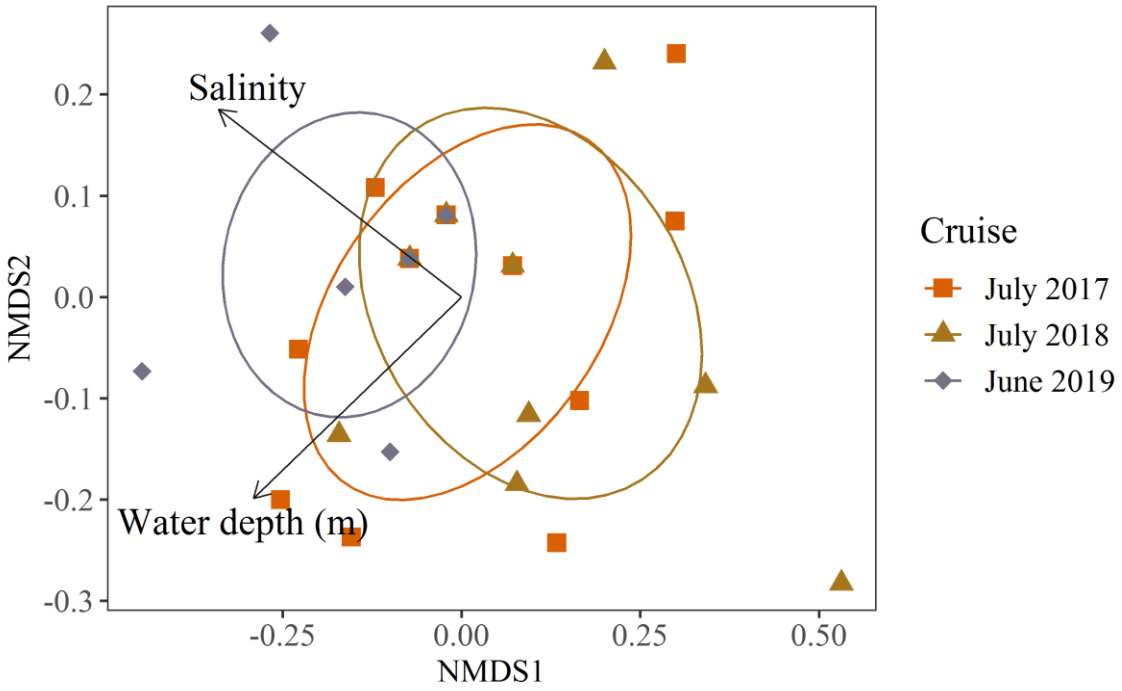


Figure 2.14 NMDS plot of *Lobotes surinamensis* diet by cruise (July 2017, July 2018, and June 2019). Direction and magnitude of vectors denote relative influence of environmental factors. Ellipses denote 50% confidence intervals of each cruise and vectors included for environmental variables determined to be in best model using a BIOENV analysis. Cruise sample sizes: July 2017 (n = 12), July 2018 (n = 12), June 2019 (n = 8).

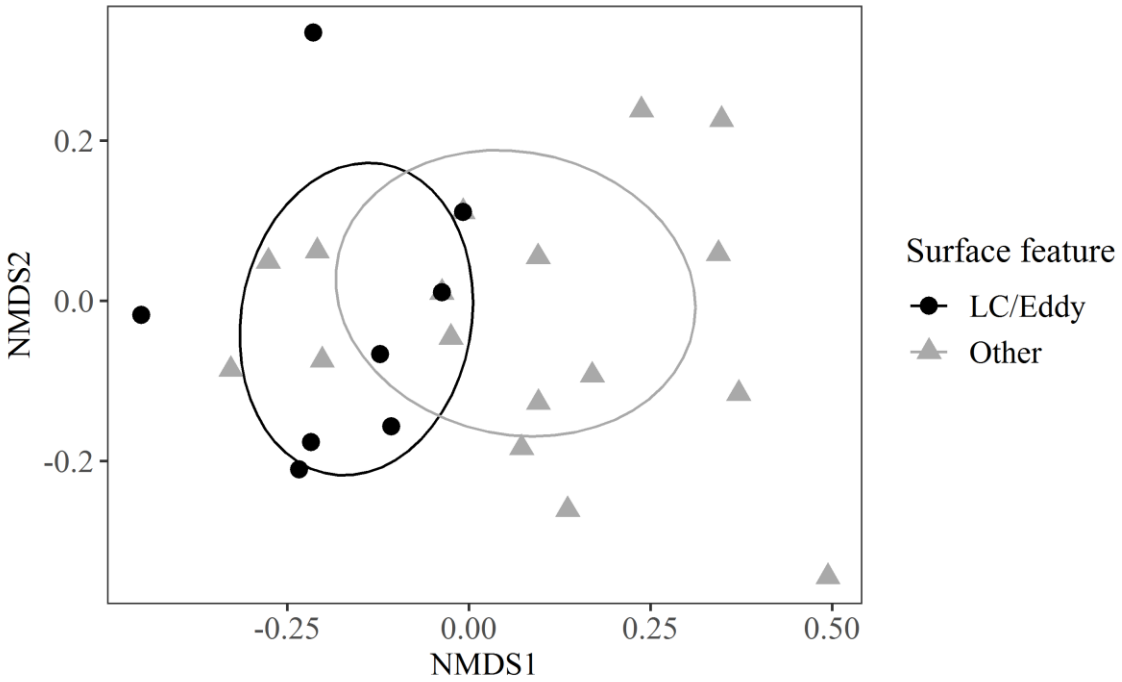


Figure 2.15 NMDS plot of *Lobotes surinamensis* diet coded by surface feature. Ellipses denote 50% confidence intervals of each surface feature type. Sample sizes: LC/Eddy (n = 10), Other (n = 24).

### 2.3.6 Diet Overlap Among Species

A high degree of overlap in diet was observed among the species examined, with the most dissimilar diets being Gray Triggerfish and Tripletail (Figure 2.16; 2D stress = 0.19; ANOSIM R = 0.24, p = 0.001). This separation was also observed when using the Schoener Index, with Gray Triggerfish having no biologically significant overlap in diet with any of the other species (Table 2.8). Greater Amberjack were found to have overlap with Lesser Amberjack, Almaco Jack and Tripletail. Lesser Amberjack was found to have biologically significant overlap with Tripletail as well as Greater Amberjack.

Table 2.8 Schoener indices of diet overlap for pairwise comparisons of species. Cells with values >0.60 (highlighted in bold) denote biologically significant overlap between species.

| | Gray Triggerfish | Greater Amberjack | Lesser Amberjack | Almaco Jack | Tripletail |
|---|---|---|---|---|---|
| Gray Triggerfish | - | | | | |
| Greater Amberjack | 0.47 | - | | | |
| Lesser Amberjack | 0.48 | **0.70** | - | | |
| Almaco Jack | 0.55 | **0.82** | **0.77** | - | |
| Tripletail | 0.51 | **0.72** | 0.59 | **0.67** | - |

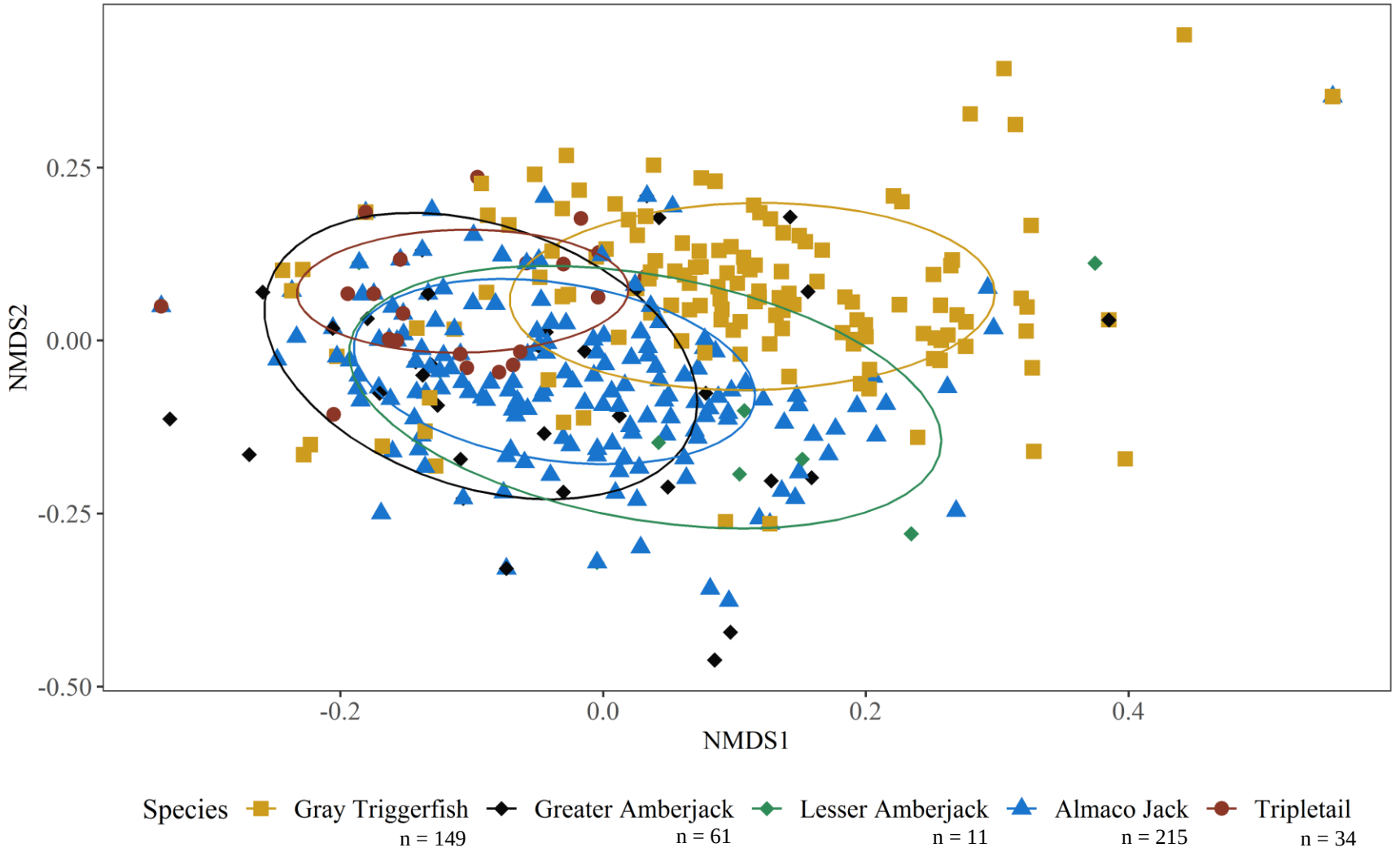


Figure 2.16 NMDS plot of all species diet coded by species. Ellipses denote 50% confidence intervals of each species.

## 2.4 Discussion

The proposed role of *Sargassum* as nursery habitat has largely been supported by observations of high juvenile fish abundances, however juvenile density is only one characteristic of nursery habitats (Beck et al. 2001). Identifying factors that contribute to the growth and survival of juvenile fishes further supports the nursery role function of *Sargassum*. In this study, among the most dominant prey items observed in the diets of the target species were *Sargassum*-associated fauna, such as epiphytes, the endemic shrimp *L. fucorum* and *L. tenuicornis*, and crabs. Although no open water collections of fishes were available for analysis, the high prevalence of these diet items suggest that juvenile Gray Triggerfish, Greater Amberjack, Lesser Amberjack, Almaco Jack, and Tripletail rely on *Sargassum* habitats for foraging. When compared in a previous study off the coast of North Carolina, the diets of fishes collected in *Sargassum* were found to have twice as many prey items as those collected in open water habitats (Casazza 2008), with the open water fishes feeding primarily on copepods and flyingfishes, and the *Sargassum*-associated fishes feeding on *L. fucorum* and *L. tenuicornis*. Although prey availability was not quantified in my study, many of the dominant prey items found in fish guts were abundant in the neuston net tows used to collect fishes, further supporting the hypothesis that *Sargassum* likely functions as a critical nursery habitat for these species.

Among the species examined, juvenile Gray Triggerfish had the most dissimilar diet relative to other species. Although all of the fish species foraged in association with *Sargassum*, the relative importance of the habitat with respect to feeding may vary by species. In this respect *Sargassum* may function as either obligate or facultative foraging

habitat. Similar habitat relationships are found in marine environments; for example reef fishes that feed directly on coral can range from obligate feeders that feed only on coral to more facultative feeders that have coral as a small portion of their diet (Graham et al. 2009). Similarly, reef fish predators include species that inhabit reef environments along with prey species, as well as those that are transient, and move throughout multiple reefs to find prey (Hixon and Carr 1997). The fishes associated with *Sargassum* fall along a similar continuum of dependency on the habitat for feeding, with some species more obligate and others more transient or mobile. Gray Triggerfish relied heavily on *Sargassum* epiphytes, such as bryozoans and a serpulid polychate (*Spirorbis* sp.), which suggests an obligate or close foraging association with *Sargassum*. In contrast, the diets of Greater Amberjack, Lesser Amberjack, and Almaco Jack included relatively high (and variable) proportions of both endemic prey (e.g., *L. fucorum* and *L. tenuicornis*), as well as pelagic zooplankton (e.g., decapod larvae, chaetognaths, stomatopods), which suggest a more transient or facultative use of the habitat. Tripletail also appear to have a more obligate use of the *Sargassum* for feeding, as the prey they consumed are found within the habitat (e.g., *L. fucorum*, *L. tenuicornis*, crabs, polychaetes). Though both Tripletail and Gray Triggerfish appear to be obligate feeders on the *Sargassum*, the diets of these species were dissimilar in that Gray Triggerfish fed on epiphytes and Tripletail fed more frequently on the two endemic shrimp species. The relative reliance of *Sargassum* habitat use has implications for the management of *Sargassum* as a habitat, and its relationship to the early life history of managed species.

Evidence for size-related shifts in diet were observed for both Greater Amberjack and Almaco Jack, which indicate that the relative importance of *Sargassum* as a foraging

habitat changes through ontogeny. For both species, *Sargassum*-associated prey items were observed in the diet throughout all predator size classes, but after reaching a size of about 100 mm TL, individuals were also observed feeding on zooplankton (e.g., decapod larvae, stomatopods). Although the larger juveniles consumed prey in the *Sargassum* as well as outside of the habitat, the smaller juveniles appear to be more dependent on the *Sargassum* for feeding. These results indicate that to determine the dependency of a species on the *Sargassum*, the size of individuals must also be considered. Size-related diet shifts have not previously been investigated in *Sargassum* habitats using gut content analysis, but shifts in trophic position have been observed between the juvenile and adult stages of *S. dumerili* using stable isotope analysis (Rooker et al. 2006). Adult *S. dumerili* were found to be enriched in $^{15}N$, and were feeding about one trophic level higher than juveniles of the same species. Diet shifts related to ontogeny have been observed using gut content analysis of juvenile carnivorous grunts and snappers in nursery habitats of the Spanish Water Bay (de la Moriniere et al. 2003). A shift in feeding from small crustaceans to larger decapods and fishes was observed as predatory juvenile grunts and snappers increased in size. de la Moriniere et al. (2003) suggest this shift to larger prey with increasing predator size could result in juveniles expanding their foraging distance at larger size classes. The authors also suggest this would promote the migrations of larger juveniles and sub-adults from the nursery habitats to coral reefs. An analogous situation may be occurring with the diet shifts of Greater Amberjack and Almaco Jack, as they appear to rely less on the *Sargassum* for feeding at larger size classes, and the observed diet shift could facilitate movement of these juveniles to their adult habitats.

Among the environmental variables examined, surface chlorophyll was found to contribute to diet variability for Almaco Jack. Specifically, surface chlorophyll was a strong predictor and had the opposite influence of distance from shelf break on the diet of Almaco Jack. This could be because higher surface chlorophyll concentrations were observed near stations collected closer to the shelf. Remote-sensed estimates of surface chlorophyll-*a* can be used as an indicator of primary productivity (Grémillet et al. 2008). Although this application of surface chlorophyll can be used to predict distributions of primary consumers, it is not always a reliable predictor of top predators and other intermediate trophic levels. For example, Grémillet et al. (2008) found that even though distribution of top predator marine birds was related to primary productivity, there was mismatch throughout the subsequent lower trophic levels of fishes in the food web. Since I observed diet for juvenile fishes at multiple trophic levels, I may be observing a similar mismatch between the different fishes and primary productivity (surface chlorophyll). For example, juvenile Gray Triggerfish in *Sargassum* have a trophic level of 1.7, and juvenile Almaco Jack feed at a trophic level of 3.7, as determined using stable isotope analysis (Rooker et al. 2006). Lower level consumers like Gray Triggerfish may have a mismatch with surface chlorophyll, and at higher trophic levels a match may be observed again with surface chlorophyll for predators like Almaco Jack. So, surface chlorophyll may be used in a bottom-up approach in observing the trophic structure of the food web associated with *Sargassum*.

I also found that variability in diet was influenced by surface feature type for Greater Amberjack, Lesser Amberjack, and Almaco Jack. There is evidence of differences in stable isotope values of invertebrates which are common prey items of

juvenile fishes in our study (e.g., *Leander tenuicornis* and *Portunus sayi* (Sargassum crab)) between eddy types (Wells et al. 2017). Stable isotope values of primary producers (POM and *Sargassum*) and consumers were compared between two different sample collections in the GOM: within the Loop Current/anticyclonic eddies, and cyclonic eddies. Mean total biomass was higher in samples collected within cyclonic eddies compared to anticylonic eddies, and the producers as well as most of the consumers were found to be more nitrogen-enriched in cyclonic eddies (Wells et al. 2017). Since anticyclonic eddies in the GOM often originate from the Loop Current, it can be inferred that the prey introduced from the Loop Current could be less abundant and of different quality than the prey already established in the GOM. Therefore, the variability observed in diets of Greater Amberjack, Lesser Amberjack, and Almaco Jack associated with different surface features could be a result of prey abundance or quality. This suggests the origin of *Sargassum* and where the community is establishing could influence its nursery-role function and the trophic relationships of different fishes associated with the habitat type. Future research should focus on making this direct relationship for *Sargassum* habitats by characterizing the prey field of Loop Current derived *Sargassum* compared to *Sargassum* established within the GOM.

Although there was little evidence of temporal variability in fish diets, spatial variability was observed. Distance from shelf break influenced diets of Gray Triggerfish, Greater Amberjack, and Almaco Jack. This suggests that the prey available throughout our sampling region was variable. Since I observed surface chlorophyll to have the opposite relationship of distance from shelf break to Almaco Jack diet, I can infer that primary productivity is decreasing with increasing distance from the continental shelf

break. This is expected as the nearshore waters are highly productive with nutrient input from rivers and estuaries into the GOM. Though surface chlorophyll was influencing the diet of Almaco Jack, it was not a factor for the other species influenced by distance from shelf break. This could suggest that for Gray Triggerfish and Greater Amberjack, feeding behavior was spatially variable but not directly associated to primary productivity. Because I observed diet to be spatially variable within the northern GOM, diets of these species should also be studied in other regions of the GOM to understand the variability in the role of *Sargassum* as a nursery for juvenile fishes at a larger scale. The results of this chapter can be used as a baseline for feeding habits of juvenile fishes in the area sampled in this study, but future efforts could build upon this data set to better understand the large-scale differences in trophic relationships in *Sargassum*.

The results of this chapter fill a current knowledge gap because diet studies of these species are limited, especially in the GOM, and at the smaller size ranges collected in this study. This study has provided a better understanding of diet variability of juvenile fishes and the spatial and environmental factors influencing diet. I provide evidence of the role of *Sargassum* as a nursery habitat for juvenile fishes in the GOM, and suggest how this function can be spatially variable. This chapter can be used to inform management about the role of *Sargassum* in the GOM as a food source for juvenile fish, and the need to protect and manage the habitat where species like Gray Triggerfish and Tripletail are depending heavily on for feeding. This study also can inform management about feeding habits of Amberjack species that are data-limited, and very little is known about their trophic variability in general.

### 2.4.1 Conclusion

*Sargassum* is a nursery habitat for juvenile fishes, and estimating the trophic variability of fishes that rely on the habitat for feeding using diet analysis can be used as a baseline for the use of the habitat by these species in anticipation of a changing ocean. Here I find that commercially- and recreationally-managed fishery species depend on *Sargassum* to feed as juveniles, which was observed as a continuum of dependence. Spatial variation in diet was most evident, as illustrated by distance from shelf break describing diet variability for Gray Triggerfish, Greater Amberjack, and Almaco Jack, as well as water depth and salinity describing diet variability of Lesser Amberjack and Tripletail. Ontogenetic shifts in diet for Greater Amberjack and Almaco Jack were also observed. The results of this chapter can be used to fill a current knowledge gap in the trophic ecology of smaller sizes classes of the selected species, as well as inform fisheries management of the variability in the role of *Sargassum* as a nursery habitat in the GOM.

Our future research will be focused on understanding the difference in prey communities between *Sargassum* and open water habitats, which will help provide a baseline for future studies that want to make conclusions about a predator's residency and reliance on the habitat for feeding, as well as make these conclusions in the current study. We also plan to compare the invertebrate prey within *Sargassum* collections of the Loop Current/anticyclonic eddies to those outside of such features. This will help us to understand the influence of surface features on the prey community, and how this can affect the feeding habits of associated juvenile fishes.

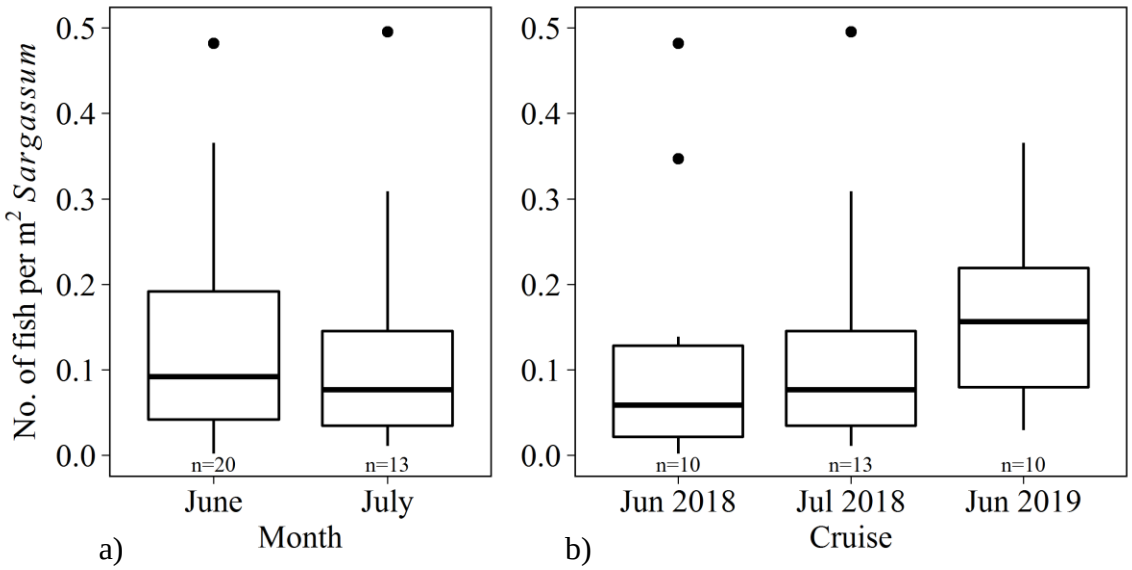


Figure A.1 Boxplots of number of fish collected in neuston nets per m$^2$ of *Sargassum* by a) month, and b) cruise. In boxplots, outside bars represent first and third quartiles and dark bar inside boxes represent median. Sample sizes are presented for each sample group.

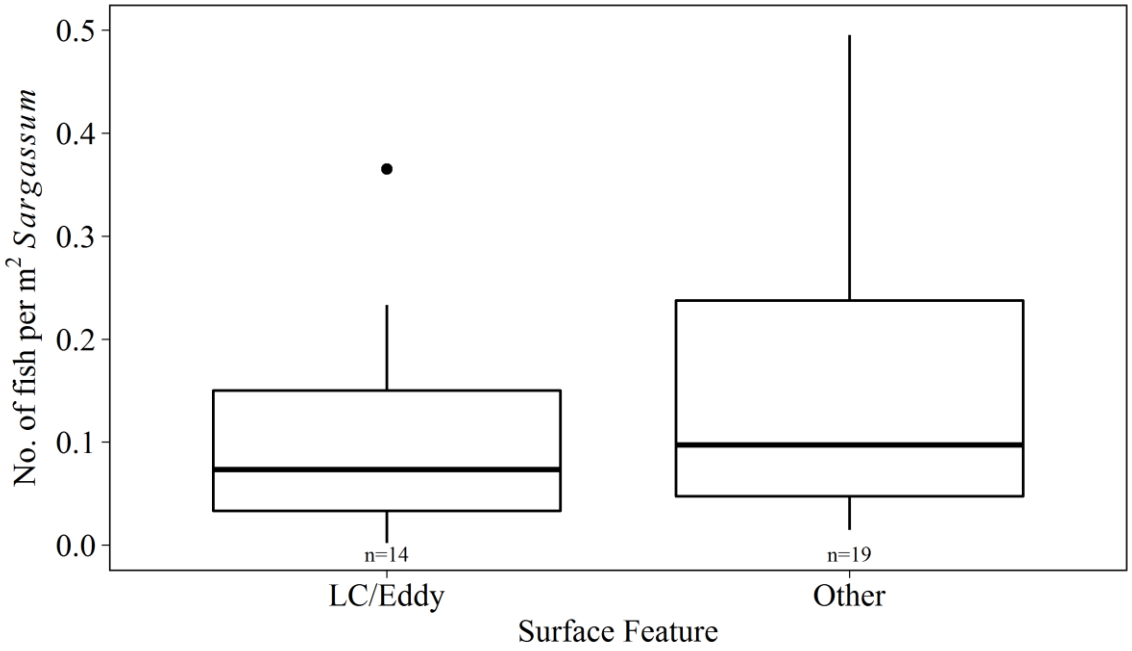


Figure A.2 Boxplot of number of fish collected in neuston nets per m$^2$ of *Sargassum* by surface feature. In boxplots, outside bars represent first and third quartiles and dark bar inside boxes represent median. Sample sizes are presented for each sample group.

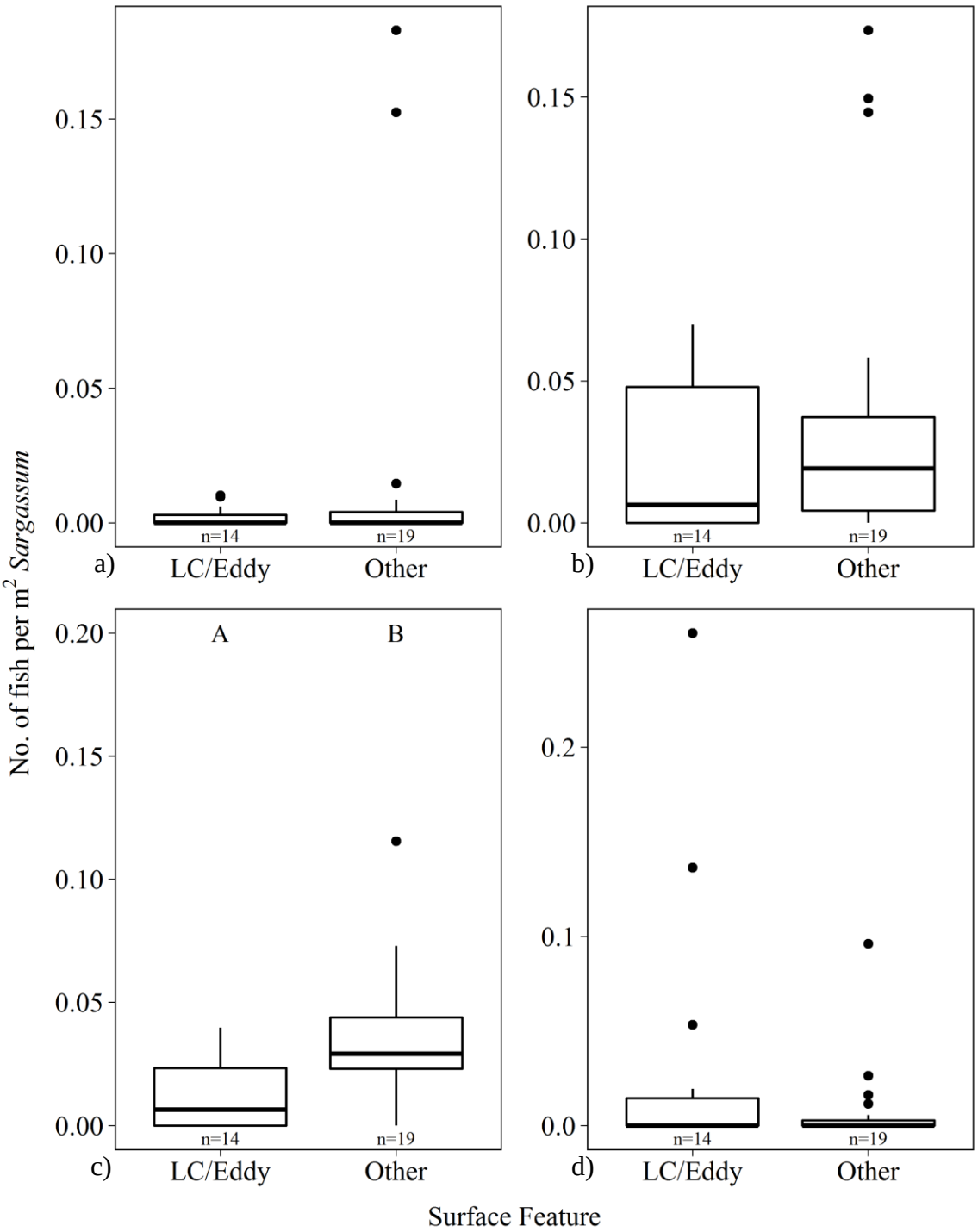


Figure A.3 Boxplots of number of fish collected in neuston nets per m$^2$ of *Sargassum* by surface feature for dominant taxa: a) *Balistes capriscus*, b) *Abudefduf saxatilis*, c) *Histrio histrio*, and d) *Stephanolepis* spp. In boxplots, outside bars represent first and third quartiles and dark bar inside boxes represent median. Sample sizes are presented for each sample group and letters indicate statistical significance among cruises as determined by a Kruskal-Wallis test and Wilcoxon rank sum pairwise test. Note the differences in y-axis values.

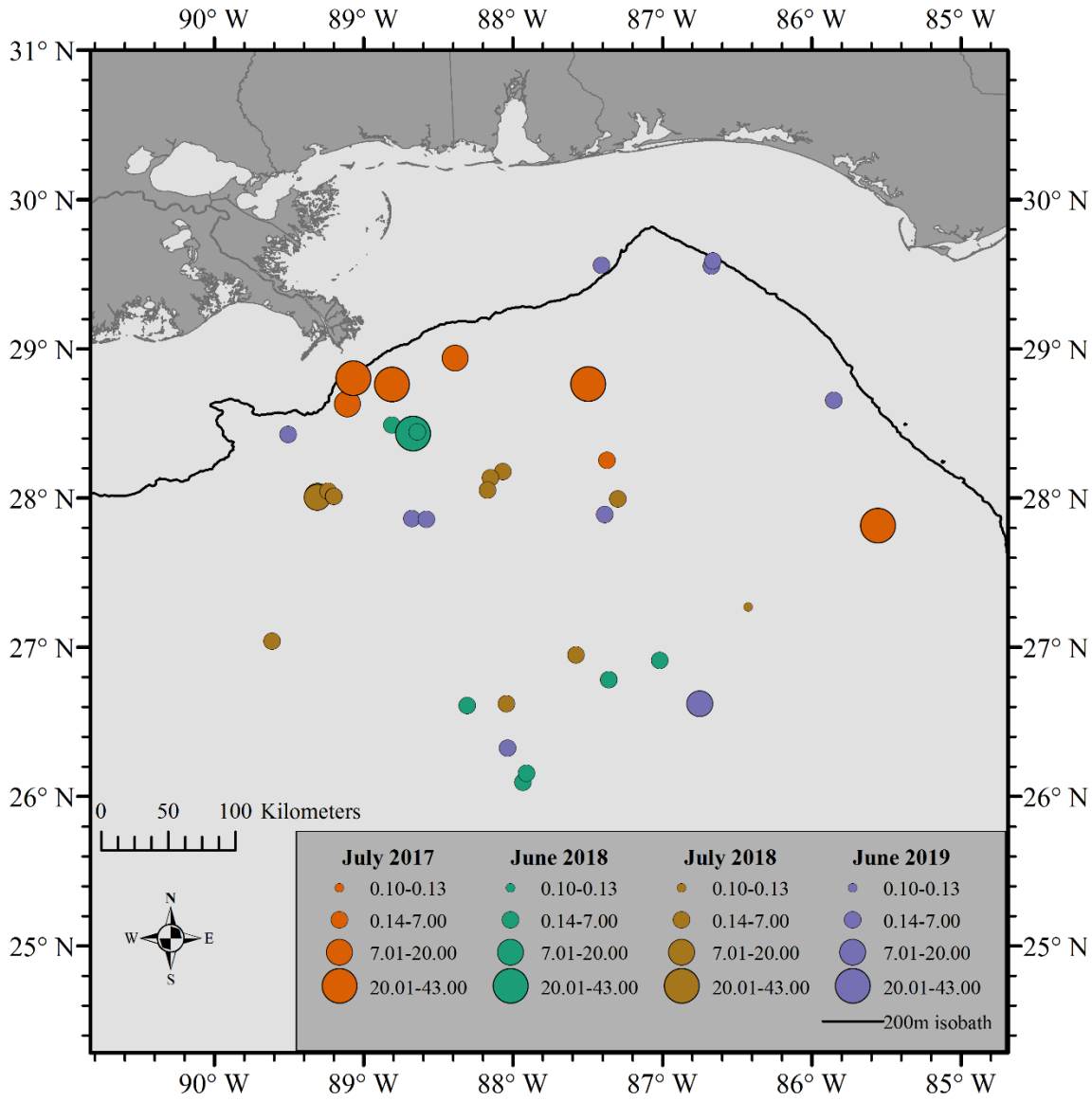


Figure A.4 Map of fish density expressed as total number of individuals per 10 kg of *Sargassum* collected. Size of point indicates which range of estimates that samples falls within, as shown in legend, and color of points indicates the cruise dates.

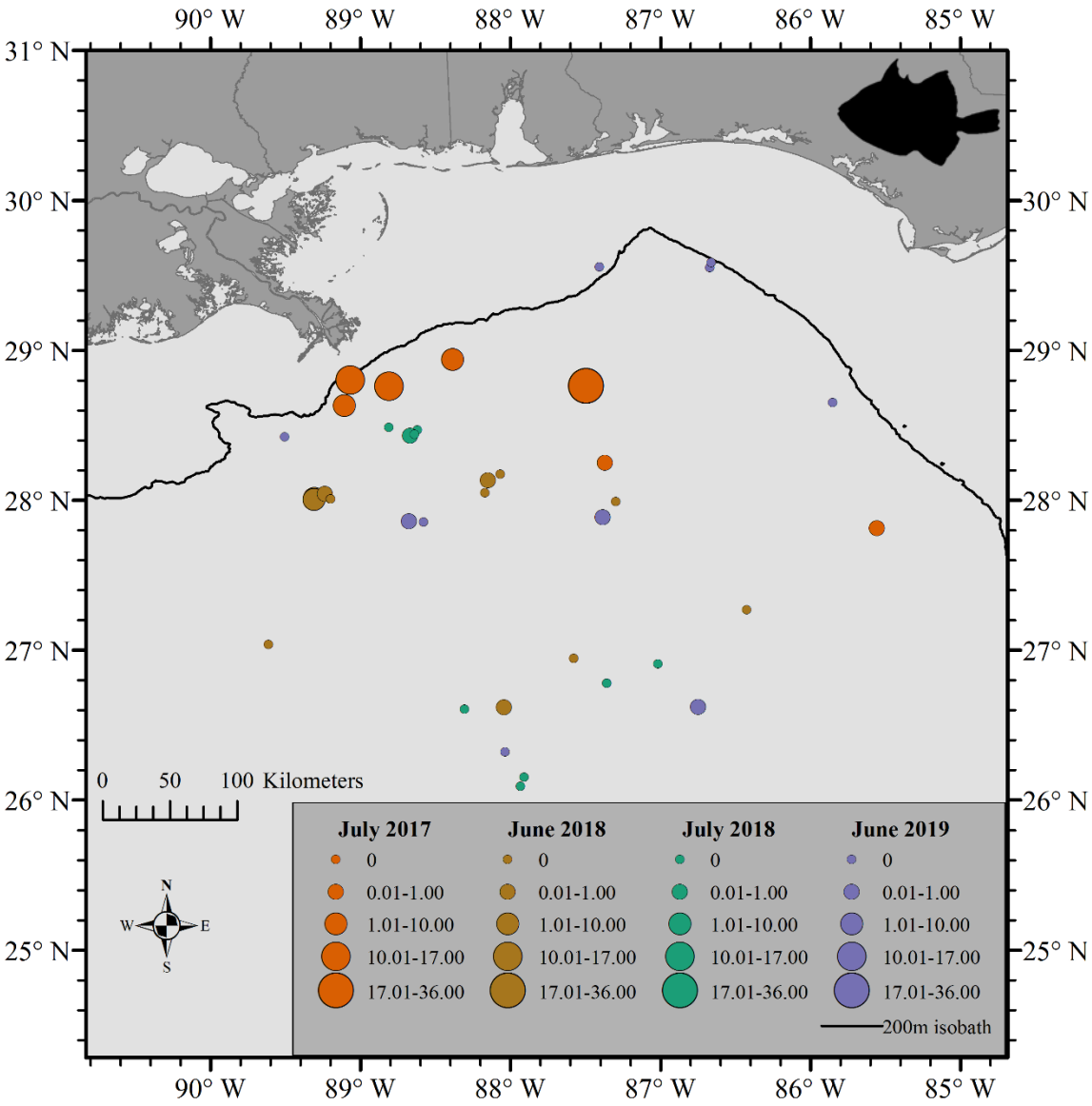


Figure A.5 Map of fish density expressed as number of *Balistes capriscus* per 10 kg *Sargassum* collected. Size of point indicates which range of estimates that samples falls within, as shown in legend, and color of points indicates the cruise dates.

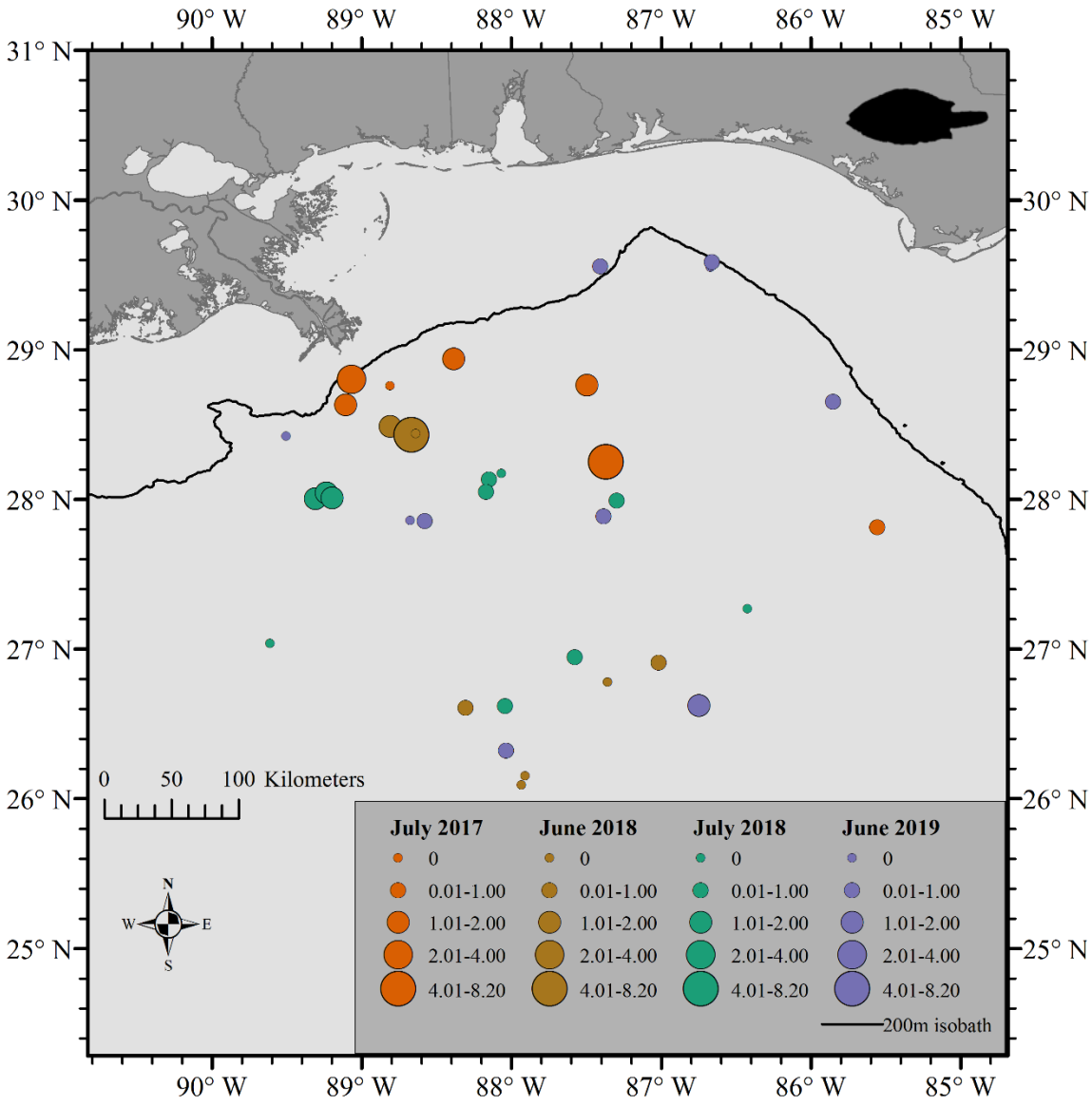


Figure A.6 Map of fish density expressed as number of *Abudefduf saxatilis* per 10 kg of *Sargassum* collected. Size of point indicates which range of estimates that samples falls within, as shown in legend, and color of points indicates the cruise dates.

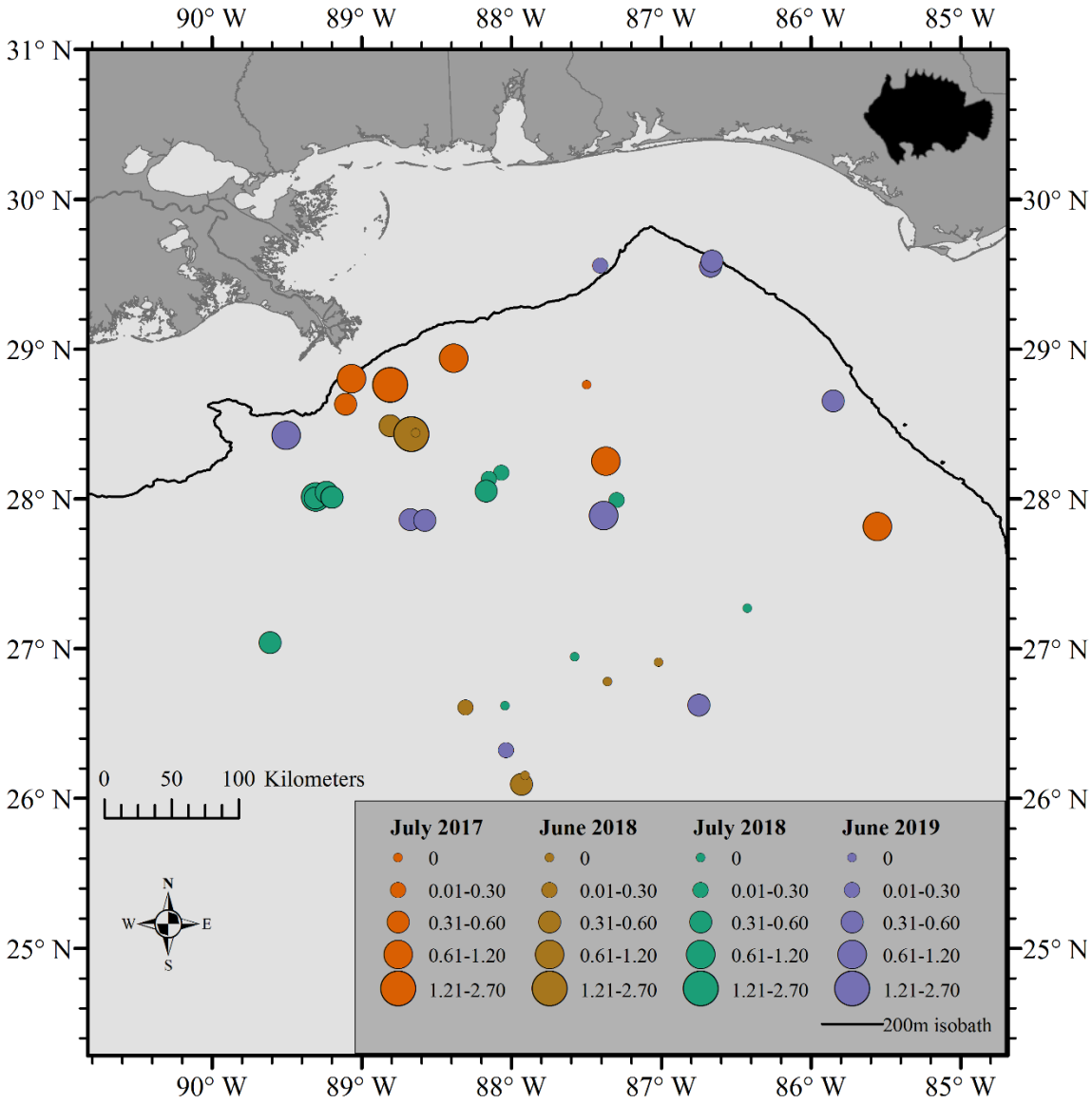


Figure A.7 Map of fish density expressed as number of *Histrio histrio* per 10 kg of *Sargassum* collected. Size of point indicates which range of estimates that samples falls within, as shown in legend, and color of points indicates the cruise dates.

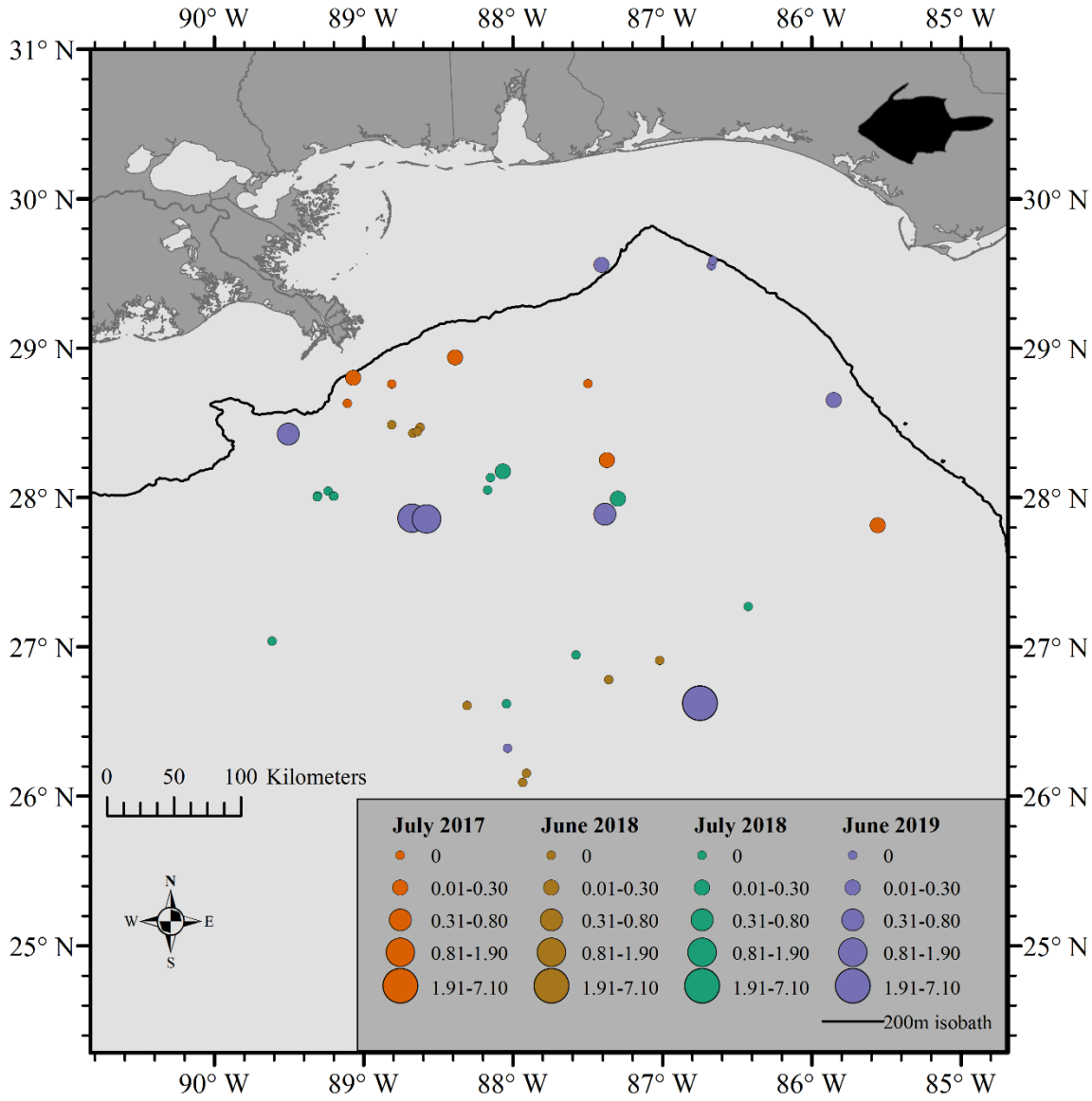


Figure A.8 Map of fish density expressed as number of *Stephanolepis* spp. per 10 kg of *Sargassum* collected. Size of point indicates which range of estimates that samples falls within, as shown in legend, and color of points indicates the cruise dates.

Table A.1 Results of GAMs for total fish density estimates based on neuston net collections (fish per $m^2$ *Sargassum*). Each model's Akaike's Information Criteria (AIC), deviance explained (DE), $r^2$, and sample size (n) provided above parameter significance values. Parameter (Par.) type given: If linear, a Wald-type 't' statistic value provided, if smooth a Wald-type 'F' statistic value provided. Significance values (p) provided for all statistics. Asterisk indicates significant p-value at alpha-level of 0.05.

| | **Model AIC = 36.8** | **DE = 66%** | **$r^2$ = 0.54** | **n = 33** | |
|---|---|---|---|---|---|
| Response Variable | Environmental Variable | Par. type | t | F | p |
| **No. total fish per $m^2$ *Sargassum*** | Water depth | linear | 1.41 | - | 0.171 |
| | Distance from shore | linear | -1.68 | - | 0.105 |
| | Temperature | smooth | - | 4.37 | 0.002* |

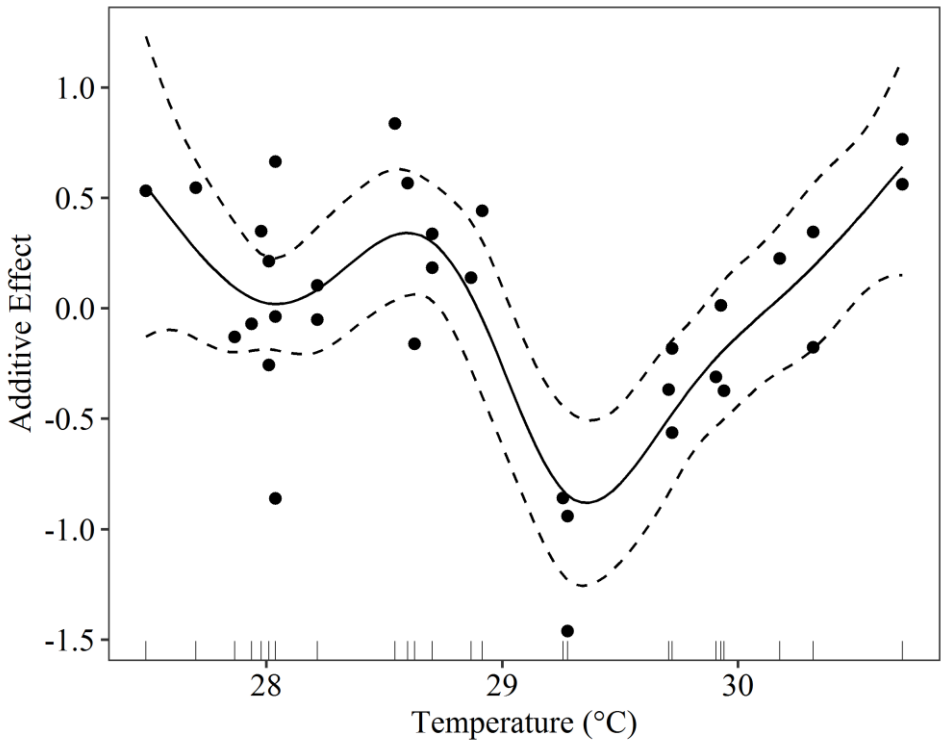


Figure A.9 Plot of $\log_{10}(x)$-transformed estimates of number of fish per $m^2$ *Sargassum* as a response to the only significant environmental variable in GAM with the lowest Akaike's Information Criteria (AIC). Solid line represents smoothed estimate and dashed lines represent 95% confidence intervals. Y-axis represents the additive effect of Temperature on the response variable.

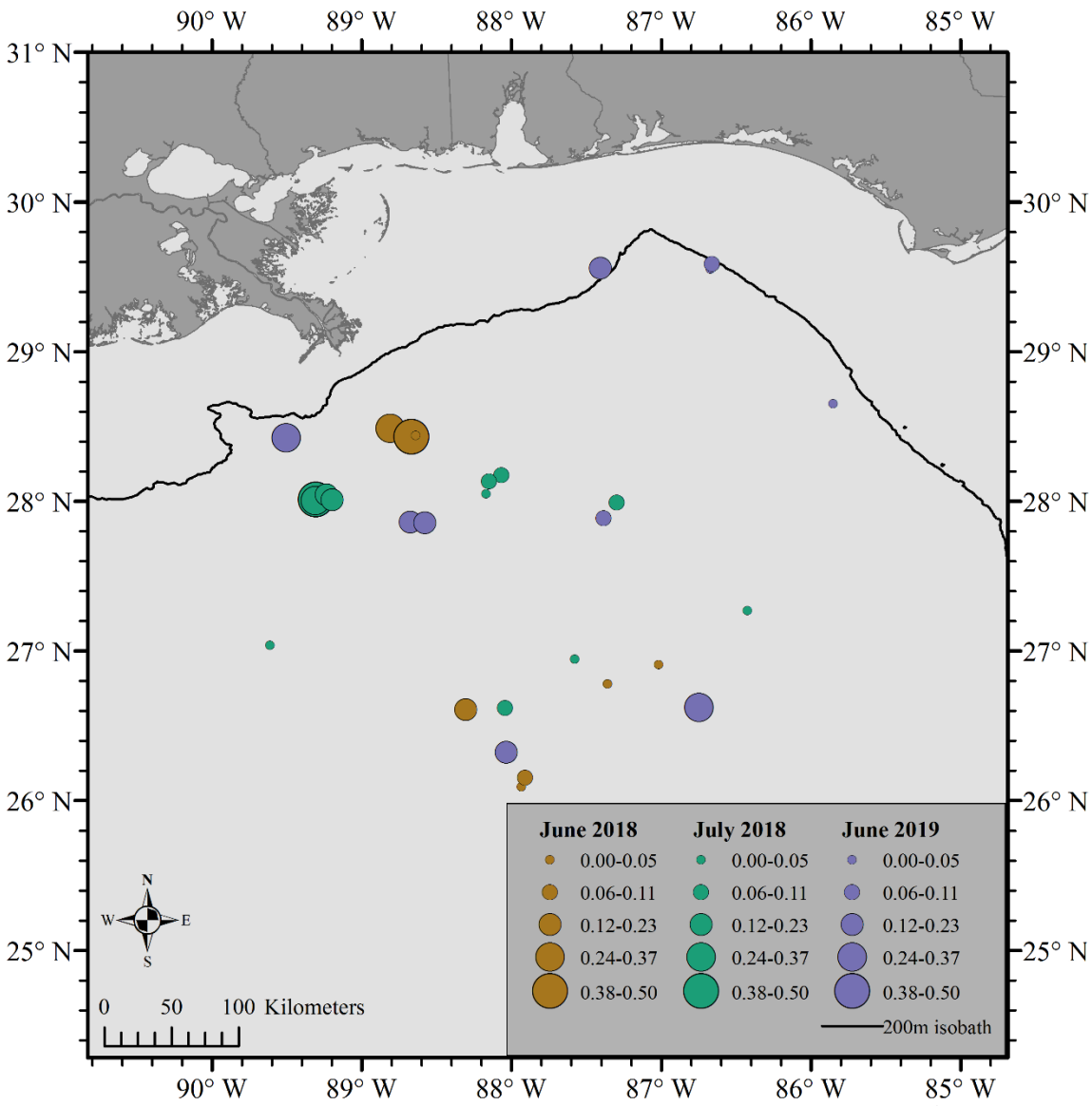


Figure A.10 Map of fish density expressed as number of fish collected per $m^2$ of *Sargassum*. Size of point indicates which range of estimates that samples falls within, as shown in legend, and color of points indicates the cruise dates.

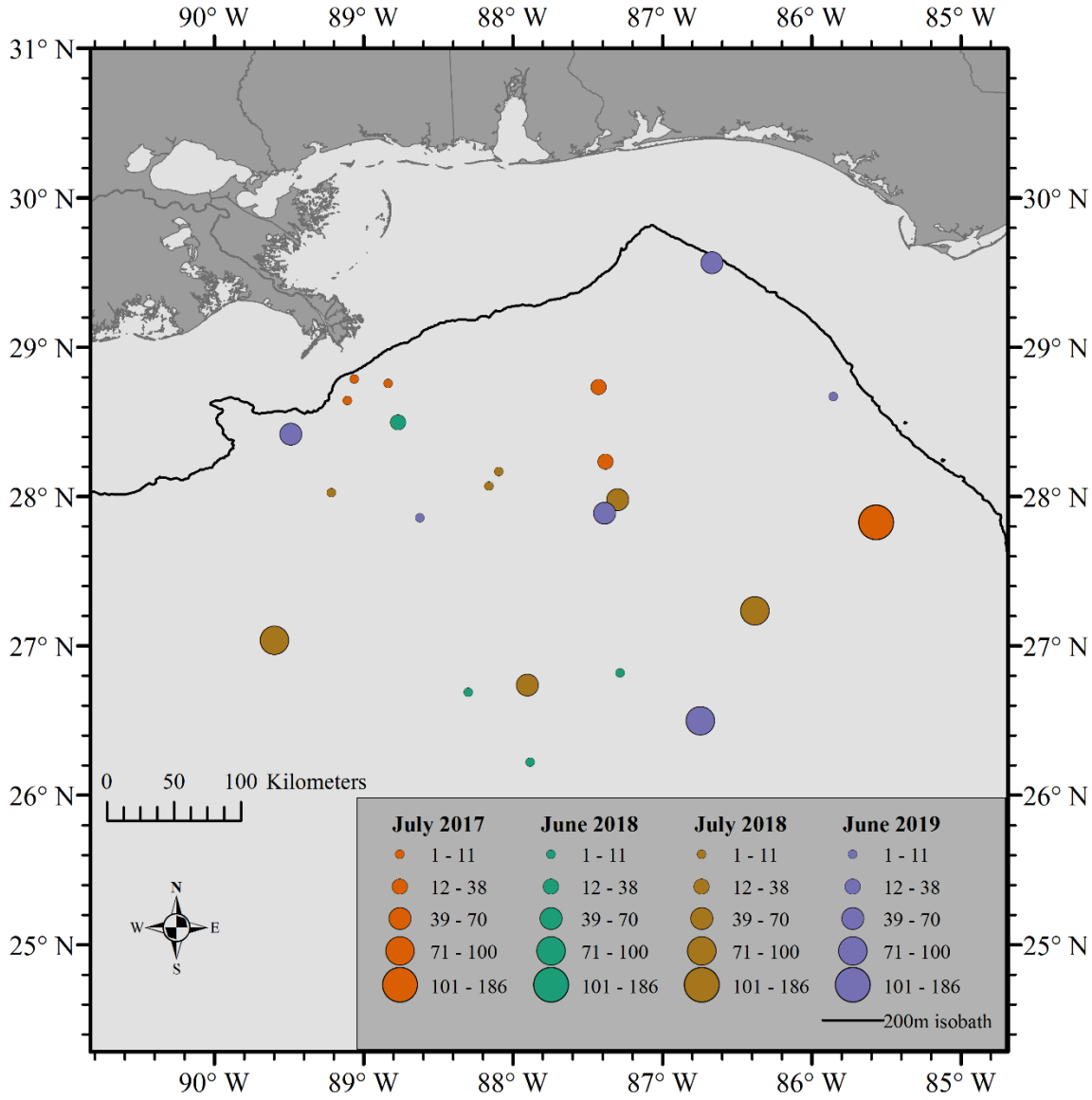


Figure A.11 Map of hook-and-line fish CPUE expressed as total number of individuals collected per 30 minute fishing period. Size of point indicates which range of estimates that samples falls within, as shown in legend, and color of points indicates the cruise dates.

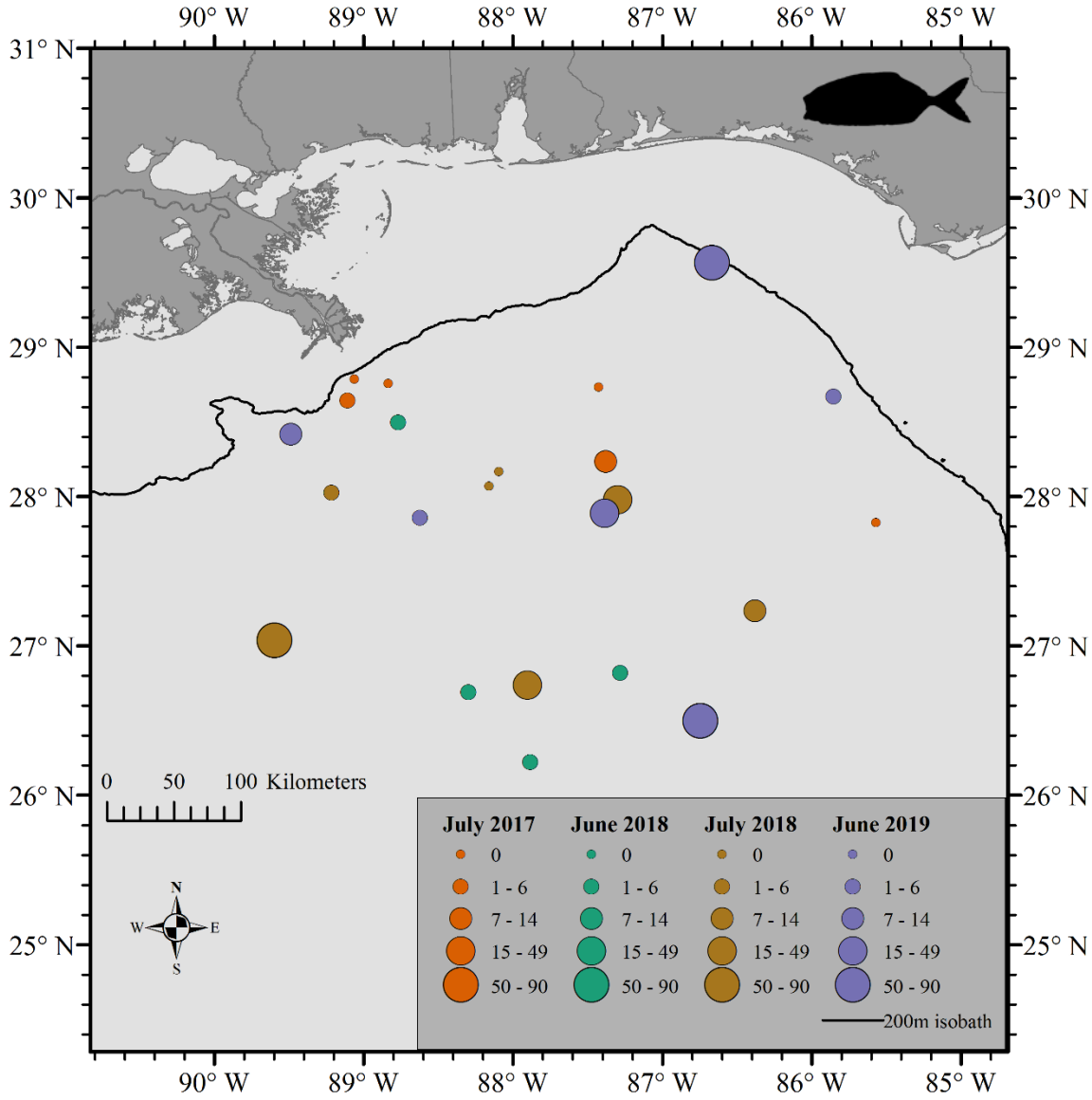


Figure A.12 Map of hook-and-line fish CPUE expressed as number of *Seriola rivoliana* collected per 30 minute fishing period. Size of point indicates which range of estimates that samples falls within, as shown in legend, and color of points indicates the cruise dates.

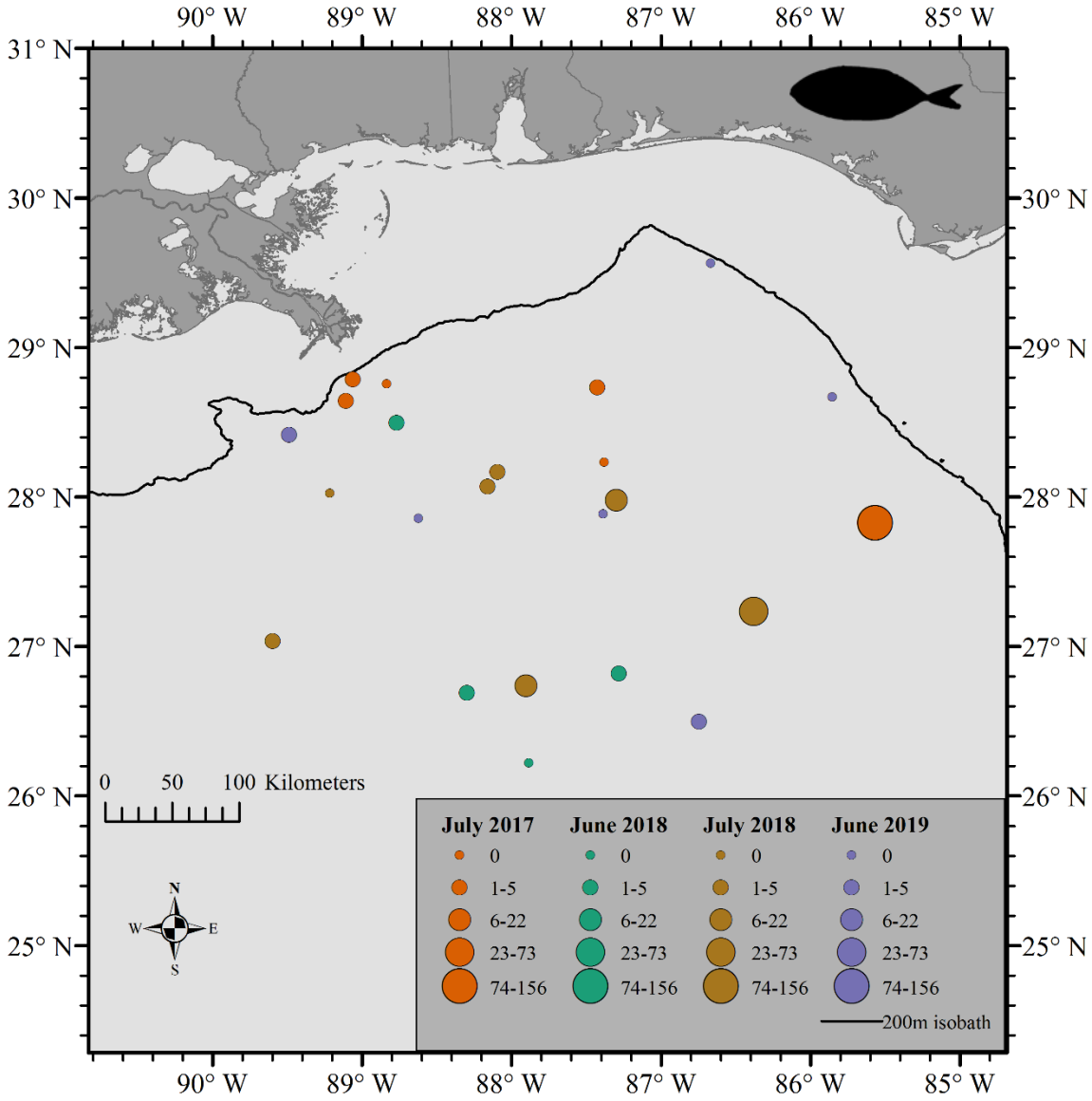


Figure A.13 Map of hook-and-line CPUE expressed as number of *Caranx crysos* collected per 30 minute fishing period. Size of point indicates which range of estimates that samples falls within, as shown in legend, and color of points indicates the cruise dates.

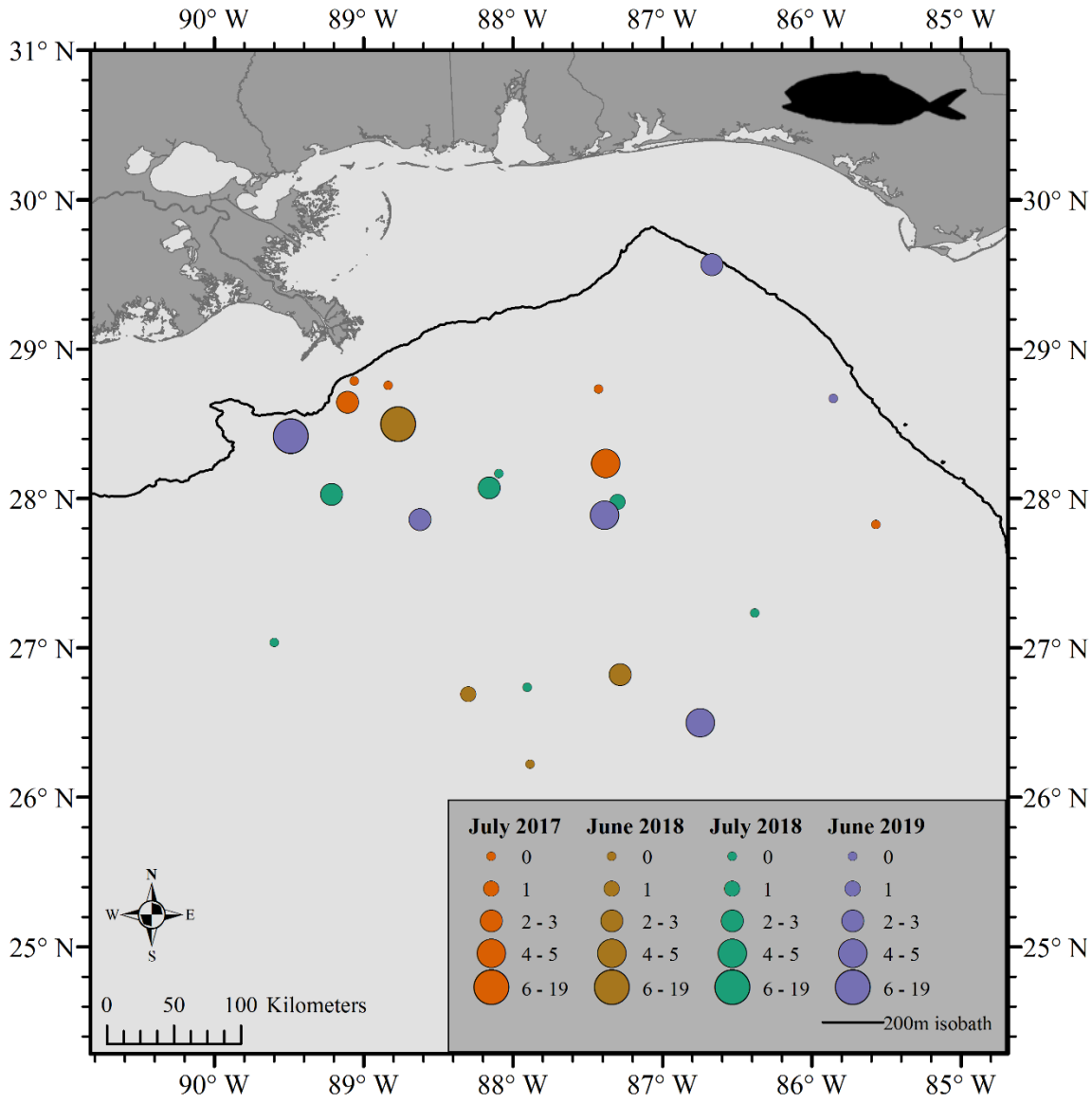


Figure A.14 Map of hook-and-line CPUE expressed as number of *Seriola dumerili* collected per 30 minute fishing period. Size of point indicates which range of estimates that samples falls within, as shown in legend, and color of points indicates the cruise dates.

Table A.2 Average (avg.) pairwise species abundances of neuston net collections by cruise based on SIMPER analysis. Taxa are ordered starting with those of highest contribution (%) to between-cruise dissimilarities with a cutoff of approximately 80% cumulative contribution.

| Species | Avg. contribution to overall dissimilarity (%) | Avg. Abundance | | Cumulative Contribution (%) |
|---|---|---|---|---|
| July 2017 - June 2018 | | July 2017 | June 2018 | |
| *B. capriscus* | 19.12 | 3.54 | 0.08 | 23.75 |
| *A. saxatilis* | 8.89 | 2.06 | 0.83 | 34.79 |
| *H. histrio* | 6.68 | 1.58 | 0.69 | 43.09 |
| *Kyphosus* spp. | 5.66 | 1.21 | 0.12 | 50.12 |
| *L. surinamensis* | 5.02 | 0.82 | 0.12 | 56.35 |
| *C. crysos* | 5.00 | 1.04 | 0.22 | 62.56 |
| *Aluterus* spp. | 4.61 | 0.94 | 0.00 | 68.28 |
| *C. pullus* | 4.02 | 0.50 | 0.57 | 73.28 |
| *S. rivoliana* | 3.47 | 0.71 | 0.35 | 77.59 |
| *Stephanolepis* spp. | 2.71 | 0.51 | 0.28 | 80.96 |
| July 2017 - July 2018 | | July 2017 | July 2018 | |
| *B. capriscus* | 15.61 | 3.54 | 0.72 | 22.72 |
| *A. saxatilis* | 7.11 | 2.06 | 1.17 | 33.07 |
| *Kyphosus* spp. | 5.34 | 1.21 | 0.56 | 40.85 |
| *H. histrio* | 4.76 | 1.58 | 1.05 | 47.77 |
| *C. crysos* | 4.48 | 1.04 | 0.25 | 54.29 |
| *Aluterus* spp. | 4.38 | 0.94 | 0.05 | 60.66 |
| *L. surinamensis* | 4.07 | 0.82 | 0.47 | 66.59 |
| *S. rivoliana* | 3.26 | 0.71 | 0.31 | 71.33 |
| *Stephanolepis* spp. | 2.73 | 0.51 | 0.45 | 75.30 |
| *C. pullus* | 2.67 | 0.50 | 0.22 | 79.19 |
| July 2017 - June 2019 | | July 2017 | June 2019 | |
| *B. capriscus* | 14.73 | 3.54 | 0.25 | 21.74 |
| *A. saxatilis* | 6.01 | 2.06 | 1.27 | 30.62 |
| *Stephanolepis* spp. | 5.89 | 0.51 | 1.62 | 39.32 |
| *Kyphosus* spp. | 4.73 | 1.21 | 0.30 | 46.31 |
| *Aluterus* spp. | 4.20 | 0.94 | 0.21 | 52.52 |
| *C. crysos* | 3.91 | 1.04 | 0.00 | 58.30 |
| *L. surinamensis* | 3.83 | 0.82 | 0.21 | 63.96 |
| *C. pullus* | 3.08 | 0.50 | 0.45 | 68.51 |
| *H. histrio* | 2.92 | 1.58 | 1.80 | 72.82 |
| *S. rivoliana* | 2.86 | 0.71 | 0.22 | 77.04 |

Table A.2 (continued) Average (avg.) pairwise species abundances of neuston net collections by cruise based on SIMPER analysis. Taxa are ordered starting with those of highest contribution (%) to between-cruise dissimilarities with a cutoff of approximately 80% cumulative contribution.

| Species | Avg. contribution to overall dissimilarity (%) | Avg. Abundance | | Cumulative Contribution (%) |
|---|---|---|---|---|
| June 2018 - July 2018 | | June 2018 | July 2018 | |
| *A. saxatilis* | 13.45 | 0.83 | 1.17 | 18.18 |
| *H. histrio* | 11.17 | 0.69 | 1.05 | 33.28 |
| *S. rivoliana* | 6.37 | 0.35 | 0.31 | 41.89 |
| *C. pullus* | 6.22 | 0.57 | 0.22 | 50.30 |
| *Stephanolepis* spp. | 5.84 | 0.28 | 0.45 | 58.20 |
| *Kyphosus* spp. | 5.41 | 0.12 | 0.56 | 65.52 |
| *L. surinamensis* | 5.01 | 0.12 | 0.47 | 72.28 |
| *B. capriscus* | 5.00 | 0.08 | 0.72 | 79.05 |
| *C. crysos* | 3.65 | 0.22 | 0.25 | 83.98 |
| *C. ruber* | 2.92 | 0.15 | 0.05 | 87.93 |
| June 2018 - June 2019 | | June 2018 | June 2019 | |
| *H. histrio* | 12.75 | 0.69 | 1.80 | 17.50 |
| *Stephanolepis* spp. | 12.55 | 0.28 | 1.62 | 34.73 |
| *A. saxatilis* | 11.06 | 0.83 | 1.27 | 49.91 |
| *C. pullus* | 6.22 | 0.57 | 0.45 | 58.44 |
| *S. rivoliana* | 4.41 | 0.35 | 0.22 | 64.49 |
| *C. bartholomaei* | 3.93 | 0.08 | 0.43 | 69.88 |
| *Kyphosus* spp. | 3.20 | 0.12 | 0.30 | 74.27 |
| *C. ruber* | 3.06 | 0.15 | 0.25 | 78.47 |
| *L. surinamensis* | 2.51 | 0.12 | 0.21 | 81.91 |
| *B. capriscus* | 2.26 | 0.08 | 0.25 | 85.01 |
| July 2018 - June 2019 | | July 2018 | June 2019 | |
| *Stephanolepis* spp. | 10.90 | 0.45 | 1.62 | 16.92 |
| *A. saxatilis* | 9.49 | 1.17 | 1.27 | 31.64 |
| *H. histrio* | 7.93 | 1.05 | 1.80 | 43.95 |
| *B. capriscus* | 4.61 | 0.72 | 0.25 | 51.11 |
| *Kyphosus* spp. | 4.59 | 0.56 | 0.30 | 58.22 |
| *C. pullus* | 4.02 | 0.22 | 0.45 | 64.47 |
| *L. surinamensis* | 3.56 | 0.47 | 0.21 | 69.99 |
| *C. bartholomaei* | 3.29 | 0.05 | 0.43 | 75.09 |
| *S. rivoliana* | 2.47 | 0.31 | 0.22 | 78.92 |
| *E. bipinnulata* | 1.94 | 0.24 | 0.07 | 81.93 |

# REFERENCES

Badalamenti, F., D'Anna, G., Lopiano, L., Scilipoti, D., and Mazzola, A. (1995). Feeding habits of young-of-the-year greater amberjack *Seriola dumerili* (Risso, 1810) along the N/W Sicilian Coast. Scientia Marina 59: 317–323.

Baker, R., Buckland, A., and Sheaves, M. (2014). Fish gut content analysis: robust measures of diet composition. Fish and Fisheries 15(1): 170–177. https://doi.org/10.1111/faf.12026

Barreiros, J. P., Morato, T., Santos, R. S., and De Borba, A. E. (2003). Interannual changes in the diet of the Almaco Jack, *Seriola rivoliana* (Perciformes: Carangidae) from the Azores. Cybium 27(1): 37-40.

Ballard, S. E., and Rakocinski, C. F. (2012). Flexible feeding strategies of juvenile Gray Triggerfish (Balistes capriscus) and Planehead Filefish (*Stephanolepis hispidus*) within *Sargassum* habitat. Gulf and Caribbean Research 24(1): 31–40. https://doi.org/10.18785/gcr.2401.05

Beck, M. W., Heck, K. L., Able, K. W., Childers, D. L., Eggleston, D. B., Gillanders, B. M., … Weinstein, M. P. (2001). The Identification, conservation, and management of estuarine and marine nurseries for fish and invertebrates. BioScience 51(8): 633. https://doi.org/10.1641/0006-3568(2001)051[0633:TICAMO]2.0.CO;2

Bortone, S. A., Hastings, P. A., and Collard, S. B. (1977). The pelagic *Sargassum* ichthyofauna of the eastern Gulf of Mexico. Northeast Gulf Science 1: 60–67. https://doi.org/10.18785/negs.0102.02

Casazza, T. L. (2008). Community structure and diets of fishes associated with pelagic *Sargassum* and open-water habitats off North Carolina. M. S. Thesis. University of North Carolina Wilmington.

Casazza, T. L. and Ross, S. W. (2008). Fishes associated with pelagic *Sargassum* and open water lacking *Sargassum* in the Gulf Stream off North Carolina. Fishery Bulletin 106(4): 348-363.

Clarke, K. R and Ainsworth, M. (1993). A method of linking multivariate community structure to environmental variables. Marine Ecology Progress Series 92: 205-219.

Clarke, K. R. and Gorley, R. N. *PRIMER v6: User Manual/Tutorial* 6th edn, Ch. 13 (PRIMER-E, 2006)

Cohen, J. (1988). *Statistical power analysis for the behavioral sciences*. 2nd ed. Hillsdale, NJ: Lawrence Erlbaum Associates.

Cortés, E. (1997). A critical review of methods of studying fish feeding based on analysis of stomach contents: application to elasmobranch fishes. Canadian Journal of Fisheries and Aquatic Science 54: 726-738. https://doi.org/10.1139/f96-316

Coston-Clements, L., Settle, LR., Hoss, DE., Cross, FA. (1991). Utilization of the *Sargassum* habitat by marine invertebrates and vertebrates— a review. NOAA Tech Memo NMFSSEFSC-296

Dagg, M. J., and Breed, G. A. (2003). Biological effects of Mississippi River nitrogen on the northern gulf of Mexico - A review and synthesis. Journal of Marine Systems 43(3–4): 133–152. https://doi.org/10.1016/j.jmarsys.2003.09.002

de la Moriniere, E. C., Pollux, B. J. A., Nagelkerken, I., Hemminga, M. A., Huiskes, A. H. L., and van der Velde, G. (2003). Ontogenetic dietary changes of coral reef fishes in the mangrove-seagrass-reef continuum: stable isotopes and gut- content analysis. Marine Ecology Progress Series 246: 279–289. https://doi.org/10.3354/meps246279

Dooley, J. (1972). Fishes associated with the pelagic *Sargassum* complex, with a discussion of the *Sargassum* community. Contributions in Marine Science 16: 1-32.

Farmer, N. A., Malinowski, R. P., McGovern, M. F., and Rubec, P. J. (2016). Stock complexes for fisheries management in the Gulf of Mexico. Marine and Coastal Fisheries, 8(1): 177–201. https://doi.org/10.1080/19425120.2015.1024359

Franks, J. S., VanderKooy, K. E., and Garber, N. M. (2003). Diet of Tripletail, *Lobotes surinamensis*, from Mississippi Coastal Waters. Gulf and Caribbean Research 15(1): 27–32. https://doi.org/10.18785/gcr.1501.05

Gower, J. F. R. and King, S. A. (2011). Distribution of floating *Sargassum* in the Gulf of Mexico and the Atlantic Ocean mapped using MERIS. International Journal of Remote Sensing 32(7): 1917-1929. https://doi.org/10.1080/01431161003639660

Graham, N. A. J., Wilson, S. K., Pratchett, M. S., Polunin, N. V. C., and Spalding, M. D. (2009). Coral mortality versus structural collapse as drivers of corallivorous butterflyfish decline. Biodiversity and Conservation 18(12): 3325–3336. https://doi.org/10.1007/s10531-009-9633-3

Gratwicke, B. and Speight, M. R. (2005). Effects of habitat complexity on Caribbean marine fish assemblages. Marine Ecology Progress Series 292: 301–310. https://doi.org/10.3354/meps292301

Grémillet, D., Lewis, S., Drapeau, L., Van Der Lingen, C. D., Huggett, J. A., Coetzee, J. C., … Ryan, P. G. (2008). Spatial match-mismatch in the Benguela upwelling zone: should we expect chlorophyll and sea-surface temperature to predict marine predator distributions? Journal of Applied Ecology 45(2): 610–621. https://doi.org/10.1111/j.1365-2664.2007.01447.x

Grimes, C. B., and Finucane, J. H. (1991). Spatial distribution and abundance of larval and juvenile fish, chlorophyll, and macrozooplankton around the Mississippi River discharge plume, and the role of the plume in fish recruitment. Marine Ecology Progress Series 75: 109-119.

Hamasaki, K, Tsuruoka, K., Teruya, K., Hashimoto, H., Hamada, K., Hotta, T., and Mushiake, K. (2009). Feeding habits of hatchery-reared larvae of greater amberjack *Seriola dumerili*. Aquaculture 288(3–4): 216–225. https://doi.org/10.1016/j.aquaculture.2008.11.032

Hastie, T. and Tibshirani, R. (2014). Generalized Additive Models. In Wiley StatsRef: Statistics Reference Online (eds N. Balakrishnan, T. Colton, B. Everitt, W. Piegorsch, F. Ruggeri and J.L. Teugels). https://doi.org/10.1002/9781118445112.stat03141

Hixon, M. A., and Carr, M. H. (1997). Synergistic predation, density dependence, and population regulation in marine fish. Science 277(5328): 946–949. https://doi.org/10.1126/science.277.5328.946

Hoffmayer, E.R., Franks, J. S., Comyns, B. H., Hendon, J. R., and Waller., R. S. (2005). Larval and juvenile fishes associated with pelagic *Sargassum* in the northcentral Gulf of Mexico. Proceedings of Gulf and Caribbean Fisheries Institute 56:259-269.

Hu, C. (2009). A novel ocean color index to detect floating algae in the global oceans. Remote Sensing of Environment 113(10): 2118-2129. https://doi.org/10.1016/j.rse.2009.05.012

Hyslop, E. J. (1980). Stomach contents analysis-a review of methods and their application. Journal of Fish Biology 17(4): 411–429. https://doi.org/10.1111/j.1095-8649.1980.tb02775.x

Kramer, L. M. (2014). Trophic dynamics and community assemblages of larval and juvenile fishes associated with floating *Sargassum* in the northern Gulf of Mexico. M.S. Thesis. University of South Alabama.

Krummel, O. (1891). Die nordatlantische Sargassosee, 1891. Petermann's Geographische Mitteilungen 37: 129–141.

Macdonald, J.S., and Green, R.H. (1983). Redundancy of variables used to describe importance of prey species in fish diets. Canadian Journal of Fisheries and Aquatic Science 40: 635-637. https://doi.org/10.1139/f83-083

Manooch, III, C. S., and Haimovici, M. (1983). Foods of Greater Amberjack, *Seriola dumerili*, and Almaco Jack, *Seriola rivoliana*, (Pisces: Carangidae), from the South Atlantic Bight. The Journal of the Elisha Mitchell Scientific Society 99(1): 1-9.

Massey, F. J. (1951). The Kolmogorov-Smirnov Test for Goodness of Fit. Journal of the American Statistical Association 46(253): 68–78. https://doi.org/10.1080/01621459.1951.10500769

Mickle, P., Harper, J., Shipley, K., Aplin, K., Kalinowsky, C., Adriance, J., … Rester, J. (2016). Biological Profile for Tripletail in the Gulf of Mexico and the Western Central Atlantic Gulf States Marine Fisheries Commission (258): 164 pp.

Phlips, E. J., Willis, M., and Verchick, A. (1986). Aspects of nitrogen fixation in *Sargassum* communities off the coast of Florida. Journal of Experimental Marine Biology and Ecology 102: 99-119. https://doi.org/10.1016/0022-0981(86)90170-X

Pietsch, T. W., and Grobecker, D. B. (1990). Frogfishes, Scientific American. 262(6): 96–103.

Rand, T. (1982). The *Sargassum* community and *Sargassum* fishes. Department of Agriculture and Fisheries, Bermuda Monthly Bulletin 53(4): 25-28.

Rooker, J. R., Turner, J. P., and Holt, S. A. (2006). Trophic ecology of *Sargassum*-associated fishes in the Gulf of Mexico determined from stable isotopes and fatty acids. Marine Ecology Progress Series 313: 249–259. https://doi.org/10.3354/meps313249

Schoener, T. (1970). Nonsynchronous spatial overlap of lizards in patchy habitats. Ecology 51: 408-418. https://doi.org/10.2307/1935376

Shadle, S., Lestrade, O., Elmer, F., and Hernandez, F. (2019). Estimation and comparison of epiphyte loading on holopelagic *Sargassum fluitans* collected in the North

Atlantic Ocean and the Gulf of Mexico. Gulf and Caribbean Research 30(1): SC42-SC46. https://doi.org/10.18785/gcr.3001.16

South Atlantic Fishery Management Council. (2002). Fishery management plan for pelagic *Sargassum* habitat of the South Atlantic Region. 1-153.

Stoner, A., and Greening, H. (1984). Geographic variation in the macrofaunal associates of pelagic *Sargassum* and some biogeographic implications. Marine Ecology Progress Series 20: 185–192. https://doi.org/10.3354/meps020185

Strelcheck, A. J., Jackson, J. B., Cowan, J. H., and Shipp, R. L. (2004). Age, growth, diet, and reproductive biology of the tripletail, *Lobotes surinamensis*, from the north-central Gulf of Mexico. Gulf of Mexico Science 22(1): 45–53. https://doi.org/10.18785/goms.2201.04

Tomczak, M. and Tomczak, E. (2014). The need to report effect size estimates revisited. An overview of some recommended measures of effect size. Trends in Sport Sciences 1(21): 19–25. ISSN 2299-9590

Turner, J. P., and Rooker, J. R. (2006). Determining the trophic relationships among flora and fauna within *Sargassum* mat communities using fatty acids. Proceedings of the Gulf and Caribbean Fisheries Institute 57: 679–691.

Wallace, R. K. (1981). An assessment of diet-overlap indexes. Transactions of the American Fisheries Society 110: 72-76. https://doi.org/10.1577/1548-8659(1981)110<72:AAODI>2.0.CO;2

Wang, M. and Hu, C. (2016). Mapping and quantifying *Sargassum* distribution and coverage in the Central West Atlantic using MODIS observations. Remote Sensing of Environment 183: 350-367. https://doi.org/10.1016/j.rse.2016.04.019

Wang, M., Hu, C., Barnes, B. B., Mitchum, G., Lapointe, B., and Montoya, J. P. (2019). The great Atlantic *Sargassum* belt. Science 364(6448): 83–87. https://doi.org/10.1126/science.aaw7912

Waters, L., Malinowski, R., Jepson, M., Freeman, M., Diagne, A., Johnson, D. H., and Lasseter, A. (2017). Amendment 46: Gray Triggerfish Rebuilding Plan.

Wells, R. J. D. and Rooker, J. R. (2003). Distribution and abundance of fishes associated with *Sargassum* mats in the NW Gulf of Mexico. Proceeds of the Gulf and Caribbean Fisheries Institute 54: 609-621.

Wells, R. J. D. and Rooker, J. R. (2004). Spatial and temporal patterns of habitat use by fishes associated with *Sargassum* mats in the Northwestern Gulf of Mexico. Bulletin of Marine Science 74(1): 81-99.

Wells, R. J. D., and Rooker, J. R. (2009). Feeding ecology of pelagic fish larvae and juveniles in slope waters of the Gulf of Mexico. Journal of Fish Biology 75(7): 1719–1732. https://doi.org/10.1111/j.1095-8649.2009.02424.x

Wells, R. J. D., Rooker, J. R., Quigg, A., and Wissel, B. (2017). Influence of mesoscale oceanographic features on pelagic food webs in the Gulf of Mexico. Marine Biology 164(4): 1–11. https://doi.org/10.1007/s00227-017-3122-0

Werner, E. E., and Gilliam, J. F. (1984). The ontogenetic niche and species interactions in size-structured populations. Annual Review of Ecology and Systematics 15: 393–425.

Wood, S. N. (2013). On p-values for smooth components of an extended generalized additive model. Biometrika, 100(1): 221–228. https://doi.org/10.1093/biomet/ass048

Wood, S. N. (2019). mgcv: Identifiability constraints. R Package Version 1.8-31.

Zar, J. H. (1999). Biostatistical Analysis. Fourth Edition. Prentice-Hall, Englewood Cliffs. 663 p.